

**PHASE 2 REPORT - REVIEW COPY
FURTHER SITE CHARACTERIZATION AND ANALYSIS
VOLUME 2D - REVISED BASELINE MODELING REPORT
HUDSON RIVER PCBs REASSESSMENT RI/FS**

JANUARY 2000



For

**U.S. Environmental Protection Agency
Region 2
and
U.S. Army Corps of Engineers
Kansas City District**

**Volume 2D - Book 1 of 4
Fate and Transport Models**

**TAMS Consultants, Inc.
Limno-Tech, Inc.
Menzie-Cura & Associates, Inc.
Tetra Tech, Inc.**



UNITED STATES ENVIRONMENTAL PROTECTION AGENCY

REGION 2
290 BROADWAY
NEW YORK, NY 10007-1866

January 25, 2000

To All Interested Parties:

The U.S. Environmental Protection Agency (EPA) is pleased to release the Revised Baseline Modeling Report for the Hudson River PCBs Superfund site. This report presents results and findings from the application of mathematical models for PCB transport and fate and bioaccumulation in the Upper Hudson River. This report provides predictions under baseline conditions, that is, without any remediation measures for the PCB-contaminated sediments in the Upper Hudson River.

The Revised Baseline Modeling Report incorporates changes made to the models based on comments received during the public comment period on the May 1999 Baseline Modeling Report (BMR) and from additional analyses that were conducted to refine the models for predicting future PCB levels in sediment, water and fish. EPA is also releasing a responsiveness summary for the BMR which provides readers with responses to significant comments, or directs them to the appropriate section of the Revised Baseline Modeling Report where the comment has been incorporated.

The Revised Baseline Modeling Report supercedes the May 1999 Baseline Modeling Report. EPA will evaluate if the revised modeling results would change the overall conclusions of the Human Health and Ecological Risk Assessments, and will update the risk and hazard values in the responsiveness summaries for the risk assessments, as necessary. The results of models used to calculate the loads leaving the Upper Hudson, which were subsequently utilized in the calculation of risks and hazards for the Mid- and Lower Hudson River, are presented in the Revised Baseline Modeling Report.


Because the Revised Baseline Modeling Report was prepared in response to public comment (with some additional analyses that were outlined in the May 1999 BMR), there is no public comment period on this document. Please remember that we will, of course, accept public comment on all aspects of the Reassessment during the comment period on the Proposed Plan.

The Revised Baseline Modeling Report is being peer reviewed by a panel of independent experts. The peer reviewers will discuss their comments on the Revised Baseline Modeling Report at a meeting that will be held on March 27 and 28, 2000 at the Sheraton Saratoga Springs Hotel and Conference Center. Observers are welcome and there will be limited time for observer comment.

If you need additional information regarding the Revised Baseline Modeling Report, please contact Ann Rychlenski, the Community Relations Coordinator for this site, at (212) 637-3672.

Sincerely yours,

A handwritten signature in cursive script that reads "William McCabe".

 Richard L. Caspe, Director
Emergency and Remedial Response Division

**PHASE 2 REPORT – REVIEW COPY
 FURTHER SITE CHARACTERIZATION AND ANALYSIS
 Volume 2D – REVISED BASELINE MODELING REPORT
 HUDSON RIVER PCBs REASSESSMENT RI/FS**

BOOK 1 of 4

CONTENTS

	<u>Page</u>
LIST OF TABLES	viii
LIST OF FIGURES	xii
GLOSSARY	xxvii
EXECUTIVE SUMMARY	ES-1
1. INTRODUCTION	1
1.1 PURPOSE OF REPORT	1
1.2 REPORT FORMAT AND ORGANIZATION	2
1.3 PROJECT BACKGROUND	3
1.3.1 Site Description	3
1.3.2 Site History	3
1.4 MODELING GOALS AND OBJECTIVES	4
2. MODELING APPROACH	7
2.1 INTRODUCTION	7
2.2 CONCEPTUAL APPROACH	7
2.3 HYDRODYNAMIC MODEL	9
2.4 DEPTH OF SCOUR MODEL	9
2.5 MASS BALANCE MODEL	10
2.6 MASS BALANCE MODEL APPLICATIONS	11
2.7 MASS BALANCE MODEL CALIBRATION	12
2.8 HUDSON RIVER DATABASE	13
3. THOMPSON ISLAND POOL HYDRODYNAMIC MODEL	15
3.1 OVERVIEW	15
3.2 HYDRODYNAMIC MODELING APPROACH	16
3.2.1 Governing Equations	16
3.2.2 Computational Sequence and Linkages	18
3.3 AVAILABLE DATA	18
3.3.1 Model Grid	19
3.3.2 Manning’s ‘n’	19
3.3.3 Boundary Conditions	19
3.4 HYDRODYNAMIC MODEL CALIBRATION	20
3.5 HYDRODYNAMIC MODEL VALIDATION	21
3.5.1 Rating Curve Velocity Measurements	21
3.5.2 FEMA Flood Studies	21
3.5.3 100-Year Peak Flow Model Results	22

**PHASE 2 REPORT – REVIEW COPY
 FURTHER SITE CHARACTERIZATION AND ANALYSIS
 Volume 2D – REVISED BASELINE MODELING REPORT
 HUDSON RIVER PCBs REASSESSMENT RI/FS**

BOOK 1 of 4

CONTENTS

	<u>Page</u>
3.6 HYDRODYNAMIC MODEL SENSITIVITY ANALYSES	22
3.6.1 Manning's 'n'	23
3.6.2 Turbulent Exchange Coefficient	23
3.7 CONVERSION OF VERTICALLY-AVERAGED VELOCITY TO BOTTOM SHEAR STRESS	23
3.8 DISCUSSION OF RESULTS	26
4. THOMPSON ISLAND POOL DEPTH OF SCOUR MODEL	27
4.1 OVERVIEW	27
4.2 DOSM MODEL DEVELOPMENT	28
4.2.1 Conceptual Approach	28
4.2.2 Formulation for Cohesive Sediments	29
4.2.2.1 Background	29
4.2.2.2 Basic Equations	29
4.2.2.3 Reparameterization to a Probabilistic Model	30
4.2.2.4 Calculation of PCB Erosion	31
4.2.3 Formulation for Non-cohesive Sediments	31
4.2.3.1 Background	31
4.2.3.2 Equations	32
4.2.4 Time Scale of Erosion Estimates	32
4.3 DOSM PARAMETERIZATION	33
4.3.1 Data	33
4.3.1.1 Distribution of Types of Bottom Sediment	33
4.3.1.2 Resuspension Experiments	33
4.3.1.3 Non-Cohesive Particle Size Distributions	34
4.3.1.4 1984 Cohesive Sediment PCB Concentration	35
4.3.2 Parameterization for Cohesive Sediments	35
4.3.3 Parameterization for Non-cohesive Sediments	36
4.4 DOSM APPLICATION	37
4.4.1 Application Framework	37
4.4.2 Probabilistic Model Application to High Resolution Coring Sites	37
4.4.3 Poolwide Model Application	38
4.4.3.1 Cohesive Sediments	38
4.4.3.2 Non-Cohesive Sediments	39
4.5 DOSM FINDINGS	39
5. FATE AND TRANSPORT MASS BALANCE MODEL DEVELOPMENT	41
5.1 INTRODUCTION	41
5.2 MODEL APPROACH	41
5.2.1 Introduction	41
5.2.2 Conceptual Framework	42

**PHASE 2 REPORT – REVIEW COPY
 FURTHER SITE CHARACTERIZATION AND ANALYSIS
 Volume 2D – REVISED BASELINE MODELING REPORT
 HUDSON RIVER PCBs REASSESSMENT RI/FS**

BOOK 1 of 4

CONTENTS

	<u>Page</u>
5.2.3 Governing Equations.....	43
5.3 WATER TRANSPORT	44
5.4 SOLIDS DYNAMICS.....	46
5.4.1 Solids Gross Settling	46
5.4.2 Cohesive Sediment Flow-Driven Resuspension.....	46
5.4.3 Non-Cohesive Sediment Resuspension.....	47
5.4.4 Sediment Bed Particle Mixing	48
5.4.5 Scour and Burial	48
5.5 PCB DYNAMICS	50
5.5.1 Equilibrium Sorption	50
5.5.2 Air-Water Exchange.....	52
5.5.3 Dechlorination	55
5.5.4 Sediment-Water Mass Transfer of PCBs	55
5.6 MODEL SPATIAL SEGMENTATION	56
5.6.1 Water Column Segments	56
5.6.2 Sediment Segments.....	57
5.7 MODEL IMPLEMENTATION.....	58
6. DATA DEVELOPMENT FOR MODEL APPLICATIONS.....	61
6.1 INTRODUCTION	61
6.2 AVAILABLE DATA.....	61
6.3 MODEL APPLICATION DATASETS.....	63
6.3.1 Sediment Datasets	63
6.3.2 Water Column Data.....	65
6.3.3 Conversion of PCB Data in Historical Calibration Datasets	66
6.3.3.1 USGS Water Column Data.....	66
6.3.3.2 1976-1978 NYSDEC Sediment Data.....	67
6.3.3.3 1984 NYSDEC Sediment Data	67
6.3.3.4 GE Water Column and Sediment Data	67
6.3.3.5 USEPA Water Column and Sediment Data	67
6.3.4 Data conversion for Total PCB and Congeners.....	68
6.4 FLOW BALANCE.....	68
6.4.1 Overview	68
6.4.2 Flow Data	69
6.4.3 Flow Estimation Methods	70
6.4.4 Results of Flow Balance.....	73
6.4.4.1 Validation of the Flow Estimation Approach	73
6.4.4.2 Application of Estimated Flows in Modeling.....	74
6.4.4.3 Summary of Flow Balance.....	74
6.5 MAINSTEM AND TRIBUTARY SOLIDS LOADS	74

**PHASE 2 REPORT – REVIEW COPY
 FURTHER SITE CHARACTERIZATION AND ANALYSIS
 Volume 2D – REVISED BASELINE MODELING REPORT
 HUDSON RIVER PCBs REASSESSMENT RI/FS**

BOOK 1 of 4

CONTENTS

	<u>Page</u>
6.5.1 Overview	74
6.5.2 Solids Data	75
6.5.3 Methods for Estimating Solids Loads	76
6.5.3.1 Mainstem Solids Loads	77
6.5.3.2 Tributary Solids Loads	81
6.5.3.3 Development of Long-term Solids Balance	82
6.5.4 Results	85
6.5.5 Summary of Solids Load Estimates.....	86
6.6 MAINSTEM AND TRIBUTARY PCB LOADS	87
6.6.1 Overview	87
6.6.2 PCB Data	87
6.6.2.1 Data Availability for Estimating PCB Loads.....	87
6.6.2.2 Thompson Island Dam West Shore Station Bias Correction.....	88
6.6.2.3 Data Development for Computing PCB Loads.....	89
6.6.2.4 Overview.....	89
6.6.2.5 Mainstem Tri+ Loads 1977-1997	90
6.6.2.6 Tributary Tri+ Loads 1977-1997.....	92
6.6.2.7 Tri+ Load Results 1977-1997	92
6.6.2.8 Mainstem and Tributary Total PCB and Congener Loads 1991-1997	94
6.6.3 Total PCB and Congener Load Results 1991-1997.....	95
6.6.4 Summary of PCB Load Estimates.....	95
6.7 SEDIMENT INITIAL CONDITIONS	96
6.7.1 Overview	96
6.7.2 Sediment Specific Weight.....	96
6.7.3 1977 Tri+ Initial Conditions	97
6.7.3.1 1977 NYSDEC Sediment Data	97
6.7.3.2 Methods.....	98
6.7.3.3 1977 Initial Condition Results	99
6.7.4 1991 Initial conditions and model calibration targets	99
6.7.4.1 Data	99
6.7.4.2 Methods.....	100
6.7.4.3 1991 Initial Condition Results	100
6.7.5 Summary	100
6.8 WATER AND AIR TEMPERATURES	101
6.9 PARTITIONING.....	102
6.9.1 Overview	102
6.9.2 Partition Coefficients	103
6.9.2.1 Water Column Organic Carbon Concentrations	105
6.9.2.2 Water Column DOC.....	105
6.9.2.3 Water Column f_{OC}	106

**PHASE 2 REPORT – REVIEW COPY
 FURTHER SITE CHARACTERIZATION AND ANALYSIS
 Volume 2D – REVISED BASELINE MODELING REPORT
 HUDSON RIVER PCBs REASSESSMENT RI/FS**

BOOK 1 of 4

CONTENTS

	<u>Page</u>
6.9.2.4 Sediment Organic Carbon Concentrations	107
6.9.2.5 Porewater DOC	107
6.9.2.6 Sediment f_{oc}	108
6.9.2.7 Distribution of PCBs in sediment and water	108
6.9.2.8 Partitioning Summary	109
6.10 VOLATILIZATION	109
6.10.1 Overview	109
6.10.2 Volatilization Mass Transfer	109
6.10.2.1 Henry’s Constant and Molecular Weight	110
6.10.2.2 Film Transfer Coefficients	110
6.10.2.3 Atmospheric PCB Concentrations	111
6.10.3 Gas Exchange at Dams	112
6.11 SEDIMENT PARTICLE MIXING	112
6.12 DECHLORINATION	113
6.13 SEDIMENT-WATER MASS TRANSFER	114
6.13.1 Overview	114
6.13.2 Calculation of k_f for Tri+	117
6.13.2.1 Data	117
6.13.2.2 Approach	118
6.13.2.3 k_f Results	119
6.13.2.4 Implementation in HUDTOX	119
6.13.3 Analysis of congener and total PCB mass transfer coefficients	120
6.13.4 Estimation of Particulate and Pore water Mass Transfer Rates	121
7. MASS BALANCE MODEL CALIBRATION	124
7.1 OVERVIEW	124
7.2 CALIBRATION STRATEGY	124
7.3 SOLIDS DYNAMICS	126
7.3.1 Calibration Approach	126
7.3.2 Solids Calibration Results	127
7.3.2.1 Burial Rates	128
7.3.2.2 High and Low-flow Solids Loads	128
7.3.2.3 Water Column Solids Concentrations	129
7.3.2.4 Spring 1994 High Flow Event Solids Mass Balance	130
7.3.2.5 Further Model-Data Comparisons	130
7.3.3 Components Analysis for Solids	131
7.3.4 Solids Calibration Summary	132
7.4 HISTORICAL TRI+ CALIBRATION	132
7.4.1 Calibration Approach	132
7.4.2 Tri+ Calibration Results	133

**PHASE 2 REPORT – REVIEW COPY
 FURTHER SITE CHARACTERIZATION AND ANALYSIS
 Volume 2D – REVISED BASELINE MODELING REPORT
 HUDSON RIVER PCBs REASSESSMENT RI/FS**

BOOK 1 of 4

CONTENTS

	<u>Page</u>
7.4.2.1 Long-Term Sediment Tri+ Concentrations.....	134
7.4.2.2 Longitudinal and Vertical Sediment Profiles.....	135
7.4.2.3 Water Column Tri+ Concentrations.....	135
7.4.2.4 High and Low-flow Tri+ Loads.....	136
7.4.2.5 Further Model-Data Comparisons.....	137
7.4.3 Components Analysis for Tri+.....	138
7.4.4 Comparison to Low Resolution Sediment Coring Report (LRC) Results.....	139
7.4.5 Tri+ Calibration Summary.....	140
7.5 SENSITIVITY ANALYSES.....	141
7.5.1 Solids loadings.....	141
7.5.1.1 Solids loads at Fort Edward.....	142
7.5.1.2 External Tributary Solids Loads.....	142
7.5.1.3 Tributary Solids Loads Based on the Original Rating Curves.....	143
7.5.2 Partition Coefficients.....	143
7.5.3 Sediment-Water Mass Transfer Rates.....	144
7.5.3.1 Variation of Sediment-water Transfer Rate.....	144
7.5.3.2 Differences in Sediment Water Transfer between Cohesive and Non-Cohesive Areas.....	144
7.5.4 Burial Rates in Cohesive Sediments.....	145
7.5.5 Particle Mixing in Sediments.....	145
7.5.6 Sediment Initial Conditions.....	146
7.5.7 Henry’s Law Constant.....	146
7.6 1991-1997 HINDCAST APPLICATIONS.....	146
7.6.1 Overview.....	146
7.6.2 Approach.....	147
7.6.3 Results.....	147
7.6.4 Hindcast Applications Summary.....	149
7.7 CALIBRATION FINDINGS AND CONCLUSIONS.....	150
8. FORECAST SIMULATIONS FOR NO ACTION.....	153
8.1 OVERVIEW.....	153
8.2 NO ACTION FORECAST SIMULATION DESIGN.....	154
8.2.1 Hydrograph.....	154
8.2.2 Solids Loads.....	155
8.2.3 PCB Loads.....	155
8.2.4 Initial Conditions for the Forecast.....	156
8.2.5 Specification Of Other Model Inputs.....	156
8.3 NO ACTION FORECAST RESULTS.....	157
8.3.1 Forecast Results: Surface Sediment PCB Concentrations.....	157
8.3.2 Forecast Results: Water Column PCB Concentrations.....	159

**PHASE 2 REPORT – REVIEW COPY
FURTHER SITE CHARACTERIZATION AND ANALYSIS
Volume 2D – REVISED BASELINE MODELING REPORT
HUDSON RIVER PCBs REASSESSMENT RI/FS**

BOOK 1 of 4

CONTENTS

	<u>Page</u>
8.3.3 Forecast Results: PCB Loads to the Lower Hudson River.....	160
8.4 100-YEAR PEAK FLOW SIMULATION DESIGN	160
8.4.1 Specification of the 100-year Flood Hydrograph and Loadings.....	160
8.5 100-YEAR PEAK FLOW SIMULATION RESULTS	161
8.6 SENSITIVITY ANALYSIS	162
8.6.1 Sensitivity to Specification of Forecast Hydrograph.....	162
8.6.2 Sensitivity to Solids Loads at Fort Edward	163
8.6.3 Sensitivity to Tributary Solids Loads.....	163
8.6.4 Sensitivity to Particle Mixing.....	164
8.6.5 Sensitivity to Sediment Initial Conditions	164
8.7 EXPOSURE CONCENTRATIONS FOR AUGUST 1999 AND DECEMBER 1999 RISK ASSESSMENTS	164
8.8 PRINCIPAL FINDINGS AND CONCLUSIONS	165
8.8.1 No Action Forecast.....	165
8.8.2 100-Year Peak Flow Simulation.....	166
9. HUDTOX VALIDATION	169
9.1 OVERVIEW	169
9.2 VALIDATION APPROACH.....	169
9.2.1 Validation Results	170
9.2.2 Validation Summary.....	170
REFERENCES.....	173

Note: Book 3 and Book 4 Tables of Contents are located in the respective books.

**PHASE 2 REPORT – REVIEW COPY
FURTHER SITE CHARACTERIZATION AND ANALYSIS
Volume 2D – REVISED BASELINE MODELING REPORT
HUDSON RIVER PCBs REASSESSMENT RI/FS**

BOOK 1 of 4

LIST OF TABLES

<u>TABLE</u>	<u>TITLE</u>
3-1	Comparison of Manning’s ‘n’ from Previous Studies
3-2	Modeled Hudson River Flows at the Upstream Boundary of Thompson Island Pool
3-3	Comparison of Model Results with Rating Curve Data
3-4	Effect of Manning’s ‘n’ on Model Results for 100-Year Flow Event
3-5	Effect of Turbulent Exchange Coefficients on Model Results
4-1	Summary of Inputs for Depth of Scour Model at Each High Resolution Core
4-2	Predicted Depth of Scour Range for 100 Year Flood at Each High Resolution Core Location
4-3	Thompson Island Pool Cohesive Sediment Expected Values of Solids Erosion and Mean Depth of Scour for 100-Year Flood, from Monte Carlo Analysis
5-1 a	HUDTOX Water Column Segment Geometry in Thompson Island Pool (2-dimensional segmentation)
5-1 b	HUDTOX Water Column Segment Geometry Below Thompson Island Pool (1-dimensional segmentation)
5-2 a	HUDTOX Sediment Segment Geometry in Thompson Island Pool for Surficial Sediment Segments (2-dimensional segmentation)
5-2 b	HUDTOX Sediment Segment Geometry Downstream of Thompson Island Pool for Surficial Sediment Segments (1-dimensional segmentation)
6-1	Sediment Data Sets Used in Development and Application of the HUDTOX Model
6-2	USGS Gage Information For Gages Used In Flow Estimation
6-3	Drainage Areas and Reference Tributaries Used to Estimate Daily Tributary Flows
6-4	Mean Seasonal USGS Flows For Select Flow Gauges in the Study Area for the Period 3/1/77 to 6/30/92
6-5	Seasonal Tributary Flow Adjustment Factors applied to Tributaries between Fort Edward and Stillwater, and between Stillwater and Waterford
6-6	Hudson River Flows Yearly Averages Estimated and USGS Gage Data
6-7	Summary of Available Solids Data for Mainstem Stations; Number of Samples and Source of Suspended Solids Sample Data by Station

PHASE 2 REPORT – REVIEW COPY
FURTHER SITE CHARACTERIZATION AND ANALYSIS
Volume 2D – REVISED BASELINE MODELING REPORT
HUDSON RIVER PCBs REASSESSMENT RI/FS

BOOK 1 of 4

LIST OF TABLES

<u>TABLE</u>	<u>TITLE</u>
6-8	Summary of Available Solids Data for Tributaries; Number of Samples and Source of Suspended Solids Sample Data by Station
6-9	Reference Tributaries for Unmonitored Tributaries
6-10	Tributary Solids Rating Curve Equations for Data-Based Rating Curves and Adjusted Rating Curves for the Long-Term Solids Balance
6-11	Cumulative Mainstem Solids (SS) Loads and Yields
6-12	Cumulative Solids Loads and Corresponding Yields by Reach (10/1/77 – 9/30/97)
6-13	Solids (TSS) Trapping Efficiencies by Reach Estimated by QEA Using SEDZL and Applied to Estimate Tributary TSS Loads in HUDTOX
6-14	Comparison of LTI and Literature-Based Annual Average Sediment Yield Estimates by Watershed
6-15	Number of Tri+ PCB Data Available by Source and Year at Each Hudson River Mainstem Sampling Station
6-16	Number of Days With Available PCB Data for Monitored Tributaries (Batten Kill, Hoosic River, Mohawk River)
6-17	Number of PCB Data Available for Each Congener and Total PCB by Source and Year at Each Hudson River Mainstem Sampling Station
6-18	Criteria and Factors Used in Adjustment of Thompson Island Dam West Shore PCB Data Bias
6-19	Tri+ and Total PCB Concentration Statistics for Monitored Tributaries
6-20	Comparison of Annual Tri+ PCB Load Estimates at Hudson River Mainstem Station Presented in the DEIR and Calculated in this Report
6-21	Estimated Average Annual Load at Fort Edward by PCB Type from 1991-1997
6-22	Cohesive/non-cohesive Sample Classification Criteria Applied to 1977 NYSDEC Data to Compute HUDTOX Sediment Tri+ Initial Conditions
6-23	Sample Count and Averaging Groups for Specifying 1977 Sediment Initial Conditions for HUDTOX from the NYSDEC Data
6-24	Averaging Groups for Specifying Sediment Initial Conditions from the 1991 GE Composite Sampling Data

PHASE 2 REPORT – REVIEW COPY
FURTHER SITE CHARACTERIZATION AND ANALYSIS
Volume 2D – REVISED BASELINE MODELING REPORT
HUDSON RIVER PCBs REASSESSMENT RI/FS

BOOK 1 of 4

LIST OF TABLES

<u>TABLE</u>	<u>TITLE</u>
6-25	Pool-Wide Average Surficial Sediment Concentrations for Each PCB State Variable
6-26	3-Phase Partition Coefficients Estimated from Phase 2 Water Column Data and GE Sediment Data
6-27	Mass Fraction of Total PCB Represented by Tri+, BZ#1, BZ#4, and BZ#8 at Mainstem Hudson River Stations Determined from GE and USEPA Phase 2 (P2) Data
6-28	Estimated Partition Coefficients (K_{POC} , K_{DOC}) for Total PCB by Source and Agency at Mainstem Hudson River Stations
6-29	Estimated Partition Coefficients (K_{POC} , K_{DOC}) for Total PCB at Mainstem Hudson River Stations and Averaged Over Study Reach
6-30	Statistical Summary of Dissolved Organic Carbon (DOC) Water Column Data
6-31	Mean DOC Concentrations by Reach in Upper Hudson River
6-32	Mean Sediment f_{OC} Values Specified from GE 1991 Composite Data for River Mile intervals in HUDTOX
6-33	Illustration of Typical Low and High Flow Partitioning Behavior During Cold Weather and Warm Weather Periods
6-34	Henry's Law Constants Developed Experimentally by Brunner, et. al. (1990) for Selected Congeners
6-35	Congener Distribution of Total PCB by Mass Fraction at Mainstem Hudson River Stations Using 1993 USEPA Phase 2 Data (Number of observations)
6-36	Congener Distribution of Total PCB by Mass Fraction at Mainstem Hudson River Stations Using 1991-1998 GE Data (Number of observations)
6-37	Estimated Henry's Law Constants (HLC) for Total and Tri+ PCB by Source and Agency at Mainstem Hudson River Stations
6-38	Estimated Henry's Law Constants (HLC) for Total PCB at Mainstem Hudson River Stations and Averaged Over Study Reach
6-39	Estimated Molecular Weight for Total and Tri+ PCB by Source and Agency at Mainstem Hudson River Stations
6-40	Estimated Molecular Weight for Total PCB at Mainstem Hudson River Stations and Averaged Over Study Reach

PHASE 2 REPORT – REVIEW COPY
FURTHER SITE CHARACTERIZATION AND ANALYSIS
Volume 2D – REVISED BASELINE MODELING REPORT
HUDSON RIVER PCBs REASSESSMENT RI/FS

BOOK 1 of 4

LIST OF TABLES

<u>TABLE</u>	<u>TITLE</u>
6-41	Estimated Henry’s Law Constants and Molecular Weight by PCB Type
6-42	Coefficients Used to Estimate Depth and Velocity as a Function of Cross-Section Average Flow in HUDTOX for Calculation of Liquid-Phase (K_L) Air-Water Transfer Rates
6-43	Annual Average Bulk Sediment Concentrations by PCB Type
6-44	Annual Average Pore Water Concentrations by PCB Type
6-45	Estimated Sediment Properties in Thompson Island Pool Based on Area Weighting by Sediment Type
6-46	Annual Time Series of Sediment-Water Mass Transfer Rate for Tri+ PCBs
6-47	Correlation of Particulate-mediated Sediment-Water Mass Transfer Coefficient with Suspended Solids Concentration, Fort Edward Flow, and Water Temperature
6-48	Annual Time Series of Pore Water and Particulate Mass Transfer Coefficients by PCB Type
7-1	HUDTOX Solids Model Calibration Parameter Values
7-2	HUDTOX Cohesive Sediment Resuspension and Armoring Parameters
7-3	HUDTOX Fraction Organic Carbon and Dissolved Organic Carbon Parameterization by Reach
7-4	HUDTOX PCB Model Calibration Parameter Values
7-5	Tri+ Mass Loads (1977-1997) at Mainstem Stations for Sensitivity Analyses
8-1	Sequencing of Annual Hydrographs to Develop 70-year Forecast Hydrograph
8-2	Surface Sediment Tri+ Initial Conditions for the No Action and 100-Year Event Simulations
8-3	Effect of the 100-Year Flood Event on the Non-cohesive (N) and Cohesive (C) Sediment Bed in Upper Hudson River Reaches between Fort Edward and Federal Dam (Year 1 – 3/28 to 4/13)

PHASE 2 REPORT – REVIEW COPY
FURTHER SITE CHARACTERIZATION AND ANALYSIS
Volume 2D – REVISED BASELINE MODELING REPORT
HUDSON RIVER PCBs REASSESSMENT RI/FS

BOOK 1 of 4

LIST OF FIGURES

<u>FIGURE</u>	<u>TITLE</u>
1-1	Hudson River Watershed
1-2	Upper Hudson River Watershed
1-3	Thompson Island Pool
2-1	Upper Hudson River Modeling Framework
2-2	Upper Hudson River Modeling Framework with Model Inputs
3-1	Thompson Island Pool Study Area
3-2	Thompson Island Pool RMA-2V Model Mesh
3-3	Thompson Island Pool Velocity Vectors for 100-Year Flow Event
3-4	Shear Stress Computed from Vertically Averaged Velocity
3-5	Thompson Island Pool Bottom Shear Stress for 100-Year Flow Event
4-1	Erosion versus Shear Stress in Cohesive Sediments
4-2	Armoring Depth versus Shear Stress
4-3 a,b	Likelihood of PCB Scour for Selected Phase 2 High Resolution Sediment Cores
4-4	Cumulative Percent versus Mean Depth of Scour for Cohesive Sediment in Thompson Island Pool
4-5	Cumulative Percent versus Total Solids Scoured from Cohesive Sediment in Thompson Island Pool
5-1	Conceptual Framework for the HUDTOX PCB Model
5-2	Illustration of Sediment Scour in the HUDTOX Model
5-3	Illustration of Sediment Burial in the HUDTOX Model
5-4 a,b	HUDTOX Model Water Column Segmentation Grid for Upper Hudson River, Parts A and B
5-4 c,d	HUDTOX Model Water Column Segmentation Grid for Upper Hudson River, Parts C and D
5-5	Thompson Island Pool Study Area
5-6	Schematic of HUDTOX Water Column Segmentation Grid
5-7	HUDTOX Water Column Segment Depths by River Mile

PHASE 2 REPORT – REVIEW COPY
FURTHER SITE CHARACTERIZATION AND ANALYSIS
Volume 2D – REVISED BASELINE MODELING REPORT
HUDSON RIVER PCBs REASSESSMENT RI/FS

BOOK 1 of 4

LIST OF FIGURES

<u>FIGURE</u>	<u>TITLE</u>
5-8	Percent Cohesive Area Represented in HUDTOX Sediment by River Mile
6-1	Upper Hudson River Basin USGS Flow Gage Stations Used in HUDTOX Modeling
6-2	Log Pearson Flood Frequency Analysis for Fort Edward gage, Hudson River, NY Analysis
6-3	USGS Flow Time Series at Fort Edward from 1/1/77 – 9/30/97
6-4	Comparison of LTI-Estimated Flow (DAR-based, seasonally & high-flow adjusted) and the USGS-Reported Flow
6-5	Estimated Daily Average Mainstem and Tributary Flows for the Upper Hudson River between Fort Edward and Federal Dam (1/1/77-9/30/97)
6-6	Relative Percent Flow Contribution from Fort Edward and Tributaries between Fort Edward and Waterford
6-7	1993 – 1997 Estimated versus USGS-Reported Daily Average Flow at Stillwater and Waterford
6-8	1993 – 1997 Estimated versus USGS-Reported Daily Average Flow Time Series at Stillwater and Waterford
6-9	Upper Hudson River Basin Primary Mainstem and Tributary Sampling Locations for Solids Used in HUDTOX Modeling
6-10	Monitored and Unmonitored Subwatersheds for Solids Between Fort Edward and Waterford
6-11	GE versus USGS TSS Data at Fort Edward for High and Low Flow Data Pairs from 4/1/91 to 9/15/97
6-12	Observed Total Suspended Solids (TSS) versus Flow, 1977-1997 and TSS Rating Curves for this Period at Fort Edward, Stillwater and Waterford
6-13	Comparison of Total Suspended Solids (TSS) High-Flow Rating Curves for Fort Edward, 1977-1997, Using MVUE (Cohn et al. 1989) and Non-linear Regression Analysis.
6-14	Comparison of 1977-1990 and 1991-1997 Total Suspended Solids (TSS) Rating Curves at Fort Edward versus the 1977-1997 Rating Curve
6-15	Tributary TSS Rating Curves: Based on Data and Adjusted to Achieve Solids Balance

PHASE 2 REPORT – REVIEW COPY
FURTHER SITE CHARACTERIZATION AND ANALYSIS
Volume 2D – REVISED BASELINE MODELING REPORT
HUDSON RIVER PCBs REASSESSMENT RI/FS

BOOK 1 of 4

LIST OF FIGURES

<u>FIGURE</u>	<u>TITLE</u>
6-16	Mainstem and Tributary Suspended Solids Watershed Loads and Yields based on HUDTOX Suspended Solids Loading Estimates (10/1/77-9/30/97)
6-17	Relative Percent Solids Contribution from Fort Edward and Tributaries between Fort Edward and Waterford
6-18	Distribution of TSS Load Over Flow Range at Fort Edward, Stillwater, and Waterford from 1977-1997
6-19	Upper Hudson River Basin Primary Mainstem and Tributary Sampling Locations for PCB Data Used in HUDTOX Modeling
6-20 a,b	Distribution of Available Tri+ PCBs Concentration Data by Flow Intervals for Mainstem Hudson River Sampling Stations (January 1977-May 1998)
6-21	Tri+ PCB concentrations and Load versus Flow at Fort Edward for Selected Years
6-22	Tri+ PCB Concentrations and Loads versus Total Suspended Solids (TSS) Concentration at Fort Edward for Selected Years
6-23	Interpolated Daily Tri+ PCB Concentration and Flow at Fort Edward, 1977-1997
6-24	Examples of Apparent Tri+ Pulse Loading Events at Fort Edward in 1983 and 1994
6-25	Estimated Annual Tri+ Load at Mainstem Hudson River Sampling Stations Compared to DEIR Estimates
6-26	Estimated Annual Tri+ Load at Hudson River Mainstem Sampling Stations
6-27	Distribution of Tri+ Load Over Flow Range at Fort Edward, Stillwater, and Waterford from 1977-1997
6-28	Distribution of Tri+ Load Gain Across Thompson Island Pool (TIP) Over Flow Range for 1993-1997
6-29	Relative Contribution of Estimated External Tri+ PCB Loads to the Upper Hudson River by Source, 1977-1997
6-30	Ratio of Congener BZ#4 to Total PCBs at Fort Edward, 1991-1997, GE and Phase2 Data
6-31	Estimated Annual Total and Congener PCB Loads at Fort Edward
6-32	1977 Sediment Tri+ PCB Initial Conditions Computed from the NYSDEC Data, Fort Edward to Federal Dam

PHASE 2 REPORT – REVIEW COPY
FURTHER SITE CHARACTERIZATION AND ANALYSIS
Volume 2D – REVISED BASELINE MODELING REPORT
HUDSON RIVER PCBs REASSESSMENT RI/FS

BOOK 1 of 4

LIST OF FIGURES

<u>FIGURE</u>	<u>TITLE</u>
6-33	1977 Sediment Tri+ PCB Initial Conditions Computed from the NYSDEC Data, Thompson Island Pool
6-34 a,b	1977 Sediment Tri+ Initial Conditions Computed from 1977 NYSDEC Data: Vertical Profiles
6-35	Comparison of Measures Total PCB & Tri+ PCB Data to 1991 Model Initial Conditions in the Top Layer (0 - 5 cm) of Cohesive and Non-cohesive Sediments
6-36	Comparison of Measured BZ#4 (#10) & BZ#52 Data to Model Initial Conditions in the Top Layer (0 to 5 cm) of cohesive and Non-cohesive Sediment
6-37	Comparison of Measured BZ#28 and BZ#90+101 Data to 1991 Model Initial Conditions in the Top Layer (0 to 5 cm) of Cohesive and Non-cohesive Sediments
6-38	Comparison of Measured BZ#138 Data to Model Initial Conditions in the Top Layer (0 to 5 cm) of Cohesive and Non-cohesive Sediments
6-39	Ratio of Average BZ#4 1991 Concentrations to Average BZ#52 1991 Concentrations by Sediment Depth
6-40	Monthly Average Water Temperature Functions Applied in HUDTOX and Observed Water Temperatures
6-41	Comparison of Monthly Mean Temperatures at Mainstem Upper Hudson River Stations
6-42	Estimated Partition Coefficients for Total PCB by Station and by Source
6-43	Observed Dissolved Organic Carbon (DOC) Concentrations versus Normalized Flow between Fort Edward and Federal Dam
6-44	Observed Dissolved Organic Carbon (DOC) Data versus River Mile between Fort Edward and Federal Dam
6-45	River-wide Fraction Organic Carbon (f_{oc}) Function Based on a Power Function Fit to f_{oc} Data for Mainstem Hudson River Stations
6-46	Specified Sediment Dissolved Organic Carbon (DOC) Concentrations in HUDTOX
6-47	f_{oc} versus River Mile from the 1991 GE Composite Sampling and Values Specified for Cohesive and Non-cohesive Sediment in HUDTOX
6-48	Estimated Henry's Law Constant for Selected Congeners Determined Experimentally by Brunner, et. al (1990)

PHASE 2 REPORT – REVIEW COPY
FURTHER SITE CHARACTERIZATION AND ANALYSIS
Volume 2D – REVISED BASELINE MODELING REPORT
HUDSON RIVER PCBs REASSESSMENT RI/FS

BOOK 1 of 4

LIST OF FIGURES

<u>FIGURE</u>	<u>TITLE</u>
6-49	Estimated Henry's Law Constants for Tri+ and Total PCB by Station and Data Source
6-50	Estimated Molecular Weight for Tri+ and Total PCB by Station and Data Source
6-51	Specification of Historical Atmospheric Gas-Phase PCB Boundary Concentrations for the 1977-1997 HUDTOX Calibration Period
6-52 a-c	Vertical Profiles of PCB ₃₊ within Finely Segmented Sediment Cores Collected from the Upper Hudson River (from QEA, 1999)
6-53	Comparison of Same-Day Suspended Solids (TSS) Concentration Data at Fort Edward and Thompson Island Dam when TSS Concentration is less Than 10 mg/L and Fort Edward Flow is less Than 10,000 cfs (1993-1997)
6-54	Temporal Patterns in Water Column Tri+ PCB Concentration at Fort Edward and Thompson Island Dam, Tri+ PCB Loading Increase Across Thompson Island Pool, and Calculated Effective Sediment-Water Mass Transfer Rates Across Thompson Island Pool
6-55	Computed Effective Mass Transfer Rate for Tri+ PCBs in Thompson Island Pool, 1993-1997
6-56	Scatter Plots of Estimated Sediment-Water Mass Transfer Rate: Congeners versus Total PCB
6-57	Comparison of Estimated Site-Specific Water Column and Sediment Koc Values for Congeners as Determined in the DEIR
6-58	Average Observed versus Porewater and Particulate Predicted Relative Load Gain at Thompson Island Dam by Season, 1991-1997
6-59	Comparison of Congener Specific Apparent Sediment-Water Mass Transfer Rates by Date
6-60	Comparison of Fit using Ratio of Pore Water to Particulate Mass Transfer Coefficients to Average Observed Predicted Relative Load Gain at Thompson Island Dam by Season, 1991-1997
7-1	Computed Annual Average Burial Rates, 1977-1997
7-2	Comparison between Model Estimated and Data Estimated In-River Solids Loadings Stratified by Fort Edward Flow at 10,000 cfs (1/1/77-9/30/97)
7-3 a,b	Comparison Between Computed and Observed Solids Concentrations at Mainstem Sampling Stations

**PHASE 2 REPORT – REVIEW COPY
FURTHER SITE CHARACTERIZATION AND ANALYSIS
Volume 2D – REVISED BASELINE MODELING REPORT
HUDSON RIVER PCBs REASSESSMENT RI/FS**

BOOK 1 of 4

LIST OF FIGURES

<u>FIGURE</u>	<u>TITLE</u>
7-4	Comparison Between Computed and Observed Total Suspended Solids Concentrations (TSS) for the Spring 1983 High Flow Event
7-5	Comparison Between Computed and Observed Total Suspended Solids Concentrations (TSS) for the Spring 1993 High Flow Event
7-6	Comparison Between Computed and Observed Total Suspended Solids Concentrations (TSS) for the Spring 1994 High Flow Event
7-7	Comparison Between Computed and Observed Total Suspended Solids Concentrations (TSS) for the Spring 1997 High Flow Event
7-8	Comparison Between Computed and Observed Suspended Solids Concentrations for Fort Edward Flows less than 10,000 cfs
7-9	Comparison Between Computed and Observed Suspended Solids Concentrations for Fort Edward Flows greater than 10,000 cfs
7-10	Comparison Between Computed and Observed Probability Distributions for Total Suspended Solids (TSS) for Fort Edward Flows less than 10,000 cfs
7-11	Comparison Between Computed and Observed Probability Distributions for Total Suspended Solids (TSS) for Fort Edward Flows greater than 10,000 cfs
7-12	Computed Cumulative Sediment Bed Elevation Change in Thompson Island Pool, 1977-1997
7-13	Computed Annual Average Solids Burial Rates, 1977-1997
7-14	Computed Solids Mass Balance Components Analysis for 1977-1997
7-15 a	Comparison between Computed and Observed (Surficial and Depth-Composited) Sediment Tri+ Concentrations for Thompson Island Pool
7-15 b	Comparison between Computed and Observed (Surficial and Depth-Composited) Sediment Tri+ Concentrations for Schuylerville Reach
7-15 c	Comparison between Computed and Observed (Surficial and Depth-Composited) Sediment Tri+ Concentrations for Stillwater Reach
7-15 d	Comparison between Computed and Observed (Surficial and Depth-Composited) Sediment Tri+ Concentrations for Waterford Reach
7-15 e	Comparison between Computed and Observed (Surficial and Depth-Composited) Sediment Tri+ Concentrations for Federal Dam Reach

PHASE 2 REPORT – REVIEW COPY
FURTHER SITE CHARACTERIZATION AND ANALYSIS
Volume 2D – REVISED BASELINE MODELING REPORT
HUDSON RIVER PCBs REASSESSMENT RI/FS

BOOK 1 of 4

LIST OF FIGURES

<u>FIGURE</u>	<u>TITLE</u>
7-16	Comparison Between Computed and Observed Depth-Averaged Sediment Tri+ Concentrations for Thompson Island Pool in 1984
7-17	Comparison Between Computed and Observed Depth-Averaged (0-5 cm) Sediment Tri+ Concentrations from Fort Edward to Federal Dam in 1991
7-18	Comparison Between Computed and Observed Depth-Averaged (5-10 cm) Sediment Tri+ Concentrations from Fort Edward to Federal Dam in 1991
7-19	Comparison Between Computed and Observed Depth-Averaged (10-26 cm) Sediment Tri+ Concentrations from Fort Edward to Federal Dam in 1991
7-20 a,b	Comparison between Computed and Observed Sediment Tri+ Concentrations at Mainstem Stations
7-20 c	Comparison between Computed and Observed Tri+ Concentrations at Thompson Island Dam, 1991-1997
7-21	Comparison of Same Day Tri+ Concentration Data by Source at Fort Edward, Stillwater, and Waterford
7-22	Comparison between Model Estimated and Data Estimated In-River Tri+ Loadings from 1977-1997 Stratified by Fort Edward Flow at 10,000 cfs
7-23	Comparison between Computed and Observed Tri+ Concentrations for the Spring 1983 High Flow Event
7-24	Comparison between Computed and Observed Tri+ Concentrations for the Spring 1993 High Flow Event
7-25	Comparison between Computed and Observed Tri+ Concentrations for the Spring 1994 High Flow Event
7-26	Comparison between Computed and Observed Tri+ Concentrations for the Spring 1997 High Flow Event
7-27	Comparison between Computed and Observed Tri+ Concentrations for Fort Edward Flow Less Than 10,000 cfs
7-28	Comparison between Computed and Observed Tri+ Concentrations for at Fort Edward Flow Greater Than 10,000 cfs
7-29	Comparison Between Computed and Observed Probability Distributions for Tri+ at Fort Edward Flow Less Than 10,000 cfs

PHASE 2 REPORT – REVIEW COPY
FURTHER SITE CHARACTERIZATION AND ANALYSIS
Volume 2D – REVISED BASELINE MODELING REPORT
HUDSON RIVER PCBs REASSESSMENT RI/FS

BOOK 1 of 4

LIST OF FIGURES

<u>FIGURE</u>	<u>TITLE</u>
7-30	Comparison Between Computed and Observed Probability Distributions for Tri+ at Fort Edward Flow Greater Than 10,000 cfs
7-31	Computed Tri+ PCB Mass Balance Components Analysis for 1977-1997
7-32	Computed Cumulative Contribution Tri+ Load Gain between Mainstem Hudson River Sampling Stations from 1991 to 1997
7-33	Sediment Responses in Thompson Island Pool to Alternate Solids Loads at Fort Edward
7-34	Sediment Responses in Waterford to Alternative Solids Loads at Fort Edward
7-35	Sediment Responses in Thompson Island Pool to Changes in Tributary Solids Loadings
7-36	Sediment Responses at Waterford to Changes in Tributary Solids Loadings
7-37	Water Column Responses to Changes in Tributary Solids Loadings
7-38	Sediment Responses in Thompson Island Pool to Changes in Tributary Solids Loads due to Specification of Rating Curves
7-39	Sediment Responses at Waterford to Changes in Tributary Solids Loads Due to Specification of Rating Curves
7-40	Water Column Responses to Changes in Tributary Solids Loadings Due to Specification of Rating Curve
7-41	Sediment Responses in Thompson Island Pool to Changes in Partitioning
7-42	Sediment Responses in Waterford Reach to Changes in Partitioning
7-43	Water Column Responses to Changes in Partitioning
7-44	Time Series for Effective Mass Transfer Rate in HUDTOX
7-45	Sediment Responses in Thompson Island Pool to Changes in Sediment-Water Mass Transfer Rate
7-46	Sediment Responses in Waterford Reach to Changes in Sediment-Water Mass Transfer Rate
7-47	Water Column Responses to Changes in Sediment-Water Mass Transfer Rate
7-48	Sediment Responses in Thompson Island Pool to Changes in Cohesive and Non-cohesive Specific Sediment to Water Effective Mass Transfer Rates

PHASE 2 REPORT – REVIEW COPY
FURTHER SITE CHARACTERIZATION AND ANALYSIS
Volume 2D – REVISED BASELINE MODELING REPORT
HUDSON RIVER PCBs REASSESSMENT RI/FS

BOOK 1 of 4

LIST OF FIGURES

<u>FIGURE</u>	<u>TITLE</u>
7-49	Sediment Responses in Waterford to Changes in Cohesive and Non-cohesive Specific Sediment to Water Effective Mass Transfer Rates
7-50	Responses of Burial Rates in Cohesive Sediments to Changes in Gross Settling Velocities
7-51	Responses of Burial Rates in Non-Cohesive Sediments to Changes in Gross Settling Velocities
7-52	Sediment Responses in Thompson Island Pool to Changes in Gross Settling Velocities
7-53	Sediment Responses in Waterford Reach to Changes in Gross Settling Velocities
7-54	Water Column Responses to Changes in Gross Settling Velocities
7-55	Sediment Responses in Schuylerville Reach to Enhanced Mixing (top 6 cm) in Non-cohesive Sediments
7-56	Sediment Responses in Stillwater Reach to Enhanced Mixing (top 6 cm) in Non-cohesive Sediments
7-57	Sediment Responses at Waterford to Enhanced Mixing (top 6 cm) in Non-cohesive Sediments
7-58	Sediment Responses in Federal Dam Reach to Enhanced Mixing (top 6 cm) in Non-cohesive Sediments
7-59	Sediment Responses in Thompson Island Pool to Changes in Sediment Initial Conditions
7-60	Sediment Responses in Waterford to Changes in Sediment Initial Conditions
7-61	Water Column Responses to Changes in Sediment Initial Conditions
7-62	Water Column Responses to Changes in Henry's Law Constant
7-63	Predicted versus Observed BZ#4, BZ#28 and BZ#52 Concentrations Using Historical Calibration Model Parameters
7-64	Comparison between Computed Surficial Sediment Tri+, BZ#28, BZ#52 and BZ#4 Concentrations for Thompson Island Pool
7-65	Predicted versus Observed BZ#4, BZ#28 and BZ#52 Concentrations Using Sediment-Specific Partitioning (from GE Data)

PHASE 2 REPORT – REVIEW COPY
FURTHER SITE CHARACTERIZATION AND ANALYSIS
Volume 2D – REVISED BASELINE MODELING REPORT
HUDSON RIVER PCBs REASSESSMENT RI/FS

BOOK 1 of 4

LIST OF FIGURES

<u>FIGURE</u>	<u>TITLE</u>
7-66 a	Predicted versus Observed BZ#4, BZ#28 and BZ#52 Concentrations Using Sediment-Specific Partitioning (from GE Data) and Particulate and Porewater Sediment-Water Mass Transfer Pathways
7-66 b	Predicted versus Observed BZ#[90+101], BZ#138 and Total PCB Concentrations Using Sediment-Specific Partitioning (from GE Data) and Particulate and Dissolved Sediment-Water Mass Transfer Pathways
7-67 a	Predicted versus Observed BZ#4 Concentrations below Thompson Island Dam, 1991-1993
7-67 b	Predicted versus Observed BZ#28 Concentrations below Thompson Island Dam, 1991-1993
7-67 c	Predicted versus Observed BZ#52 Concentrations below Thompson Island Dam, 1991-1993
7-67 d	Predicted versus Observed BZ#[90+101] Concentrations below Thompson Island Dam, 1991-1993
7-67 e	Predicted versus Observed BZ#138 Concentrations below Thompson Island Dam, 1991-1993
7-67 f	Predicted versus Observed Total PCB Concentrations below Thompson Island Dam, 1991-1993
7-68 a	Comparison of Model versus Observed Congener Concentrations Ratios: Thompson Island Pool, September 25, 1996 Float Study
7-68 b	Comparison of Model versus Observed Congener Concentrations Ratios: Thompson Island Pool, September 26, 1996 Float Study
7-68 c	Comparison of Model versus Observed Congener Concentrations Ratios: Thompson Island Pool, June 4, 1997 Float Study
7-68 d	Comparison of Model versus Observed Congener Concentrations Ratios: Thompson Island Pool, June 17, 1997 Float Study
7-69	Model versus Observed Down-river [BZ#28]/[BX#52] Ratios by Season, 1991-1997
7-70	Model versus Observed Down-river [BZ#28]/[BZ#52] Ratios Stratified by Fort Edward Flow (<10,000 cfs and >10,000 cfs), 1991-1997
8-1	70-Year Hydrograph for the No Action Forecast Simulation: 1998-2067

PHASE 2 REPORT – REVIEW COPY
FURTHER SITE CHARACTERIZATION AND ANALYSIS
Volume 2D – REVISED BASELINE MODELING REPORT
HUDSON RIVER PCBs REASSESSMENT RI/FS

BOOK 1 of 4

LIST OF FIGURES

<u>FIGURE</u>	<u>TITLE</u>
8-2	Observed Total PCB and Tri+ PCB Concentrations at Fort Edward During 1997 and 1998
8-3	Data-Based Estimate of Annual Total and Tri+ PCB Load by Year at Fort Edward, 1991-1997
8-4 a	Forecast Sediment Tri+ Concentrations for Thompson Island Pool with Constant Upstream Tri+ Concentrations at 10 ng/L, 30 ng/L, and 0 ng/L, 1998-2067
8-4 b	Forecast Sediment Tri+ Concentrations for the Schuylerville Reach with Constant Upstream Tri+ Concentrations at 10 ng/L, 30 ng/L, and 0 ng/L, 1998-2067
8-4 c	Forecast Sediment Tri+ Concentrations for the Stillwater Reach with Constant Upstream Tri+ Concentrations at 10 ng/L, 30 ng/L, and 0 ng/L, 1998-2067
8-4 d	Forecast Sediment Tri+ Concentrations for the Waterford Reach with Constant Upstream Tri+ Concentrations at 10 ng/L, 30 ng/L, and 0 ng/L, 1998-2067
8-4 e	Forecast Sediment Tri+ Concentrations for the Federal Dam Reach with Constant Upstream Tri+ Concentrations at 10 ng/L, 30 ng/L, and 0 ng/L, 1998-2067
8-5 a	Predicted Sediment Tri+ Concentrations for Thompson Island Pool with Forecasted Constant Upstream Tri+ Concentration at 10 ng/L
8-5 b	Predicted Sediment Tri+ Concentrations for Schuylerville Reach with Forecasted Constant Upstream Tri+ Concentration at 10 ng/L
8-5 c	Predicted Sediment Tri+ Concentrations for Stillwater Reach with Forecasted Constant Upstream Tri+ Concentration at 10 ng/L
8-5 d	Predicted Sediment Tri+ Concentrations for Waterford Reach with Forecasted Constant Upstream Tri+ Concentration at 10 ng/L
8-5 e	Predicted Sediment Tri+ Concentrations for Federal Dam Reach with Forecasted Constant Upstream Tri+ Concentration at 10 ng/L
8-6 a	Forecast Average Annual Tri+ Concentrations at Thompson Island Dam and Schuylerville with Constant Upstream Concentrations of 10 ng/L, 30 ng/L, and 0 ng/L, Tri+ at Fort Edward, 1998-2067
8-6 b	Forecast Average Annual Tri+ Concentrations at Stillwater and Waterford with Constant Upstream Concentrations of 10 ng/L, 30 ng/L, and 0 ng/L, Tri+ at Fort Edward, 1998-2067

PHASE 2 REPORT – REVIEW COPY
FURTHER SITE CHARACTERIZATION AND ANALYSIS
Volume 2D – REVISED BASELINE MODELING REPORT
HUDSON RIVER PCBs REASSESSMENT RI/FS

BOOK 1 of 4

LIST OF FIGURES

<u>FIGURE</u>	<u>TITLE</u>
8-7 a	Forecast Average Summer Tri+ Concentrations at Thompson Island Dam and Schuylerville with Constant Upstream Concentrations of 10 ng/L, 30 ng/L, and 0 ng/L Tri+ at Fort Edward, 1998-2067
8-7 b	Forecast Average Summer Tri+ Concentrations at Stillwater and Waterford with Constant Upstream Concentrations of 10 ng/L, 30 ng/L, and 0 ng/L Tri+ at Fort Edward, 1998-2067
8-8 a	Predicted Average Annual Water Column Tri+ Concentrations at Thompson Island Dam and Schuylerville with Forecasted Constant Upstream Tri+ Concentration at 10 ng/L,1977-2067
8-8 b	Predicted Average Annual Water Column Tri+ Concentrations at Stillwater and Waterford with Forecasted Constant Upstream Tri+ Concentration at 10 ng/L,1977-2067
8-9 a	No-action Forecast Annual Tri+ Load to the Lower Hudson River with Constant Upstream Concentrations of 10 ng/L, 30 ng/L, and 0 ng/L Tri+ at Fort Edward, 1998-2067
8-9 b	No-action Forecast Cumulative Annual Tri+ Load to the Lower Hudson River with Constant Upstream Concentrations of 10 ng/L, 30 ng/L, and 0 ng/L Tri+ at Fort Edward, 1998-2067
8-10	Adjustment of the Fort Edward Hydrograph to Include the 100 Year Flow (47,330 cfs)
8-11	Predicted 100 Year Event (3/28 to 4/13) Impact on Tri+ PCB Levels at Thompson Island Dam (West)
8-12	Predicted 100 Year Event (3/28 to 4/13) Impact on Tri+ PCB Levels at Federal Dam
8-13	Cumulative Net Increase of Tri+ PCB Mass Loading at Various Locations in the Upper Hudson River Due to the 100 Year Flood Event (versus the No Action Scenario)
8-14 a	Forecast Sediment Tri+ Concentrations for Thompson Island Pool for Alternative Hydrographs (Constant Upstream Tri + Concentration of 10 ng/L) at Fort Edward
8-14 b	Forecast Sediment Tri+ Concentrations for Schuylerville Reach for Alternative Hydrographs (Constant Upstream Tri + Concentration of 10 ng/L) at Fort Edward

PHASE 2 REPORT – REVIEW COPY
FURTHER SITE CHARACTERIZATION AND ANALYSIS
Volume 2D – REVISED BASELINE MODELING REPORT
HUDSON RIVER PCBs REASSESSMENT RI/FS

BOOK 1 of 4

LIST OF FIGURES

<u>FIGURE</u>	<u>TITLE</u>
8-14 c	Forecast Sediment Tri+ Concentrations for the Stillwater Reach for Alternative Hydrographs (Constant Upstream Tri + Concentration of 10 ng/L) at Fort Edward
8-14 d	Forecast Sediment Tri+ Concentrations for the Waterford Reach for Alternative Hydrographs (Constant Upstream Tri + Concentration of 10 ng/L) at Fort Edward
8-14 e	Forecast Sediment Tri+ Concentrations for the Federal Dam Reach for Alternative Hydrographs (Constant Upstream Tri + Concentration of 10 ng/L) at Fort Edward
8-15 a	Forecast Annual Average Tri+ Concentrations at Thompson Island Dam and Schuylerville for Alternative Hydrographs (Constant Upstream Tri + Concentration of 10 ng/L at Fort Edward), 1998-2067
8-15 b	Forecast Annual Average Tri+ Concentrations at Stillwater and Waterford for Alternative Hydrographs (Constant Upstream Tri + Concentration of 10 ng/L at Fort Edward), 1998-2067
8-16	Sensitivity of Thompson Island Pool Surface Sediment Tri+ Concentrations to an Alternative Total Suspended Solids Load at Fort Edward, 1998-2047
8-17 a	Sensitivity of Thompson Island Pool Surface Sediment Tri+ Concentrations to Changes in External Tributary Solids Loadings, 1998-2067
8-17 b	Sensitivity of Thompson Island Dam to Schuylerville Surface Sediment Tri+ Concentrations to Changes in External Tributary Solids Loadings, 1998-2067
8-17 c	Sensitivity of Schuylerville to Stillwater Surface Sediment Tri+ Concentrations to Changes in External Tributary Solids Loadings, 1998-2067
8-17 d	Sensitivity of Stillwater to Waterford Surface Sediment Tri+ Concentrations to Changes in External Tributary Solids Loadings, 1998-2067
8-17 e	Sensitivity of Waterford to Federal Dam Surface Sediment Tri+ Concentrations to Changes in External Tributary Solids Loadings, 1998-2067
8-18 a	Sensitivity of Thompson Island Pool Surface Sediment Tri+ Concentrations to Enhanced Mixing (top 6cm) in Non-Cohesive Sediments, 1998-2067
8-18 b	Sensitivity of Thompson Island Dam to Schuylerville Surface Sediment Tri+ Concentrations to Enhanced Mixing (top 6cm) in Non-Cohesive Sediments, 1998-2067
8-18 c	Sensitivity of Schuylerville to Stillwater Surface Sediment Tri+ Concentrations to Enhanced Mixing (top 6cm) in Non-Cohesive Sediments, 1998-2067

PHASE 2 REPORT – REVIEW COPY
FURTHER SITE CHARACTERIZATION AND ANALYSIS
Volume 2D – REVISED BASELINE MODELING REPORT
HUDSON RIVER PCBs REASSESSMENT RI/FS

BOOK 1 of 4

LIST OF FIGURES

<u>FIGURE</u>	<u>TITLE</u>
8-18 d	Sensitivity of Stillwater to Waterford Surface Sediment Tri+ Concentrations to Enhanced Mixing (top 6cm) in Non-Cohesive Sediments, 1998-2067
8-18 e	Sensitivity of Waterford to Federal Dam Surface Sediment Tri+ Concentrations to Enhanced Mixing (top 6cm) in Non-Cohesive Sediments, 1998-2067
8-19	Sensitivity of Tri+ Concentrations at Stillwater to Enhanced Mixing (top 6 cm) in Non-cohesive Sediments, 1998-2067
8-20 a	Sensitivity of Thompson Island Pool Surface Sediment Tri+ Concentrations to Specification of Sediment Initial Conditions, 1998-2067
8-20 b	Sensitivity of Schuylerville Reach Surface Sediment Tri+ Concentrations to Specification of Sediment Initial Conditions, 1998-2067
8-20 c	Sensitivity of Stillwater Reach Surface Sediment Tri+ Concentrations to Specification of Sediment Initial Conditions, 1998-2067
8-20 d	Sensitivity of Waterford Reach Surface Sediment Tri+ Concentrations to Specification of Sediment Initial Conditions, 1998-2067
8-20 e	Sensitivity of Federal Dam Reach Surface Sediment Tri+ Concentrations to Specification of Sediment Initial Conditions, 1998-2067
8-21 a	Sensitivity of Forecasted Average Annual Tri+ Concentrations to Specification of Initial Conditions at Thompson Island Dam and Schuylerville, 1998-2067
8-21 b	Sensitivity of Forecasted Average Annual Tri+ Concentrations to Specification of Initial Conditions at Stillwater and Waterford, 1998-2067
9-1	HUDTOX Validation: Comparison of Predicted and Observed Thompson Island Dam Tri+ Concentrations
9-2	HUDTOX Validation: Comparison of Predicted and Observed Schuylerville Tri+ Concentrations
9-3	HUDTOX Validation: Predicted versus Observed Tri+ Concentrations at Thompson Island Dam and Schuylerville
9-4	Monthly Average Scatter Plots of Observed Data and Model Output at Thompson Island Dam, 1998-1999
9-5	Monthly Average Scatter Plots of Observed Data and Model Output at Schuylerville, 1998-1999

GLOSSARY

BAF	Biota Accumulation Factor
Bayesian updating	calibration procedure based on conditional probability in Bayes Rule (optimizes predicted distribution based on observed distribution).
BMR	Baseline Modeling Report
BSRE	Beale's Stratified Ratio Estimator
BURE	Beale's Unstratified Ratio Estimator
CEAM	Center for Exposure Assessment Modeling
CD-ROM	Compact Disc - Read Only Memory
cfs	Cubic feet per second
cm	Centimeter
Corp.	Corporation
DAR	Drainage Area Ratio
deg. C	Degree Celsius
DEIR	Data Evaluation and Interpretation Report
DOC	Dissolved Organic Carbon
DOSM	Depth of Scour Model
e.g.	For example
et al.	and others
FA	Flow Average (Phase 2 Water Column Monitoring Program)
FEMA	Federal Emergency Management Agency
foc	Fraction organic carbon
fps	Feet per second
g	Gram
GBTOX	Green Bay Toxic Chemical Model
GE	General Electric
GIS	Geographic Information System
GLI	Great Lake Initiative
HEC-2	US Army Corps of Engineers, Hydraulic Engineering Center, Surface Water Profile Model
HOC	Hydrophobic Organic Chemicals
HUDTOX	Hudson River Toxic Chemical Model
i.e.	That is
IADN	Integrated Atmospheric Deposition Network
kg	Kilogram
LDEO	Lamont-Doherty Earth Observatory
Likelihood profile	maximum likelihood estimation technique to determine parameters of prior and posterior distributions
LRC	Low Resolution Sediment Coring Report
m/s	Meters per second
mg/l	Milligrams per liter
mi ²	Square miles
MT	Metric Ton
MVUE	Minimum Variance Unbiased Estimator
NAPL	Non-aqueous Phase Liquid
NPDES	National Pollutant Discharge Elimination System

ng/m ³	Nanograms per cubic meter
ng/l	Nanograms per liter
NGVD	National Geodetic Vertical Datum
NOAA	National Oceanic and Atmospheric Administration
NWS	National Weather Service
NYSDEC	New York State Department of Environmental Conservation
NYSDOH	New York State Department of Health
NYSDOT	New York State Department of Transportation
OC	Organic Carbon
PCBs	Polychlorinated Biphenyls
PMCR	Preliminary Model Calibration Report
Posterior distribution	optimized input distribution based on Bayesian updating calibration procedure; revised prior distribution
Prior distribution	empirical or likelihood-function-based probability distribution initially specified in FISHRAND before implementing any calibration procedure; "best guess"
RBMR	Revised Baseline Modeling Report
RMA-2V	Thompson Island Pool Hydrodynamic Model
ROD	Record of Decision
RPI	Rensselaer Polytechnic Institute
SS	Suspended Solids
TID	Thompson Island Dam
TIN	Triangulated Irregular Network
TIP	Thompson Island Pool
TSCA	Toxic Substances Control Act
TSF (tsf)	Temperature slope factor
TSS	Total Suspended Solids
ug/g (ppm)	Micrograms per gram (parts per million)
ug/L	Micrograms per liter
USACE	United States Army Corps of Engineers
USEPA	United States Environmental Protection Agency
USGS	United States Geological Survey
WASP5	(USEPA) Water Quality Analysis Simulation Program, Version 4
TOXI5	Toxic Chemical Module in WASP5
WY	Water year

EXECUTIVE SUMMARY
REVISED BASELINE MODELING REPORT
JANUARY 2000

This report presents results and findings from the application of mathematical models for PCB physical/chemical transport and fate, as well as PCB bioaccumulation in the Upper Hudson River. The modeling effort for the Hudson River PCBs site Reassessment has been designed to predict future levels of PCBs in Upper Hudson River sediment, water and fish. This report provides predictions under baseline conditions, that is, without remediation of PCB-contaminated sediment in the Upper Hudson River (equivalent to a No Action scenario). The predicted sediment, water and fish PCB concentrations from the models are used as inputs in the Human Health and Ecological Risk Assessments. Subsequently, the models will be used in the Feasibility Study (the Phase 3 Report) to help evaluate and compare the effectiveness of various remedial scenarios.

The Revised Baseline Modeling Report (RBMR or Revised BMR) incorporates changes to the May 1999 Baseline Modeling Report (BMR) based on public comments and additional analyses, and supercedes the May 1999 report. The Revised BMR consists of four books. Books 1 and 2 are on the transport and fate models, with Book 1 containing the report text and Book 2 containing the corresponding tables, figures and plates. Similarly, Books 3 and 4 are on the bioaccumulation models, with Book 3 containing the report text and Book 4 containing the corresponding tables, figures and plates. Predictions of future PCB concentrations in sediment and water from the transport and fate models are used as input values for the bioaccumulation models. The bioaccumulation models forecast PCB concentrations in various fish species based on these inputs.

MODELING OBJECTIVES

The overall goal of the modeling is to develop scientifically credible models capable of answering the following principal questions:

- When will PCB levels in fish populations recover to levels meeting human health and ecological risk criteria under continued No Action?
- Can remedies other than No Action significantly shorten the time required to achieve acceptable risk levels?
- Are there contaminated sediments now buried that are likely to become “reactivated” following a major flood, possibly resulting in an increase in contamination of the fish population?

The work presented in this Revised BMR provides information relevant to the first and third questions. Forecasts regarding the potential impacts of various remedial scenarios, thus addressing the second question, will be presented in the Feasibility Study (the Phase 3 Report).

MODEL DEVELOPMENT

A large body of information from site-specific field measurements (documented in Hudson River Database Release 4.1), laboratory experiments and the scientific literature was synthesized within the models to develop the PCB transport and fate and the PCB bioaccumulation models. Data from numerous sources were utilized including USEPA, the New York State Department of Environmental Conservation, the National Oceanic and Atmospheric Administration, the US Geological Survey and the General Electric Company.

The proposed modeling approach and preliminary demonstrations of model outputs were made available for public review in the Preliminary Model Calibration Report (PMCR), which was issued in October 1996. The modeling framework of the PMCR was revised based on a peer review and public comment, as well as the incorporation of additional data. The baseline modeling effort and results were documented in the Baseline Modeling Report (BMR) issued in May 1999. USEPA decided to revise the BMR to reflect changes to the models based on public comment and additional analyses that were conducted. The Revised BMR includes model refinements, additional years of data, longer model forecasts, validation to an independent dataset, and additional model sensitivity analyses. This Revised BMR supercedes the May 1999 BMR.

Transport and Fate Models

HUDTOX - The backbone of the modeling effort is the Upper Hudson River Toxic Chemical Model (HUDTOX). HUDTOX was developed to simulate PCB transport and fate for 40 miles of the Upper Hudson River from Fort Edward to Troy, New York. HUDTOX is a transport and fate model, which is based on the principle of conservation of mass. The fate and transport model simulates PCBs in the water column and sediment bed, but not in fish. It balances inputs, outputs and internal sources and sinks for the Upper Hudson River. Mass balances are constructed first for water, then solids and bottom sediment, and finally PCBs. External inputs of water, solids loads and PCB loads, plus values for many internal model coefficients, were specified from field observations. Once inputs are specified, the remaining internal model parameters are calibrated so that concentrations computed by the model agree with field observations. Model calculations of forecasted PCB concentrations in water and sediment from HUDTOX are used as inputs for the forecasts of the bioaccumulation models (as described in Books 3 and 4).

Depth of Scour Model (DOSM) - The Depth of Scour Model was principally developed to provide spatially-refined information on sediment erosion depths in response to high-flow events such as a 100-year peak flow. The DOSM is a two-dimensional, sediment erosion model that was applied to the Thompson Island Pool. The Thompson Island Pool is characterized by high levels of PCBs in the cohesive sediments. DOSM is linked with a hydrodynamic model that predicts the velocity and shear stress (force of the water acting on the sediment surface) during high flows. There is also a linkage between the

DOSM and HUDTOX. Relationships between river flow and cohesive sediment resuspension were developed using the DOSM for a range of flows below the 100-year peak flow. These relationships were used in the HUDTOX model for representing flow-dependent resuspension.

Bioaccumulation Models

Three separate bioaccumulation models were developed in a sequential manner, beginning with a simple, data-driven empirical approach (Bivariate BAF Analysis), followed by a probabilistic food chain model, and ending with a time-varying, mechanistic approach (FISHRAND). The three approaches are complementary, with each progressively more complex model building on the results of the preceding, simpler effort. All three bioaccumulation models are presented in the Revised BMR; however, the FISHRAND model is the final bioaccumulation model that is used to predict future fish PCB body burdens.

Bivariate BAF Analysis - The Bivariate BAF (Bioaccumulation Factor) Analysis is a simple empirical approach that draws on the wealth of historical PCB data for the Hudson River to relate PCB levels in water and sediments (two variables, or “bivariate”) to observed PCB levels in fish. This analysis is useful in understanding the relative importance of water and sediment sources on particular species of fish. As this empirical approach does not describe causal relationships, the analysis has limited predictive capabilities and accordingly was not used for forecasts.

Empirical Probabilistic Food Chain Model - The Empirical Probabilistic Food Chain Model is a more sophisticated representation of the steady-state relationships between fish body burdens and PCB exposure concentrations in water and sediments. The model combines information from available PCB exposure measurements with knowledge about the ecology of different fish species and the food chain relationships among larger fish, smaller fish, and invertebrates in the water column and sediments. The Probabilistic Model provides information on the expected range of uncertainty and variability associated with the estimates of average fish body burdens.

(FISHRAND) Mechanistic Time-Varying Model - The FISHRAND model is based on the peer-reviewed uptake model developed by Gobas (1993 and 1995) and provides a mechanistic, process-based, time-varying representation of PCB bioaccumulation. This is the same form of the model that was used to develop criteria under the Great Lakes Initiative (USEPA, 1995). The FISHRAND model incorporates distributions instead of point estimates for input parameters, and calculates distributions of fish body burdens from which particular point estimates can be obtained, for example, the median, average, or 95th percentile. FISHRAND was used to predict the future fish PCB body burdens for the Human Health and Ecological Risk Assessments.

MODEL CALIBRATION

The principal HUDTOX application was a long-term historical calibration for a 21-year period from 1977 through 1997. Consistent with the Reassessment principal questions, emphasis was placed on calibration of the model to long-term trends in sediment and water column PCB concentrations. However, a short-term hindcast calibration test was also conducted from 1991 to 1997 to establish model performance for certain individual PCB congeners.

Model applications included mass balances for seven different PCB forms: total PCBs, Tri+, and five individual PCB congeners (BZ#4, BZ#28, BZ#52, BZ#[90+101] and BZ#138). Total PCBs represents the sum of all measured PCB congeners and represents the entire PCB mass. Tri+ represents the sum of the trichloro- through decachlorobiphenyl homologue groups. Use of Tri+ as the historical calibration parameter allows for the comparison of data that were analyzed by congener-specific methods with data analyzed by packed-column methods (that did not separate the various PCBs as well and did not measure many of the mono- and dichlorobiphenyls). Therefore, use of the operationally defined Tri+ term allows for a consistent basis for comparison over the entire period for which historical data were available. Tri+ is also a good representation of the PCBs that bioaccumulate in fish.

The five PCB congeners were selected for model calibration based primarily on their physical-chemical properties and frequencies of detection in environmental samples across different media. These individual congener simulations help provide a better understanding of the environmental processes controlling PCB dynamics in the river by testing the model with PCBs with widely varying properties. BZ#4 is a dichloro congener that represents a final product of PCB dechlorination in the sediments. BZ#28 is a trichloro congener that has similar physical-chemical properties to Tri+. BZ#52 is a tetrachloro congener that was selected because of its resistance to degradation and based on its presence in Aroclor 1242, the main Aroclor used by General Electric at the Hudson River capacitor plants. BZ#[90+101] (a pentachloro congener) and BZ#138 (a hexachloro congener) represent higher-chlorinated congeners that strongly partition to solids in the river and bioaccumulate in fish.

The HUDTOX model calibration strategy can be considered minimal and conservative. It is minimal in that external inputs and internal model parameters were determined independently to the fullest extent possible from site-specific data and only a minimal number of parameters were adjusted during model calibration. It is conservative in that parameters determined through model calibration were held spatially and temporally constant unless there was supporting information to the contrary. Consistent with the Reassessment principal questions, emphasis was placed on calibration to long-term trends in sediment and water column PCB concentrations, not short transient changes or localized variations.

The 21-year historical calibration for Tri+ served as the main development vehicle for the PCB fate and transport model used in the Reassessment. This calibration was successful in reproducing observed long-term trends in water and sediment PCB concentrations over

the 21-year period. This was primarily demonstrated through comparisons between model results and available data for long-term Tri+ surface sediment concentrations, in-river solids and Tri+ mass transport at low and high flows, and water column solids and Tri+ concentrations. Many different metrics were used collectively in a “weight of evidence” approach to demonstrate model reliability.

The calibration of the FISHRAND model was conducted by a process known as Bayesian updating. This approach optimizes the agreement between predicted distributions of fish concentrations from the FISHRAND model as compared to empirical distributions based on the data by adjusting three input distributions (percent lipid in fish, total organic carbon in sediment, and the octanol-water partition coefficient or K_{ow}). Initial input distributions (referred to as prior distributions) are specified based on site-specific data and values from the published scientific literature. The model is run and calculates the likelihood of obtaining an output distribution that matches observed measurements given the input distribution. The prior input distributions are then adjusted (within constraints of the data) and these adjusted distributions are referred to as posterior distributions. The focus of the calibration was on the wet weight concentrations (as opposed to the lipid-normalized concentrations) because the wet weight concentrations are generally of primary interest to USEPA and other regulators, the lipid content of any given fish is difficult to predict, and the model predicts fish body burdens on a wet weight basis and then lipid-normalizes. It was determined that, overall, the FISHRAND model predicts wet weight Tri+ PCB fish body burdens to within a factor of two, and typically significantly less than that.

MODEL VALIDATION

Model validation is the comparison of model output to observed data for a dataset that was not included in the calibration of the model. A HUDTOX model validation was conducted to compare predicted and observed water column concentrations for Tri+ using a dataset acquired in 1998 for the Upper Hudson River by General Electric. Results indicated good agreement at both Thompson Island Dam and Schuylerville over an entire year, spanning a range of environmental conditions in the river. The validation was judged successful and it enhances the credibility of the model as a predictive tool.

Several approaches were used to validate the FISHRAND model. One method was to calibrate FISHRAND for one river mile, and then to run the model for a different river mile. Satisfactory agreement for both river miles implied model validity across locations in the Hudson River. In addition, a calibration was conducted using only part of the available dataset, and then the model results were compared with the remaining portion of the dataset. The posterior distributions obtained using only the partial dataset were compared to the posterior distributions obtained using the full dataset. Finally, the partial-data calibrated model was run for the forecast period and these results compared to the full-data calibrated model results. Good agreement across all three metrics implied confidence in the performance of the model.

MODEL FORECAST

In the Revised BMR, the HUDTOX model was run for a 70-year forecast period from 1998 through 2067 for Tri+. The forecast period was lengthened from the 21-year forecast in the May 1999 BMR for two reasons. First, the fish body burdens attained for the 21-year forecast presented risks and hazards above levels of concern as documented in the risk assessments (*i.e.*, the 21-year forecast was too short to predict when PCB concentrations in fish would decrease below levels of concern). Second, the 70-year forecast period was selected in order to provide exposure concentrations that can be used directly in the Monte Carlo analysis in the Human Health Risk Assessment. Tri+ was simulated because it reflects PCB congeners that bioaccumulate in fish and hence are key to the risk assessment.

In order to conduct forecast simulations with the HUDTOX model, it was necessary to specify future conditions in the Upper Hudson River for flows, solids loads, and upstream Tri+ loads. These model inputs are not easily predicted (similar to predicting the future weather), but reasonable estimates were made based on historical observations and current information regarding PCB loading trends.

The baseline forecast simulation was run for an assumed constant Tri+ concentration of 10 ng/L at the model's upstream boundary at Fort Edward. This level represented the annual average Tri+ concentration that was observed in 1997 and assumes that there will be no future load increases or reductions from upstream sources. In particular, it also assumes that the PCB migration from the GE Hudson Falls Plant site would not increase or decrease and that there would not be any type of event similar to the releases that occurred with the partial failure of the Allen Mill gate structure in 1991. Recognizing the uncertainty in this upstream load, model sensitivity runs were conducted for an assumed Tri+ concentration of zero (0 ng/L) to represent a lower bound on future loads due to the implementation of remedial measures upstream, and for an assumed concentration of 30 ng/L to reflect increased loads similar to observations in 1998.

Results from 70-year forecast simulations contain inherent uncertainty due to uncertainties in estimating future flow and solids loading conditions. Furthermore, various model input assumptions, while less influential in 21-year simulations, can become more important in 70-year forecast simulations. This uncertainty can be assessed and accounted for in USEPA's decision making by evaluating predictions across a range of alternate scenarios for these inputs. For this reason, model sensitivity runs were also conducted for three additional hydrologic conditions: plus/minus 50 percent changes in future tributary solids loads, a different assumption for the depth of particle mixing in the surface sediments, and different starting concentrations for Tri+ in the sediments.

Risk-based target levels for fish PCB body burdens have not yet been established. In the Feasibility Study, site-specific target levels to be protective of human health and the environment will be developed from the risk assessments. However, it is beneficial at this time to compare forecasted fish PCB levels against example target levels as a matter of perspective. The target levels used for this analysis provide several concentrations spanning two orders-of-magnitude. Again, these are not endorsements of these values for

decision making. Appropriate values will be developed in the Feasibility Study for the site.

MAJOR FINDINGS

The primary objective of the modeling effort is to construct a scientifically credible tool to help in the understanding of PCB transport and fate and bioaccumulation in the Upper Hudson River, and to use that tool for making forecasts of what will happen in the future. As such, one of the major findings was that it was possible to construct models that simulate conditions that match the observed data reasonably well. Consequently, the model predictions can be reliably used to evaluate future ecological and human health risks and to assess the relative time it takes for the river to recover under various remedial scenarios.

There are numerous general observations about the river that are apparent from the mass balance exercises. Some important observations that impact the understanding of the system include:

- The river is net depositional for solids in Thompson Island Pool, and apparently also in downstream reaches;
- Solids loads are dominated by tributary inputs;
- PCB (Tri+) loads to the water column are dominated by sediment to water mass transfer under non-scouring flow conditions; and,
- Water column and PCB (Tri+) surface sediment concentrations are gradually declining due to reduced input loads and natural attenuation.

Beyond the general observations above, the model forecasts provide the following findings regarding PCBs in the Upper Hudson River. It should be noted that the findings below are made based on the evaluation of Tri+, and that some of the findings may differ for other mixtures of PCBs, such as total PCBs or individual congeners.

1. PCB (Tri+) concentrations in the surface sediment are forecasted to decline at annual rates of approximately 7 to 9 percent over the next two decades, consistent with long-term historical trends.
2. PCB (Tri+) loads from upstream of the model boundary at Fort Edward control the long-term responses of PCB (Tri+) concentrations in the water column and surface sediments, and accordingly, body burdens in fish.
 - For the first two to three decades of the model forecast, depending on location, the in-place PCB (Tri+) reservoir in the sediments and sediment-water transfer processes control responses of surface sediment concentrations.
 - Water column PCB (Tri+) concentrations are increasingly controlled by the upstream boundary at Fort Edward over the long term. The rate at which water

column concentrations approach an asymptote depends upon the assumed magnitude of the upstream boundary load and location within the river.

3. Forecasted surface sediment PCB (Tri+) concentrations in several localized areas in the Stillwater reach and the Thompson Island Pool increase after 40 to 50 years, despite exponential-type decreases up to that time. These computed increases are due to relatively small annual erosion rates that eventually, over an extended length of time, expose PCB concentrations that were previously at depth.
 - The relative magnitudes of computed increases in surface sediment PCB (Tri+) concentrations are small within the context of long-term trends in historical concentrations.
 - The occurrence, magnitude and timing of these computed increases are dependent on forecast assumptions.
 - It is reasonable to assume that localized erosion occurs within the river, but at scales smaller than the spatial scale of the model. Therefore, the model may not accurately reflect the areal extent of such erosion or its timing.
4. Results of the 100-year peak flow show that a flood of this magnitude would result in only a small additional increase in sediment erosion beyond what might be expected for a reasonable range of annual peak flows.
 - The small sediment scour depths produced by the 100-year peak flow result in only very small increases in surface sediment PCB (Tri+) concentrations. These increases decline to values in the base forecast simulation (without the 100-year peak flow) in approximately four years.
 - Increases in water column PCB (Tri+) concentrations in response to a 100-year peak flow are very short-lived (on the order of weeks) and decline rapidly after occurrence of the event.
 - The 100-year event causes an increase of less than 30 kg (70 lbs) in cumulative PCB (Tri+) mass loading across the Thompson Island Dam by the end of the first year of the forecast. This increase represents approximately 13 percent of the average annual PCB (Tri+) mass loading across Thompson Island Dam during the 1990's.
5. The FISHRAND model results for the 70-year forecasts show that predicted wet weight PCB (Tri+) fish body burdens asymptotically approach steady-state concentrations. These concentrations are species-specific, depending on the relative influence of sediment versus water sources, and reflect the upstream boundary assumption. That is, the asymptotic value is lowest for the 0 ng/L upstream boundary condition and approximately an order of magnitude higher for the 10 ng/L upstream boundary condition. Under the 30 ng/L upstream boundary condition, the asymptotic value is approximately a factor of five higher than the 10 ng/L result.

6. FISHRAND model results show that PCB (Tri+) uptake in fish is predominantly attributable to dietary sources, with a smaller contribution from direct water uptake. Analysis of relative sediment and water contributions within the food chain yielded the following results. Brown bullhead are most sensitive to changes in sediment concentration and not very sensitive to changes in water concentration; largemouth bass are more sensitive to sediment concentrations than to water concentrations, but water plays a larger role than for brown bullhead; yellow perch are driven primarily by the water; white perch show greater sensitivity to sediment; and pumpkinseed and spottail shiner are sensitive to small changes in water concentration.
7. The time it takes to attain acceptable target levels in fish tissue is greatly dependent upon the target level selected. Target levels will be selected as part of the Feasibility Study for the site.

SUMMATION

The modeling effort for the Reassessment has provided USEPA with valuable insights regarding factors that control transport and fate and bioaccumulation of PCBs in the Upper Hudson River. Forecasted responses of water column and surface sediment PCB (Tri+) concentrations in the Upper Hudson River, as calculated by HUDTOX, are sensitive to changes in hydrology, solids loadings, sediment particle mixing depth and sediment initial conditions. Forecasted responses of fish body burdens using the FISHRAND model are sensitive to changes in lipid content of fish, total organic carbon in sediment, and the octanol-water partitioning coefficient (K_{ow}).

The models are useful tools for forecasting future sediment, water and fish PCB concentrations. The forecasts can be reliably used to evaluate future ecological and human health risks and to assess the relative time it takes for the river to recover under various remedial scenarios.

1. INTRODUCTION

1.1 PURPOSE OF REPORT

This volume is the fourth in a series of reports describing the results of the Phase 2 investigation of Hudson River sediment polychlorinated biphenyls (PCB) contamination. This investigation is being conducted under the direction of the U.S. Environmental Protection Agency (USEPA). This investigation is part of a three phase remedial investigation and feasibility study intended to reassess the 1984 No Action decision of the USEPA concerning sediments contaminated with PCBs in the Upper Hudson River. Figure 1-1 contains a location map for the Hudson River watershed. For purposes of the Reassessment, the area of the Upper Hudson River considered for remediation is defined as the river bed between the Fenimore Bridge at Hudson Falls (just south of Glens Falls) and Federal Dam at Troy, New York (Figure 1-2).

In December 1990, USEPA issued a Scope of Work for reassessing the No Action decision for the Hudson River PCB Site. The scope of work identified three phases:

- Phase 1 – Interim Characterization and Evaluation
- Phase 2 – Further Site Characterization and Analysis
- Phase 3 – Feasibility Study

The Phase 1 Report (USEPA, 1991) is Volume 1 of the Reassessment documentation and was issued by USEPA in August 1991. It contains a compendium of background material, discussion of findings and preliminary assessment of risks.

The Final Phase 2 Work Plan and Sampling Plan (USEPA, 1992) detailed the following main data collection tasks to be completed during Phase 2:

- High- and low-resolution sediment coring;
- Geophysical surveying and confirmatory sampling;
- Water column sampling (including transects and flow-averaged composites); and,
- Ecological field program.

The data available from the Phase 2 investigation and other historical datasets are documented in the Database Report (Volume 2A in the Phase 2 series of reports; (USEPA, 1995) and accompanying CD-ROM database. This database provides the validated data for the Phase 2 investigation. This Revised Baseline Modeling Report (RBMR or Revised BMR) utilized the Hudson River Database, Release 4.1b, which was updated in Fall 1998 (USEPA, 1998b).

This Revised Baseline Modeling Report is Volume 2D of the Reassessment documentation. It presents results and findings from application of mathematical models for PCB transport and fate, and PCB bioaccumulation in the Upper Hudson River.

There were two modeling reports preceding this RBMR in the Reassessment documentation. The Preliminary Model Calibration Report (USEPA, 1996) was issued for public review in October 1996. The purpose of the PMCR was to document the conceptual approaches, databases and preliminary calibration results for the transport and fate, and bioaccumulation models. The PMCR did not contain results for any forecast simulations with the preliminary models. The modeling approaches in the PMCR were reviewed by an independent peer review panel in September 1998. The modeling approaches were revised in response to comments from the peer review panel and from the public. The Baseline Modeling Report (USEPA, 1999c) was issued for public review in May 1999. The BMR contained model refinements recommended by reviewers, results from a long-term historical calibration of the transport and fate and bioaccumulation models, and results from forecast simulations designed to estimate long-term responses to continued No Action and impacts due to a 100-year peak flow. USEPA decided to revise the BMR to reflect changes in the models based on public comment and additional analyses that were conducted. The Revised BMR supercedes the May 1999 BMR.

The purpose of this Revised Baseline Modeling Report is to document:

- Additional model refinements;
- Sensitivity of the historical calibration;
- Model validation to an independent dataset;
- Longer (70-year) model forecasts for continued No Action; and,
- Sensitivity of forecast simulations for continued No Action.

1.2 REPORT FORMAT AND ORGANIZATION

The information gathered and the findings of this phase are presented here in a format that is focused on answering questions critical to the Reassessment, rather than report results strictly according to Work Plan tasks. In particular, results are presented in a way that facilitates input to other aspects of the projects.

This report is presented in four books. Books 1 and 2 contain results and findings from the PCB transport and fate models. Book 1 contains the report text and Book 2 contains all tables, figures and plates for the transport and fate models. Books 3 and 4 contain results and findings from the PCB bioaccumulation models. Book 3 contains the report text and Book 4 contains all tables, figures and plates for the bioaccumulation models.

Books 1 and 2 contain results and findings for applications of PCB transport and fate models to existing historical data, and for forecast simulations designed to estimate both long-term responses to continued No Action and impacts due to a 100-year peak flow. Books 1 and 2 chapters are as follows:

- Chapter 1 herein provides the report introduction;

- Chapter 2 presents the overall conceptual approach used for the mathematical models and the relationships among individual models;
- Chapter 3 presents the hydrodynamic model used for Thompson Island Pool (TIP);
- Chapter 4 presents the Depth of Scour Model (DOSM) used to estimate masses of solids and PCBs eroded from cohesive and non-cohesive sediment areas in Thompson Island Pool (TIP) in response to peak flows;
- Chapter 5 presents the development of the Hudson River Toxic Chemical Model (HUDTOX) including conceptual framework, governing equations and spatial-temporal scales;
- Chapter 6 presents results from data synthesis tasks necessary to provide model inputs and to support processing and interpretation of model output;
- Chapter 7 presents results and findings from calibration of the HUDTOX model to historical data, including data collected as part of the USEPA Phase 2 investigation;
- Chapter 8 presents results and findings from forecast simulations with the HUDTOX model designed to estimate long-term responses to continued No Action and impacts due to a 100-year peak flow; and,
- Chapter 9 presents results from a model validation simulation using an independent dataset acquired in 1998 by General Electric.

1.3 PROJECT BACKGROUND

1.3.1 Site Description

The Hudson River PCBs Superfund site encompasses the Hudson River from Hudson Falls (river mile [RM] 198) to the Battery in New York Harbor (RM 0), a river distance of nearly 200 miles. Because of different physical and hydrologic regimes, approximately 40 miles of the Upper Hudson River, from Hudson Falls to Federal Dam (RM 153.9), is distinguished from the Lower Hudson River below Federal Dam. Emphasis was placed on Thompson Island Pool (TIP), a 6-mile portion of the river between Fort Edward and Thompson Island Dam (TID) (Figure 1-3), because a substantial amount of PCB-contaminated sediment is contained in this location.

1.3.2 Site History

Over a 30-year period ending in 1977, two General Electric (GE) facilities, one in Fort Edward and the other in Hudson Falls, NY, used PCBs in the manufacture of electrical capacitors. Various sources have estimated that between 209,000 and 1,300,000 pounds (95,000 to 590,000 kilograms [kg]) of PCBs were discharged between 1957 and 1975 from these two GE facilities (Sofaer, 1976; Limburg, 1984). Discharges resulted from washing PCB-containing capacitors and PCB

spills. Untreated washings are believed to have been discharged directly into the Hudson from about 1951 through 1973 (Brown et al., 1984). No records exist on which to base estimates of discharges from the beginning of PCB capacitor manufacturing operations in 1946 to 1956; however, discharges during this period are believed to be less than in subsequent years. Discharges after 1956 have been estimated at about 30 pounds (14 kg) per day or about 11,000 pounds (5,000 kg) per year (Bopp, 1979, citing 1976 litigation; Limburg, 1984, citing Sofaer, 1976). In 1977, manufacture and sale of PCBs within the U.S. was stopped under provisions of the Toxic Substances Control Act (TSCA). PCB use ceased at the GE facilities in 1975 and only minor discharges (about 0.5 kg/day or less [Brown et al., 1984; Bopp, 1979]) are believed to have occurred during facility shutdown and cleanup operations through mid-1977 when active discharges ceased. GE had been granted a National Pollutant Discharge Elimination System (NPDES) permit allowing up to 30 lbs/day to be discharged during this period (Sanders, 1989). According to scientists at GE, at least 80 percent of the total PCBs discharged are believed to have been Aroclor 1242, with lesser amounts of Aroclors 1254, 1221 and 1016 (USEPA, 1997).

A significant portion of the PCBs discharged to the river adhered to suspended particulates and subsequently accumulated downstream in bottom sediments as they settled in the impounded pool behind the former Fort Edward Dam (RM 194.8), as well as in other impoundments farther downstream. Because of the proximity to the GE discharges, sediments behind the Fort Edward Dam were probably among the most contaminated to be found in the Hudson, although this was not well known in the 1970s. The Fort Edward Dam was removed in 1973 because of its deteriorating condition. During subsequent spring floods, the highly contaminated sediments trapped behind the Fort Edward Dam were scoured and transported downstream. Substantial portions of these sediments were stored in relatively quiescent areas of the river. These areas, which were surveyed by New York State Department of Environmental Conservation (NYSDEC) in 1976 to 1978 and 1984, have been described as PCB “hotspots”. Exposed sediments from the former pool remaining behind the dam site, called the “remnant deposits”, have been the subject of several remedial efforts.

PCB releases from the GE Hudson Falls Plant site near the Bakers Falls Dam have also occurred through migration of PCB oil through bedrock. The extent and magnitude of these releases are not well quantified. This release through bedrock continued until at least 1996, when remedial activities by GE brought the leakage under better control. Despite some evidence for its existence prior to 1991 based on U.S. Geological Survey (USGS) data, this leakage was not identified until the partial failure of the abandoned Allen Mill gate structure near the GE Hudson Falls plant site in 1991. This failure caused a large release of what were probably PCB-bearing oils and sediments that had accumulated within the structure. This failure also served to augment PCB migration from the bedrock beneath the plant to the river until remedial measures by GE over the period 1993 to 1997 greatly reduced the release rate. A more in-depth discussion of PCB sources is contained in the Data Evaluation and Interpretation Report (DEIR) (USEPA, 1997).

1.4 MODELING GOALS AND OBJECTIVES

The goal of the PCB transport, fate and bioaccumulation modeling was to assist in answering the following principal Reassessment questions:

1. When will PCB levels in fish populations recover to levels meeting human health and ecological risk criteria under continued No Action?
2. Can remedies other than No Action significantly shorten the time required to achieve acceptable risk levels?
3. Are there contaminated sediments now buried that are likely to become “reactivated” following a major flood, possibly resulting in an increase in contamination of the fish population?

The approach to the PCB transport and fate modeling was to develop and field validate a scientifically credible mass balance model that was capable of predicting future PCB concentrations in the water and sediments. The model would be used for evaluating and comparing the impacts of continued No Action, major flood events and various remedial scenarios. The model also provides water column and sediment PCB exposures for the PCB bioaccumulation model and the ecological and human health risk assessments.

The specific objectives of the transport and fate modeling work in this RBMR were the following:

- Develop a mass balance model for PCB levels in the water column and bedded sediments in the Upper Hudson River;
- Calibrate the mass balance model to available historical data, including data collected as part of the Phase 2 investigation;
- Conduct forecast simulations with the calibrated mass balance model to estimate long-term responses to continued No Action and impacts due to a 100-year peak flow; and
- Estimate short-term, fine-scale erosion of solids and PCBs in Thompson Island Pool in response to a 100-year peak flow.

Through these objectives, the modeling work in this Revised Baseline Modeling Report is directed at answering Reassessment questions pertaining to continued No Action (Question 1 above) and impacts of a major flood (Question 3). During Phase 3, the Feasibility Study, the models will be used for evaluation and comparison of the impacts of various remedial scenarios (Question 2).

THIS PAGE INTENTIONALLY LEFT BLANK

2. MODELING APPROACH

2.1 INTRODUCTION

Mass balance models were developed for transport and fate of PCBs in the water column and bedded sediments, and for PCB bioaccumulation in fish. The report herein (Books 1 and 2) focuses only on the PCB transport and fate model, whereas the bioaccumulation model is described in Books 3 and 4. The spatial domain of these models was the Upper Hudson River between Fort Edward and Federal Dam at Troy (Figure 1-2). However, special emphasis was placed on Thompson Island Pond (TIP), a 6-mile portion of the river between Fort Edward and Thompson Island Dam (TID) (Figure 1-3), because this reach contains the highest PCB concentrations and a disproportionately high PCB mass reservoir relative to downstream reaches.

The following major sections are contained in Chapter 2:

- Section 2.2 presents the overall modeling framework used in this Reassessment;
- Section 2.3 describes the hydrodynamic model developed for Thompson Island Pool which was linked to the Depth of Scour Model and the HUDTOX model;
- Section 2.4 describes the Depth of Scour Model (DOSM) for Thompson Island Pool;
- Section 2.5 describes the Hudson River Toxic Chemical Model (HUDTOX) that was developed and applied to the Upper Hudson River between Fort Edward and Federal Dam at Troy;
- Section 2.6 describes the various applications conducted with the HUDTOX model; and,
- Section 2.7 presents an overview of the database used for model development and applications.

2.2 CONCEPTUAL APPROACH

The conceptual approach for the PCB transport and fate models of the Upper Hudson River was driven by the principal Reassessment questions:

1. When will PCB levels in fish populations recover to levels meeting human health and ecological risk criteria under continued No Action?
2. Can remedies other than No Action significantly shorten the time required to achieve acceptable risk levels?

3. Are there contaminated sediments now buried that are likely to become “reactivated” following a major flood, possibly resulting in an increase in contamination of the fish population?

Answers to the first two questions required reliable representation of long-term trends in water column and sediment PCB exposure concentrations to fish populations in the Upper Hudson River. To accomplish this objective, a mass balance model, HUDTOX, was developed to simulate water, solids and PCBs over the long-term historical period and a long-term forecast period. Inputs, outputs, and internal sources and sinks were balanced on a daily time scale in order to simulate long term conditions for the entire Upper Hudson River from Fort Edward to Troy, New York.

An answer to the third question required reliable representation of flow-driven sediment resuspension from highly contaminated areas, especially PCB “hotspots” associated with fine-grain, cohesive sediments. To accomplish this objective, a two-step approach was used. First, a fine-scale hydrodynamic and sediment scour model, DOSM, was used to estimate flow-driven resuspension of sediments and associated PCBs in Thompson Island Pool, the most heavily contaminated portion of the river, in response to a 100-year peak flow. Second, the PCB mass balance model, HUDTOX, was used to estimate water column and sediment responses in the entire Upper Hudson River to the same 100-year peak flow. The hydrodynamic and resuspension models provided an estimate of the likelihood that high PCB concentrations now buried in the sediments would become re-exposed due to flow-driven scour of the sediment bed. Results from the PCB mass balance model (HUDTOX) provided estimates of the resultant water column and sediment concentration responses due to flow-driven scour and subsequent transport and redistribution of contaminated sediments.

The operational framework for the Reassessment models is illustrated in Figure 2-1, which depicts the principal individual modeling components and their inter-relationships. In Figure 2-2, the specific information input to each of these models is also presented. The hydrodynamic model, the DOSM and HUDTOX comprise the transport and fate models. The Thompson Island Pool models consist of a coupled hydrodynamic and resuspension model (DOSM) for sediments. HUDTOX is the mass balance model that represents water, solids and PCBs in the entire Upper Hudson River, including Thompson Island Pool. There is a linkage module that serves to process output from the hydrodynamic model and the DOSM for use in HUDTOX. These transport and fate models are described in the following sections. The Bivariate Biota Accumulation Factor (BAF) Model and the bioaccumulation models (FISHPATH and FISHRAND) quantify linkages between PCB water column and sediment concentrations and fish body burdens. These models are the subject of Books 3 and 4, and not described herein.

Different models with different attributes were developed to most effectively answer the three Reassessment questions while balancing the issues of complexity, computational burden, supporting data and system characteristics. The Thompson Island Pool Hydrodynamic and Depth of Scour Models were more refined and complex, as necessary to answer the issue of episodic scour. Thompson Island Pool, although only 6 miles (15 percent) of the entire model domain, contains almost half of the PCB mass reservoir in the Upper Hudson (Tofflemire and Quinn, 1979) and the highest PCB concentrations. Hence, the Pool has been the focus of remedial considerations, and more specialized modeling was warranted. The same framework was not

applied to the remainder of the river because substantially fewer supporting data were available, and the additional computational burden and model complexity were not warranted.

2.3 HYDRODYNAMIC MODEL

The hydrodynamic model used for Thompson Island Pool was the U.S. Army Corps of Engineers RMA-2V. This model is two-dimensional and vertically-averaged. It was applied to Thompson Island Pool to provide velocity information for bottom shear stress calculations at the sediment-water interface using DOSM. It also provided flow routing, water depth, and velocity information to the HUDTOX model for Thompson Island Pool only. The hydrodynamic model includes explicit representation of the existing river geometry as well as the flood plains to account for overbank flow during flood events.

The hydrodynamic model was not directly integrated with the HUDTOX model. Hydrodynamic model results were spatially and temporally processed using a linkage module that transformed water velocities into flows that were routed among the HUDTOX model spatial segments in Thompson Island Pool. Water velocities were also transformed into applied shear stresses at the sediment-water interface for use in the DOSM. The hydrodynamic model was run to steady state for a range of different river flows, including the 100-year peak flow.

2.4 DEPTH OF SCOUR MODEL

The DOSM is a two-dimensional, GIS-based model of sediment erosion that was applied to Thompson Island Pool. It is a specialized tool for providing spatially-refined information on sediment erodibility in response to high flows, including a catastrophic flood. It calculates sediment bed scour based on flow-induced shear stress and site-specific measurements of sediment properties and resuspension behavior. Information on applied shear stresses at the sediment-water interface was calculated based on output from the hydrodynamic model.

The DOSM was developed principally to answer questions related to the likelihood that flood-induced erosion of bottom sediment would reactivate buried PCB. It was first used as a stand-alone tool to provide mass estimates of solids and PCBs eroded, and depth of sediment bed scour, in response to a 100-year peak flow. A constant 100-year flow was simulated with the hydrodynamic model as a worst case scenario. This simulation produced a map of bottom shear stress throughout Thompson Island Pool for the 100-year flow. This shear stress map was used to compute estimates of depth of scour throughout the entire cohesive sediment bed in Thompson Island Pool. Based on various uncertainties in model inputs, DOSM also calculates a probability distribution for scour depth addressing the question of “likelihood”. The relationship between cohesive sediment resuspension and applied shear stress was based on a formulation from the published literature and parameterized using site-specific measurements from Thompson Island Pool. The DOSM shear stress map was also used to compute an upper bound estimate of depth of scour that could be expected for the non-cohesive sediment area in Thompson Island Pool.

The DOSM was also used to develop relationships between river flow and cohesive sediment resuspension for use in the HUDTOX model. The hydrodynamic model was run for a range of flow conditions spanning typical summer flows to the 100-year flow. The DOSM was used to estimate cohesive sediment resuspension for each of these flow conditions, thus producing a family

of resuspension-flow relationships. These relationships were used as input to the HUDTOX model to represent cohesive sediment resuspension across all flow conditions in the Thompson Island Pool portion of the River.

2.5 MASS BALANCE MODEL

HUDTOX is the principal transport and fate modeling tool in this Reassessment. HUDTOX is a time-variable, three-dimensional model that includes three types of mass balances: (1) a water balance; (2) a solids balance; and (3) a PCB mass balance. A water balance is necessary because PCB dynamics are influenced by river flow and mixing rates. A solids balance is necessary because PCB dynamics are influenced by the tendency of PCBs to sorb (attach) to both suspended and bedded solids in the river. Finally, a PCB mass balance is necessary to account for all inputs, outputs, and internal sources and sinks of PCBs in the river. HUDTOX has a fully-integrated representation of solids and PCB concentrations in the water column and bedded sediments.

The spatial scales of the HUDTOX model application were determined by the Reassessment questions and available site-specific data. HUDTOX was applied to the entire Upper Hudson River from Fort Edward to Federal Dam at Troy. Because a substantial amount of PCB-contaminated sediment is contained in Thompson Island Pool, this portion of HUDTOX included greater spatial resolution than the portion downstream of Thompson Island Dam. In the Pool, HUDTOX is two-dimensional in the water column and three-dimensional in the sediments. Between Thompson Island Dam and Federal Dam, HUDTOX is one-dimensional in the water column and two-dimensional in the sediments.

With respect to temporal scale, the HUDTOX model was developed to represent long-term average water column and sediment PCB exposure concentrations. It was not developed to represent short-term behavior associated with high flow events. The reason is that PCB body burdens in fish are driven primarily by long-term average exposure concentrations, not short-term, event-scale exposures. The model does, however, represent differences between low-flow and high-flow sediment resuspension processes, and differences between cohesive and non-cohesive sediment areas. In this sense the model was designed to capture both mean low-flow and mean high-flow solids and PCB dynamics.

In HUDTOX, hydraulic routing downstream of Thompson Island Dam was one-dimensional and was specified using USGS flow gage data at Fort Edward and estimated flows for downstream tributaries. In Thompson Island Pool, the two-dimensional flow routing was defined by the hydrodynamic model.

Sediment scour in HUDTOX was determined through use of output from DOSM. The hydrodynamic model results were used to calculate the bottom shear stress required for DOSM. Output from the DOSM was linked to HUDTOX in the form of relationships between flow and cohesive sediment resuspension. This linkage ensured internal consistency in representation of flow-dependent resuspension between these two models for cohesive sediment areas. In Thompson Island Pool, the hydrodynamic, DOSM and HUDTOX models were linked in terms of flow routing, depth, velocity, applied shear stress and cohesive sediment resuspension. Neither the hydrodynamic model nor the DOSM was applied to the portion of the river below Thompson

Island Dam. Average relationships for cohesive sediment resuspension developed from the DOSM in Thompson Island Pool were used in this portion of the river.

2.6 MASS BALANCE MODEL APPLICATIONS

The HUDTOX mass balance model was applied in a structured sequence as follows:

- Historical calibration for Tri+ (sum of trichloro through decachloro homologue groups) for a 21-year period from 1977 to 1997;
- Hindcast applications for total PCB and five congeners for 1991 to 1997;
- Independent model validation for 1998;
- 70-year model forecasts from 1998 to 2067; and,
- Sensitivity analysis for the historical calibration and the forecast simulation periods.

Model applications included a total of seven different PCB forms: total PCBs, Tri+, and five congeners, BZ#4, BZ#28, BZ#52, BZ#[90+101] and BZ#138. Total PCBs represents the sum of all measured PCB congeners and is the only PCB form that completely represents total PCB mass. A limitation to the use of total PCBs is that data were available for only the period from 1991 to 1997. To extend the period of time for the HUDTOX historical calibration, Tri+ was used as a surrogate for total PCBs and served as the principal calibration and forecast model state variable. Tri+ represents the sum of only trichloro through decachloro homologue groups. Due to differences in analytical methods among individual datasets, Tri+ was the only internally-consistent PCB form that could be operationally defined to approximate total PCBs over the entire period from 1977 to 1997 (USEPA, 1998a). Tri+ was also an appropriate choice for calibration and forecast simulations because it represents the principal distribution of PCB congeners that bioaccumulate in fish.

The historical calibration was the principal development vehicle for the model, which was focused on representing long-term PCB trends in water and sediment for a 21-year period. Tri+ was the principal focus of the calibration because comparable measurements were available for the entire 21-year period. However, a subsequent 7-year hindcast application of the model to total PCB and five congeners provided a test of the historical calibration to Tri+. The calibrated model was then subjected to validation using an independent set of water column PCB data for 1998. Following successful validation of the model, 70-year forecast simulations were developed. The forecasts were intended to assess the long-term system responses to continued No Action and impacts due to a 100-year peak flow. Additionally, model performance over the historical calibration and forecast periods was assessed through sensitivity analyses.

The congener simulations were conducted to gain better understanding of the environmental processes controlling PCB dynamics in the river and to strengthen and support the long-term historical calibration. The five congeners were selected based primarily on their physical-chemical properties and frequencies of detection in environmental samples across different media.

BZ#4 is a dichloro congener that represents a final product of PCB dechlorination in the sediments (USEPA, 1997). BZ#28 is a trichloro congener that has similar physical-chemical properties to total PCBs. BZ#52 is a tetrachloro congener that was selected as a normalizing parameter for congener patterns based on its presence in Aroclor 1242, the main Aroclor used by GE, and on its resistance to degradation or dechlorination in the environment (USEPA, 1997). BZ#[90+101] (a pentachloro congener) and BZ#138 (a hexachloro congener) represent higher-chlorinated congeners that are more strongly associated with suspended and bedded solids in the river.

2.7 MASS BALANCE MODEL CALIBRATION

The calibration strategy can be described as minimal and conservative. It was minimal in the sense that external inputs and internal model parameters were determined independently to the fullest extent possible from site-specific data and only a minimal number were determined through model calibration. It was conservative in the sense that parameters determined through model calibration were held spatially and temporally constant unless there was supporting information to the contrary. Consistent with the Reassessment questions, emphasis was placed on calibration to long-term trends in sediment and water column PCB concentrations, not short transient changes or localized variations.

The following factors were found to be the most important in controlling long-term trends in sediment and water column Tri+ concentrations in the Upper Hudson River:

- Hydrology;
- External solids loads;
- External Tri+ loads;
- Tri+ partitioning;
- Sediment-water mass transfer under non-scouring flow conditions;
- Solids burial rates; and,
- Particle mixing depth in the sediments.

The first three of these factors are external inputs defined largely by data, and the last four factors are internal processes within the river defined by data, scientific literature and model calibration. Long-term solids burial rates were the principal factor controlling long-term Tri+ responses in the river. Partitioning controls the distribution of Tri+ mass between sorbed and truly dissolved phases, thus influencing sediment-water and water-air mass transfer rates, and bioavailability to fish. Sediment-water mass transfer under non-scouring flow conditions was found to be the principal source of Tri+ inputs to the water column. Particle mixing depth strongly influenced long-term responses and the vertical distribution of Tri+ in the sediments. With the exception of solids burial rates and particle mixed depth, all model inputs and parameter values were determined using site-specific data and were not adjusted during the model calibration.

Most of the effort during the HUDTOX model calibration consisted of determining solids burial rates. Solids burial rates were determined for the 21-year historical calibration for four major reaches, including Thompson Island Pool and three downstream reaches. The principal calibration constraints on solids burial rates were the following:

- Measured burial rates from dated sediment cores;
- Computed burial rates from a sediment transport model;
- Tri+ surface sediment concentration trends; and,
- In-river solids and Tri+ mass transport at high and low flows.

The historical calibration was conducted by applying simultaneous, mutual constraints on the coupled solids and Tri+ mass balances. Operationally, the approach consisted of adjusting four model parameters: gross settling velocities into cohesive and non-cohesive sediment areas; resuspension rates from non-cohesive sediment areas; depth of particle mixing in the sediment bed; and magnitude of sediment particle mixing.

2.8 HUDSON RIVER DATABASE

All modeling work in this report utilized the extensive database that was created to support this Reassessment. The Database Report (USEPA, 1995) and accompanying CD-ROM database provides the validated data for the Phase 2 investigation. This Revised Baseline Modeling Report (RBMR) utilized the Hudson River Database, Release 4.1b, which was updated in fall 1998 (USEPA, 1998b). This database contains information from a large variety of different sources, including:

- New York State Department of Environmental Conservation (NYSDEC)
- New York State Department of Health (NYSDOH)
- New York State Department of Transportation (NYSDOT)
- General Electric Company (GE)
- Lamont-Doherty Earth Observatory (LDEO)
- Rensselaer Polytechnic Institute (RPI)
- U.S. Geological Survey (USGS)
- National Oceanic and Atmospheric Administration (NOAA)
- National Weather Service (NWS)
- U.S. Environmental Protection Agency (USEPA).

To supplement the database in Release 4.1b, a portion of the 1997 USGS flow, suspended solids and PCB data were obtained directly from the USGS in Albany, New York. Where necessary and appropriate, information from the scientific literature and various technical reports was also used in this modeling work. These sources are cited in the report text.

3. THOMPSON ISLAND POOL HYDRODYNAMIC MODEL

3.1 OVERVIEW

The six-mile long Thompson Island Pool is a special area of focus in the Reassessment because it contains a disproportionate amount of the PCB mass (nearly half) in the 40-mile long portion of Upper Hudson River. Additionally, the highest PCB concentrations occur in the Pool. These factors have made the Pool a focus area for possible remediation. The Pool is also the most extensively sampled reach of the Upper Hudson. As a result of the special focus on the Pool and the greater data availability, a fine scale, two-dimensional hydrodynamic model was applied for the Pool to provide input to the PCB fate and transport model (Chapter 5) and the Depth of Scour Model (Chapter 4). The Depth of Scour Model uses fine scale velocity information from the hydrodynamic model to compute scour of sediments, especially under high flow conditions.

The Thompson Island Pool is defined as the reach of the Hudson River upstream from the Thompson Island Dam at RM 188.5 and downstream from the former Fort Edward Dam, as shown in Figure 3-1. The purpose of the hydrodynamic modeling effort for Thompson Island Pool was to provide information on bottom shear stresses at the sediment-water interface for the DOSM and HUDTOX models. Additionally, the model provided flow routing, depth and velocity information for the two-dimensional portion of the HUDTOX model in Thompson Island Pool.

The hydrodynamic model was used to calculate two-dimensional, vertically-averaged velocity fields for a range of different river flows, including the 100-year peak flow in the Hudson River, (estimated to be 47,330 cfs by Butcher, 2000a). The computation of a two-dimensional, vertically averaged velocity field is necessary to account for the lateral variability of the flow and resultant bed shear. The bed shear is used to compute the mass of cohesive sediments eroded in the Depth of Scour Model (DOSM). Because sediment properties and PCB concentrations are not uniformly distributed, the bottom shear stresses must be determined for each element used in the river model to correctly estimate Poolwide resuspension of PCBs.

The hydrodynamic model was applied for a range of steady flow conditions in the Thompson Island Pool. Transient effects due to storage and drainage were not included in the simulations because the historical flow record at Fort Edward shows that the Hudson River high flow events occur over several days, which gives the Pool enough time to establish approximate steady state conditions. This means simulation of transient water storage and drainage could be reasonably omitted from calculations of bottom shear at peak flow conditions. Additionally, the Depth of Scour Model (DOSM) presented in Chapter 4 requires only simulation of the peak flow hydraulic conditions to estimate solids resuspension losses from cohesive sediment bed areas during flood events. The credibility of the numerical simulation results was established by applying the model to events where the flow in the river had been measured. The model was run for the 100-year peak flow to provide the velocity field used by the DOSM.

The following major sections are included in Chapter 3:

- 3.2 Hydrodynamic Modeling Approach
- 3.3 Available Data
- 3.4 Hydrodynamic Model Calibration
- 3.5 Hydrodynamic Model Validation
- 3.6 Hydrodynamic Model Sensitivity Analyses
- 3.7 Conversion of Vertically Averaged Velocity to Bottom Shear Stress
- 3.8 Discussion of Results

3.2 HYDRODYNAMIC MODELING APPROACH

The hydrodynamic model used to compute the flow is the US Army Corps of Engineers RMA-2V. RMA-2V uses the finite element method to compute vertically-averaged velocities and water surface elevations in the flow field. The model has been extensively studied and applied widely (Berger, 1990; Lin and Richards, 1993; McAnally et. al., 1984; and Richards, 1990). The selection of a two-dimensional, vertically averaged model and the density of the grid mesh were largely determined by the resolution needed to adequately define the flow field variations and river bathymetry, and hence, shear stress variation. The shear stress exerted on the river bottom is parameterized by the magnitude of the vertically averaged velocity and the depth of flow, as is described in Section 3.7

A short summary of the modeling procedure is as follows: A finite element grid was first constructed for the Thompson Island Pool section of the river and floodplain. RMA-2V uses a finite element procedure to solve the governing equations that describe the vertically-averaged velocities and water surface elevation. The boundary conditions consist of a specified upstream flow, the water elevation downstream and the resistance to flow. The downstream boundary was obtained from a rating curve developed for the stage-discharge gage near the Thompson Island Dam, and the resistance to flow is parameterized by Manning's 'n'.

3.2.1 Governing Equations

The RMA-2V model formulation is based on the conservation of mass and momentum equations in order to simulate water elevation and two-dimensional velocity. A brief description of the model equations and framework is provided here. A more rigorous presentation of the model is available in the user's manual.

The two governing equations for continuity of mass and momentum focus on three state variables, water elevation (h) and downstream and cross-stream velocity (u and v). To solve for these three variables, three equations are needed. Bottom stress is computed based on the vertically-averaged velocity using an additional equation. The equations are presented below.

1. Continuity

$$\frac{\partial h}{\partial t} + \frac{\partial(uh)}{\partial x} + \frac{\partial(vh)}{\partial y} = 0 \quad (3-1)$$

2. Linear Momentum

a. x-direction (longitudinal) momentum

$$\frac{\partial u}{\partial t} + u \frac{\partial u}{\partial x} + v \frac{\partial u}{\partial y} = -g \frac{\partial(h + a_0)}{\partial x} - C_f q \frac{u}{h} + \frac{1}{\mathbf{r}} \left(E_{xx} \frac{\partial^2 u}{\partial x^2} + E_{xy} \frac{\partial^2 u}{\partial y^2} \right) \quad (3-2)$$

b. y-direction (transverse) momentum

$$\frac{\partial v}{\partial t} + u \frac{\partial v}{\partial x} + v \frac{\partial v}{\partial y} = -g \frac{\partial(h + a_0)}{\partial y} - C_f q \frac{v}{h} + \frac{1}{\mathbf{r}} \left(E_{yx} \frac{\partial^2 v}{\partial x^2} + E_{yy} \frac{\partial^2 v}{\partial y^2} \right) \quad (3-3)$$

3. Bottom Friction Coefficient

(English Units)

$$C_f = \frac{gn^2}{(1.486)^2 h^{(1/3)}} \quad (3-4)$$

(Metric Units)

$$C_f = \frac{gn^2}{h^{(1/3)}} \quad (3-5)$$

where:

h	=	water depth [L]
u	=	vertically-averaged flow velocity in the x-direction (longitudinal) [L/T]
v	=	vertically-averaged flow velocity in the y-direction (lateral) [L/T]
x	=	distance in the longitudinal direction [L]
y	=	distance in the lateral direction [L]
t	=	time [T]
g	=	acceleration due to gravity [L/T ²]
a_o	=	bottom elevation [L]
C_f	=	bottom friction coefficient [dimensionless]
n	=	Manning's 'n' channel roughness coefficient [T/L ^{1/3}]
E_{xx}	=	normal turbulent exchange coefficient in the x direction [M/(LT)]

E_{xy}	=	tangential turbulent exchange coefficient in the x direction [M/(LT)]
E_{yy}	=	normal turbulent exchange coefficient in the y direction [M/(LT)]
E_{yx}	=	tangential turbulent exchange coefficient in the y direction [M/(LT)]
ρ	=	water density [M/L ³]
q	=	velocity magnitude = $(u^2 + v^2)^{1/2}$ [L/T].

The Coriolis apparent force and the force imposed by wind stress have been neglected here because these forces are small compared to forces induced by gravitation and friction.

3.2.2 Computational Sequence and Linkages

The hydrodynamic model for the Thompson Island Pool was not incorporated directly in either the HUDTOX model or the Depth of Scour Model because its calculations could be performed independently. As a result, output from the hydrodynamic model needed to be linked to the other models.

The RMA-2V model was first calibrated to the measured hydraulic data for the river, with Manning's 'n' as the primary calibration parameter. River data, such as river stage-discharge relations for the upstream (Lock 7) gaging station, were used to calibrate the model. Other data, such as velocity measurements made by the USGS during high flow events, were also used to validate the model results.

The specific steps used in the modeling procedure to provide information to the other models are as follows:

1. The flow field, velocity and depth for each node were calculated using the RMA-2V model for a range of flow conditions, and bottom shear velocities (u^*) were computed from depth and vertically-averaged velocity.
2. The Depth of Scour Model calculates the bottom shear stress from the bottom shear velocities using the relation:

$$\tau = r (u^*)^2$$

3. Intersegment flows between the larger HUDTOX segments were defined by integrating velocity field results from the hydrodynamic model at the various corresponding nodes.

3.3 AVAILABLE DATA

The hydrodynamic model RMA-2V requires specific input data describing the hydraulic conditions of the system chosen for simulation. These input data consist of the grid used for the computation, Manning's 'n' to parameterize the bottom friction, the forcing functions or upstream boundary conditions, and the downstream and side-channel boundary conditions. These are described below.

3.3.1 Model Grid

The RMA-2V model uses a six-node triangular element scheme to describe the physiography of the TIP system. The model grid consists of approximately 6,000 nodes defining 3,000 elements. Each node is defined by an x-y coordinate and its corresponding elevation. The depth associated with each grid node for the main channel is based on the bathymetric survey performed by General Electric in 1991 (O'Brien & Gere, 1993b). Figure 3-2 shows the finite element grid used in the model calibration. The finite element grid in the floodplain was constructed using elevations taken from the USGS topographic maps. As seen in Figure 3-2, the grid in the floodplain is much coarser than in the Thompson Island Pool channels. This is justified because velocities in the floodplain are much smaller than in the Pool channels and do not vary as much. The nodes of the finite element grid in the main channel are located approximately every 50 feet across the River (laterally) and approximately 300 feet along the channel (longitudinally).

During the course of model calibrations and runs, it was necessary to refine the grid so that the water mass was conserved at the various transects corresponding with HUDTOX segment boundaries. Conservation was achieved within a few percentage points for each transect. This level of accuracy was sufficient to allow post-processing of the RMA-2V results to meet the mass balance of water requirements for the HUDTOX model without significantly affecting the routing of advective flows through segments in the Thompson Island Pool. The refining of the grid consisted of eliminating isolated nodes along the sides of the flow and smoothing the bottom elevations. These changes were minor and had little impact on the calculated overall velocity field.

3.3.2 Manning's 'n'

The input parameter, Manning's 'n', expresses the river's hydraulic resistance to flow. Conceptually, resistance to flow reflects the character of the sediments and the nature of the flow pathways. This parameter is commonly a calibration parameter, because its value cannot be determined accurately from a measurement of the physical dimensions of the river or from a description of the sediment type. Two site-specific hydraulic flow modeling studies, Zimmie (1985) and FEMA (1982), had been conducted previously; the Manning's 'n' values can be expected to be near the values used in these studies. Table 3-1 contains the Manning 'n' values used in these two studies.

For this study, the values of Zimmie were used initially and subsequently calibrated to best fit the recorded observations of the river, especially those at high flow. The sensitivity of the model to changes in this parameter is discussed below in Section 3.6.1.

3.3.3 Boundary Conditions

The principal input to the model is the upstream boundary condition, the incoming flow. The model was run for the eight different flows at Fort Edward shown in Table 3-2. The first four flows are of interest because the concentration of suspended sediment in the river was sampled when they occurred. The fifth flow is of interest because it is the highest flow recorded in TIP after the Fort Edward dam was removed in 1973. The final three flows are of interest because they represent high flow events with a specified return period. The model results for these eight

flow simulations were used in the DOSM to develop relationships between river flow and cohesive sediment resuspension.

Other boundary conditions of the model consist of the side-channel boundary condition and the downstream water elevations. The side-channel boundary condition is the requirement that the velocity normal to the sides of the channel be zero. This is implicitly performed in the RMA-2V model. The downstream boundary condition consists of specifying the water surface elevation at the most downstream transect, which is the Thompson Island Dam. The downstream boundary must be specified as an elevation in order to incorporate the backwater effects of the dam into the model.

The downstream boundary surface elevation was taken from the rating curve for USGS Gage 118, which is located just above Thompson Island Dam. The rating curve was developed from a regression analysis performed on the discharge-water level data accumulated during the 11 year period of 1983 to 1993 (USEPA, 1997). Examination of this rating curve showed that the regression is good for flows up to 30,000 cfs; however, the third-order polynomial developed in the regression fails to accurately predict increasing river elevations for flows above 30,000 cfs. Refined extrapolation using best engineering judgment and a theoretical rating curve (Zimmie, 1985) was used to determine the water levels at Thompson Island Dam above these flows.

3.4 HYDRODYNAMIC MODEL CALIBRATION

The hydrodynamic model calibration approach consisted of specifying an appropriate value for the turbulent exchange coefficients based on literature values and then varying the Manning's 'n' so that computed river levels agree with elevations from the upstream rating curve. The agreement with the upstream rating curve was assessed for each flow input at the most upstream transect of the grid. Note that only one value of Manning's 'n' was used for the entire length of the main channel, because there are no physical data on which to base a variation of Manning's 'n'. The upstream rating curve used for comparing to model output during calibration was USGS Gage 119, near Lock Number 7, which is near the southern tip of Rogers Island (Figure 3-1).

Because the calculation of velocity is of primary interest for larger flows on the Hudson River, the calibration first focused on the flow of 30,000 cfs, which is the highest flow for which the rating curves for both USGS Gage 119 (upstream) and USGS Gage 118 (downstream) are substantiated. The Manning's 'n' values were calibrated for 30,000 cfs and were then used in the model to predict water elevations for lesser flows. These predicted water elevations were then compared with the elevations from the Gage 119 elevations.

The turbulent exchange coefficients were set to 4,790 Pa-sec (100 lb-sec/ft²) which is within the range of longitudinal turbulent dispersion (K_{ij}) values measured in a variety of rivers (Fischer et.al., 1979). The measured dispersion numbers can be directly translated into turbulent momentum exchange coefficients, since for most turbulent flows the turbulent Prandtl number (E_{ij}/K_{ij}) equals 1.0 (Tennekes and Lumley, 1972).

As described above, the model was primarily calibrated for the flow of 30,000 cfs. The Manning's 'n' values for the final calibration were 0.020 for the main channel and 0.060 for the floodplain. The model computed the same river water surface elevation as was observed at Gage

119 using these Manning's 'n' calibration values. Table 3-3 shows this result, along with the comparison of model output vs. rating curve water levels for lesser flows. The elevations in the table are listed in feet relative to the National Geodetic Vertical Datum (NGVD).

Comparing the last two columns in Table 3-3 shows that the model's results are slightly higher than the rating curve for the smaller flows, implying that the calibrated Manning's 'n' might be somewhat low for the lower-flow cases. It is possible that the rating curve used in the calibration was biased at either low or high flow, making calibration difficult across the entire flow range. Nevertheless, it was judged that a higher value could not be justified, given the model's close fit for 30,000 cfs, (a higher Manning's 'n' would unacceptably increase the model's prediction of the upstream water surface in that case).

The excellent model fit at the calibration flow of 30,000 cfs, along with good results from two validation exercises described below, provide confidence in using the model to simulate high-flow events.

3.5 HYDRODYNAMIC MODEL VALIDATION

There were two additional and independent sources of information used to verify the calibration results. The first source is the Hudson River velocity measurements made in the Thompson Island Pool by the USGS. The second source is the flood study conducted by FEMA. A comparison of model results with these sources of information is discussed below.

3.5.1 Rating Curve Velocity Measurements

The USGS periodically measures the flow in the Hudson River in the Thompson Island Pool to develop and update the river's rating curves. For the rating curve located at Scott Paper, which is upstream of Rogers Island, the flow is measured by measuring the depth and velocity at numerous points over the cross-section of the river at Rogers Island. These data are taken at the bridges over the Hudson River on both sides of Rogers Island. The model's simulated velocities can be compared to these measured velocities as a check on the accuracy of the model.

The model was run for the discharge (29,800 cfs) that was measured on April 18, 1993. The velocities computed by the model for locations along the cross-section of the river were approximately equal to or slightly lower than measured. For example, the river velocities measured in the middle of the channel by the USGS were approximately 4.3 feet per second (fps), while the model computed velocities of approximately 4.1 fps. These values are sufficiently close for validation. It should be noted that since the velocities were measured from a bridge, it is to be expected that the measured velocities are slightly higher than the computed ones, since the bridge piers will cause a localized acceleration in the flow. Constraints on model resolution inhibit the ability to capture these localized effects on the flow.

3.5.2 FEMA Flood Studies

The Federal Emergency Management Agency (FEMA) regularly conducts studies to predict the flood elevations in rivers for flows of various return periods. The results of the study conducted by FEMA in 1984 for the Upper Hudson River were used as an additional validation of the credibility of the model. The 100-year flow used by FEMA (52,400 cfs) is greater than the 100-

year flow used in this study (47,330 cfs) so that a direct comparison of 100-year flood elevations was not initially possible. Estimates of the 100-year flow magnitude are different due to use of different datasets and estimation methods. However, the model was also run for the 100-year FEMA flow of 52,400 cfs, and the model predicted a river elevation at Fort Edward of 130.4 ft. NGVD (National Geodetic Vertical Datum, formerly Sea Level Datum of 1929). The FEMA flood study using the HEC-2 program predicted a river elevation of 130.7 ft. NGVD. These results are comparable considering that the two models reflect a slightly different representation of the river hydraulics.

The RMA-2V model developed here was also run for 52,400 cfs with a Manning's 'n' of 0.030 for the main channel and 0.075 for the floodplain (approximately the same as the FEMA study). This resulted in a predicted river elevation of 131.7 ft. Most importantly, the river velocities do not vary appreciably for the various representations. Therefore, the model results are judged to be comparable to those produced from the FEMA flood study.

3.5.3 100-Year Peak Flow Model Results

The model was used to simulate the 100-year peak flow of 47,330 cfs. The predicted river elevation at the downstream tip of Rogers Island was 128.6 ft. This elevation is slightly lower than the extrapolated rating curve's elevation of 129.1, but is reasonably close.

The vertically-averaged velocity field produced by RMA-2V for the 100-year peak flow is shown in Figure 3-3. The velocity magnitudes are reflected by the length of the vectors in accordance with the scale provided near the bottom of the figure. The vectors in the floodplain that have no visible tail indicate slow moving water in the overbank area. A vector was printed where the water depth was greater than zero, even if the velocity was small, to indicate the extent of the flow.

The RMA-2V velocity field was used to compute the shear stresses in the DOSM within the normal river banks of the Thompson Island Pool, not in the floodplain. Floodplain simulation was only included to ensure an appropriate representation of the in-river, vertically-averaged velocity field.

3.6 HYDRODYNAMIC MODEL SENSITIVITY ANALYSES

The sensitivity of the model to the principal inputs was evaluated by varying the finite element grid size, the Manning's 'n', and the turbulent exchange coefficient. The model's sensitivity to the grid size was checked by running the model for a flow of 40,000 cfs with a finite element grid having approximately two times the number of elements as the baseline finite element grid. The results obtained with the larger grid resolution were essentially the same as the smaller grid and, therefore, it was concluded that the finite element grid used here was of sufficient resolution to simulate the river flow. The sensitivity of the model to the Manning's 'n' and the turbulent exchange coefficient was measured by the effect on the predicted water elevations for the 100-year peak flow at the downstream tip of Rogers Island (Gage 119). The sensitivity results are presented in the following discussion.

3.6.1 Manning's 'n'

The Manning's 'n' was varied from 0.015 to 0.035 for the main channel and 0.040 to 0.080 for the floodplain. These values of 'n' are consistent with what has been previously used for this reach of the Hudson (Zimmie, 1985; FEMA, 1982), and with literature values (Chow, 1959; Hicks and Mason, 1998). The model was run for the 100-year peak flow of 47,330 cfs; the results are contained in Table 3-4. These results indicate that changes in Manning's 'n' do not significantly affect results from the calibrated model. It is also evident that the main channel Manning's 'n' generally affects the results much more than the floodplain Manning's 'n', as would be expected because most of the flow occurs in the main channel. The model insensitivity to Manning's 'n' is due to the fact that the flows are large and the system is strongly forced. The accurate prediction of stages and velocities in this flow regime depends more on having an accurate representation of the depth of the main channel and the flood plains.

3.6.2 Turbulent Exchange Coefficient

The four turbulent exchange coefficients, E_{xx} , E_{xy} , E_{yx} , and E_{yy} were all set to a value of 4,790 Pa-sec (100 lb-sec/ft²) in the baseline run. Table 3-5 shows the effects of varying these turbulent exchange coefficient values on the water surface elevation at Rogers Island.

It can be concluded that variations in turbulent viscosities do not affect the river elevation dramatically, especially evidenced by the small increase in the river elevation for each doubling of the coefficients. The model predicts higher elevations for higher turbulent exchange coefficients in much the same way that it would predict higher elevations with a larger Manning's 'n'. Both the Manning's 'n' and the turbulent exchange coefficients parameterize energy loss in the system. This means that if higher turbulent exchange coefficients were used in the calibration, then a lower Manning's 'n' would be required to obtain an equally good agreement with the observed rating curve. Given these results, it was judged that a turbulent exchange coefficient of 100 lb-sec/ft² was reasonable and that further calibration was not required.

3.7 CONVERSION OF VERTICALLY-AVERAGED VELOCITY TO BOTTOM SHEAR STRESS

Conversion of the vertically-averaged River velocities, as obtained from the RMA-2V model, to bottom shear stresses is required to compute resuspension of Thompson Island Pool bed sediments in the DOSM and HUDTOX models. Several formulations were investigated. One of these formulations computes shear stress directly from the vertically-averaged velocity, while the other three provide computed values of bottom shear velocity, u^* , for use in computing shear stress as $\tau = \rho(u^*)^2$. The four methods, with a short description of each, are presented below.

1. Smooth wall log velocity profile

This conversion method (Thomas and McNally, 1990; Schlichting, 1979) derives from the assumption that the vertical velocity profile at any point in the river conforms to the "smooth wall log velocity profile". The following equation describes this velocity profile:

$$\frac{u}{u^*} = 2.5 \ln \left(\frac{3.32 u d}{n} \right) \quad (3-6)$$

where:

$$\begin{aligned} u &= \text{vertically-averaged velocity [L/T]} \\ u^* &= \text{shear velocity [L/T]} \\ d &= \text{depth of flow [L]} \\ \mathbf{n} &= \text{kinematic viscosity [L}^2\text{/T].} \end{aligned}$$

The applicability of this relation to the Upper Hudson River is suspect, because it is known that the bottom of the river is not hydraulically smooth.

2. Gailani Method

This empirical method was used by Gailani (Gailani et al., 1991) for the Lower Fox River, as follows:

$$\frac{\mathbf{t}_b}{\mathbf{r}_0} = 0.003 u^2 \quad (3-7)$$

where:

$$\begin{aligned} \mathbf{t}_b &= \text{bottom shear stress [M/L/T}^2\text{].} \\ \rho_0 &= \text{reference density [M/L}^3\text{].} \end{aligned}$$

3. Rough wall log velocity profile

$$\frac{u}{u^*} = 6.25 + 2.5 \ln(d/k) \quad (3-8)$$

where:

$$\begin{aligned} u &= \text{vertically averaged velocity [L/T],} \\ u^* &= \text{shear velocity (friction velocity) [L/T],} \\ d &= \text{depth of flow [L],} \\ k &= \text{equivalent Nikuradse roughness [L].} \end{aligned}$$

This relation (Thomas and McNally, 1990) describes the velocity profile for a rough wall river flow, which is typically the condition for river flows. The only free parameter for this equation is k , the roughness factor. This parameter can be estimated from the Manning's roughness (Chow, 1960): for 'n' = 0.02, k was determined to be 0.04 feet.

4. Manning shear stress equation

The fourth formulation, the Manning shear stress equation was selected for use in the Depth of Scour Model. It involves a combination of the cross-section average velocity and bottom shear stress equations (Thomas and McNally, 1990). Specifically, the bed shear velocity is expressed as:

$$u^* = \frac{\sqrt{g} \cdot u \cdot n}{(1.486)d^{1/6}} \quad \text{(English Units)} \quad (3-9)$$

$$u^* = \frac{\sqrt{g} \cdot u \cdot n}{d^{1/6}} \quad \text{(Metric Units)} \quad (3-10)$$

The channel average velocity is defined from the one-dimensional Manning equation, which is given below, as:

$$u = \frac{1.486}{n} R^{2/3} S^{1/2} \quad \text{(English Units)} \quad (3-11)$$

$$u = \frac{1}{n} R^{2/3} S^{1/2} \quad \text{(Metric Units)} \quad (3-12)$$

The definition of the cross-sectional average shear stress (τ_0), can be written as,

$$\mathbf{t}_o = wRS = \mathbf{r}gRS \quad (3-13)$$

where:

u	=	channel averaged velocity [L/T],
n	=	Manning's 'n' [T/L ^{1/3}],
g	=	acceleration due to gravity [L/T ²],
ρ	=	density of fluid [M/L ³]
w	=	weight of the water (ρg) [M/L ² /T ²],
R	=	hydraulic radius [L],
S	=	the slope of the river [dimensionless].

The definition of the friction velocity u^* can be combined with Equation 3-13 to yield;

$$u^* = \sqrt{\frac{\mathbf{t}_o}{\mathbf{r}}} = (gRS)^{1/2} \quad (3-14)$$

For flow in a wide open channel, the wetted perimeter is approximated by the depth ($R \approx d$). Combining this assumption with Equations 3-12 and 3-14 will yield Equation 3-10.

Results comparing the model calculations using the four different methods are presented in Figure 3-4, which shows the variation of shear stress with the average vertical velocity among methods. In Figure 3-4, the depth used to calculate the conversion for methods 1,2 and 4 was 10 feet. As seen in Figure 3-4, Method 1, the smooth wall velocity profile, and Method 2, the Gailani method, yield the smaller shear stresses, especially at higher flows. Methods 3 and 4, the rough wall and Manning's methods respectively, yield appreciably higher values for stress at high velocity flows. Method 4 (Manning's) was chosen to estimate shear stress because it is consistent with the RMA-

2V approach, and it provides the most critical (highest) estimates of bottom shear stress for the DOSM.

The shear stress field for the Thompson Island Pool 100-year peak flow, as computed by the Manning method using the velocity field shown in Figure 3-3, is plotted in Figure 3-5. Maximum stresses are observed in the flood plain, which is to be expected since the depths of the flow are smaller and the Manning's 'n' is 0.06, compared to 0.02 in the main channel.

3.8 DISCUSSION OF RESULTS

The calibrated RMA-2V model is a good representation of Thompson Island Pool hydraulics for various flow regimes. This conclusion is based on the good agreement found between model output for water levels and rating curve results at Lock 7, and the good agreement between model output for velocities and those measured by the USGS. The model's ability to simulate flows well above the calibration flow, 30,000 cfs, is supported by the reasonable agreement between the 100-year peak flow predictions by this model and the FEMA model, and also by the lack of sensitivity of high-flow results to changes in internal model parameters.

The sensitivity analyses show that the RMA-2V model is not appreciably sensitive to changes in the calibration parameters. However, the analysis of the conversion of the flow field output (vertically-averaged velocity and depth) to river-bed shear stress shows that shear stress can vary significantly at high flow, depending on the conversion method used. The lower bound estimate for the smooth wall profile is not applicable. However, the other three methods are potentially valid and provide similar results. The most conservative method, that method which predicts the largest shear stress given the magnitude of the vertically-averaged velocity, was chosen to provide shear stress to the DOSM. However, overall differences among the three methods are approximately less than 30 percent.

4. THOMPSON ISLAND POOL DEPTH OF SCOUR MODEL

4.1 OVERVIEW

The Depth of Scour Model (DOSM) is a two-dimensional model of sediment erosion depth that was applied to Thompson Island Pool. This model was developed as a stand-alone tool specifically to address one of the three principal study questions:

- Are there contaminated sediments now buried that are likely to become “reactivated” following a major flood, possibly resulting in an increase in contamination of the fish population?

The DOSM formulations were also integrated into the HUDTOX mass balance model, providing consistency between these two models in Thompson Island Pool for cohesive sediment resuspension.

The DOSM has different formulations for cohesive and non-cohesive sediment scour. Cohesive sediment scour is calculated on the basis of site-specific measurements of resuspension properties for Thompson Island Pool cohesive sediments. Non-cohesive sediment scour depth is computed via formulations available in the scientific literature, using sediment physical property data for the Pool. Scour depth calculations in each sediment type for the Thompson Island Pool are based on the depth of scour equations, linked to steady-state hydrodynamic model predictions of overlying water velocity (Chapter 3).

The cohesive scour depth calculations are probabilistic estimates. The 5th to 95th percentile estimates were used to define the “likelihood” that buried contaminated sediments are reactivated in a flood. However, the mean estimate at each location is used in HUDTOX transport and fate simulations. For non-cohesive scour depths, only a singular theoretical estimate is available. Both cohesive and non-cohesive estimates assume that the flow condition of interest persists long enough to achieve the estimated scour depth. For cohesive sediments, laboratory observations show that maximum scour will occur within approximately one hour for all flow conditions. The time to maximum scour cannot be determined for non-cohesive sediment in the DOSM framework and hence, the model calculations are viewed as an upper bound.

The DOSM is used to answer the principal study question presented above by estimating probable ranges of sediment scour depth expected in cohesive sediment areas with the occurrence of a 100-year flood event in Thompson Island Pool. These depth of scour ranges are compared to vertical PCB sediment concentration profiles at five specific locations. Additionally, these ranges are used to estimate PCB mass and sediment eroded from cohesive sediments through a poolwide application of DOSM. Cohesive sediment areas are of special interest relative to the non-cohesive sediment areas due to their higher levels of contamination. Observed PCB hotspots generally coincide with cohesive sediment areas and exhibit the highest buried PCB concentrations.

The DOSM cohesive sediment resuspension algorithms are also used in the HUDTOX mass balance model (described in Chapter 5). Although the DOSM does not account for transport or redeposition of scoured sediment and PCBs, the HUDTOX mass balance model does. The HUDTOX model incorporates cohesive sediment resuspension algorithms obtained through

application of the DOSM model to a range of flow conditions. Median values were used from the probabilistic DOSM model application. Equations were developed to relate the predicted cohesive sediment mass scoured to flow at Fort Edward for each HUDTOX cohesive sediment segment in Thompson Island Pool. Through this approach, consistency between the DOSM and HUDTOX models is achieved for cohesive sediment resuspension. In contrast to cohesive sediments, time to maximum scour for non-cohesive sediments is uncertain. Therefore the DOSM non-cohesive sediment scour depths were viewed as an upper bound estimate, with actual resuspension values calibrated in HUDTOX.

The findings from the Depth of Scour Model application show that the expected impact of a 100-year flood on surface sediment PCB concentrations in the Thompson Island Pool is small because computed scour does not expose higher concentrations of PCB in the sediments. Results suggest that the 100-year event is not an important concern from the standpoint of a potential remediation decision for PCBs in the Thompson Island Pool. Specific findings are presented at the end of this chapter. These findings were corroborated by HUDTOX simulation of long-term response to a 100-year peak flow, presented in Chapter 8.

The following major sections are included in Chapter 4:

- 4.2 DOSM Model Development
- 4.3 DOSM Parameterization
- 4.4 DOSM Application
- 4.5 Major DOSM Findings

Section 4.4 presents results of the DOSM estimates regarding depth of scour, likelihood of “reactivating” buried PCBs at the five high resolution core locations, and an estimate of the mass of PCB eroded from cohesive sediment areas due to a 100-year peak flow.

4.2 DOSM MODEL DEVELOPMENT

4.2.1 Conceptual Approach

Two categories of information are necessary to compute the depth of erosion and total mass of solids eroded from bedded sediments for a high-flow event. First, the hydrodynamic conditions at the sediment-water interface need to be specified. The primary forcing function for entrainment of bottom sediments into the flowing water is the shear stress exerted at the sediment-water interface by flowing water. The Thompson Island Pool Hydrodynamic Model yields estimates of vertically-averaged flow velocities at a fine spatial resolution. Bottom shear stresses are computed from the velocities by a simple formula (Section 3.7). Second, the physical-chemical properties of the bedded sediments greatly influence the magnitude and rate of entrainment of sediments for a given event, and the resulting depth of scour. These are specified from data.

Entrainment mechanisms can be classified into two distinct categories based on sediment bed properties. The main parameters affecting the entrainment of non-cohesive sediments include grain size and shape (and their distributions), the applied shear stress, bed roughness, and specific

weight. Bed sediments that are primarily fine grained and/or possess a high clay content exhibit interparticle effects that are cohesive in nature. The resulting entrainment properties are very different from non-cohesive sediments. Since the toxic contaminants of interest (PCBs) are associated preferentially with fine grained sediments, this distinction is of considerable importance. Each approach is described separately below.

4.2.2 Formulation for Cohesive Sediments

4.2.2.1 Background

Particle diameter has a significantly lower influence on the entrainment characteristics of cohesive sediments compared to electrochemical influences. Relatively small amounts of clay in the sediment-water mixture can result in critical shear stresses far larger than those in non-cohesive materials of similar size distribution (Raudkivi, 1990). Previous studies on the entrainment of cohesive sediments hypothesize that the scour magnitude is primarily influenced by the excess applied shear stress (i.e., the difference between the applied shear stress and the critical shear stress of the surficial sediments), and the state of consolidation (or age after deposition) of the bed sediments (Partheniades, 1965; Mehta et al., 1989; Xu, 1991). The mass of material resuspended can be expressed in the following functional form:

$$M = f(\tau - \tau_c; \text{age, other sediment properties}) \quad (4-1)$$

where M is the mass of material resuspended, τ is the applied shear stress, and τ_c is the bed critical shear stress. The function f has been expressed in a variety of different forms, including linear, (e.g. Partheniades, 1965), exponential, (e.g. Parchure and Mehta, 1985), and the power relationship, (e.g. Lick et al., 1995; Gailani et al., 1991).

4.2.2.2 Basic Equations

Lick et al. (1995), proposed an erosion equation based on statistical analysis of laboratory and field data. This work forms the basis of DOSM calculations for cohesive sediments and is expressed as follows:

$$e = \frac{a_0}{t_d^n} \times \left(\frac{\tau - \tau_c}{\tau_c} \right)^m \quad (4-2)$$

where:

ε = the net total amount of material resuspended (g/cm^2);

τ = the applied shear stress (dynes/cm^2);

τ_c = the bed critical shear stress (dynes/cm^2);

t_d = the time after deposition (days); and

a_0 , n , and m = empirical constants.

The empirical constants a_0 , n , and m are obtained through fitting of Equation 4-2 to experimental data. The critical shear stress, τ_c , is also determined through experimentation. The depth of scour can then be calculated as:

$$Z_{scour} = \frac{e}{C_{bulk}} \quad (4-3)$$

where Z_{scour} is the depth of scour (cm), and C_{bulk} is the dry bulk sediment density (g/cm^3). These equations have been applied to site-specific data for several rivers (Fox, Detroit, and Buffalo) by McNeil (1994).

4.2.2.3 Reparameterization to a Probabilistic Model

The reassessment study asks if buried contaminated sediments are “likely” to become reactivated following a major flood. To address this issue of likelihood, the resuspension formulation was adapted to provide probabilistic calculations of scour, as described below.

If the value of τ_c is assumed to have been defined from resuspension experiments, while the other parameters are unknown, then Equation 4-2 can be reduced from five parameters to two using a dimensionless shear stress parameter, τ' :

$$e = A \times (\tau')^m \quad (4-4)$$

where:

$$\begin{aligned} \tau' &= (\tau - \tau_c) / \tau_c, \\ A &= a_0 / t_d^n \end{aligned}$$

Equation 4-4 can be linearized as follows:

$$\ln(e) = \ln(A) + m \times \ln(\tau') \quad (4-5)$$

Therefore, a linear regression may be performed to fit a straight line to data for erosion vs. dimensionless shear stress in “log-log” space. The slope obtained from this regression will correspond to the exponent “m” from Lick’s equation, while the intercept will correspond to the logarithm of the lumped term a_0/t_d^n . Characterization of the distribution of errors around this regression will allow estimation of the uncertainty in erosion predictions due to uncertainty in measured resuspension properties.

Given a regression line with normally distributed residuals, prediction limits for new observations (for a given value of the independent variable) fall on a Student-t distribution (Neter et. al., 1990). For large sample sizes, the Student-t distribution is approximately normal. Predicted values for new observations are therefore calculated as percentiles of normal distributions, in log-log space. The resulting predicted distribution in ordinary space (again, for given values of shear stress) is log-normal, and is calculated according to Equation 4-6.

$$e = \exp(A + m \times \ln(\tau') + u) \quad (4-6)$$

where:

$$u = \mathbf{Z} \times \sqrt{MSE \times \left[1 + \frac{1}{ns} + \frac{(\ln(\mathbf{t}') - X_{avg})^2}{\sum_i (X_i - X_{avg})^2} \right]}$$

and

- τ' = $(\tau - \tau_c) / \tau_c$,
- exp** = exponentiation operator
- Z** = a value of the standard normal distribution variable
- MSE* = mean square error of regression
- ns* = number of data used in the regression
- X_{avg} = mean of the natural log dimensionless shear stresses
- X_i = a particular natural log dimensionless shear stress value.

Division of the erosion by the bulk density gives the depth of scour in centimeters, as shown in Equation 4-3.

4.2.2.4 Calculation of PCB Erosion

Equations 4-3 and 4-6 define a probabilistic model for predicting bottom cohesive sediment mass erosion and depth of scour as a function of shear stress and sediment physical properties. The model is probabilistic in that it presents a range of depth of scour estimates with associated probabilities based on the variability in experimental resuspension measurements. For a given scour depth, an estimate of the PCB erosion from cohesive sediments can then be estimated as a function of sediment PCB concentration using Equation 4-7.

$$P = \frac{S \times C_{PCB}}{\left(\frac{1000mg}{1g} \right)} \quad (4-7)$$

where:

- P* = quantity of PCBs eroded from cohesive sediments (g)
- S* = mass of solids eroded from cohesive sediments (kg)
- C_{PCB} = average cohesive sediment surficial PCB concentration (mg/kg).

In a stand-alone application of DOSM used to evaluate the impact of a 100 year peak flow, average surficial sediment PCB concentrations were used to provide a conservative screening estimate of eroded PCB. However, in long-term forecasts with HUDTOX, model simulations of PCB in individual PCB layers was used, rather than surficial averages.

4.2.3 Formulation for Non-cohesive Sediments

4.2.3.1 Background

Net erosion of non-cohesive sediments occurs when the sediment transport capacity of the flow exceeds the actual sediment burden being carried by the flow. A flow will have transport capacity for a *particular* particle diameter (size class) when the shear stress applied to those particles by

the flow exceeds the critical shear stress of the particle size class. The transport capacity of the flow is inversely related to the particle size; hence, differential scouring takes place, with the smaller particles being removed in greater proportion than the larger particles. The particle size distribution of the bed surface then shifts progressively towards larger particles. If sufficient large particles are present that cannot be transported under the flow conditions, the bed surface will come to consist primarily of the larger particles, with the smaller particles underneath sheltered from scour. This layer of coarse particles, called the armor layer, may persist until higher flows and their associated shear stresses erode it, causing further coarsening and the establishment of a new armor layer. The armor layer can be degraded by vertical mixing with the parent bed material and replenishment of fine material via deposition from the water column.

4.2.3.2 Equations

Borah (1989) gives equations for the depth of scour that will occur before the establishment of an armor layer. His formulation assumes a well-mixed surface layer with constant particle specific gravity, but different particle sizes. After a scour event and armoring, the result is a single surface layer of the smallest non-transportable particle size. The formulation may be viewed as conservative because the potential for finer particles to be trapped (hiding) in the armor layer is ignored. This means that the mass of sediment scoured to achieve armoring may be high because the fine particles that may be trapped are assumed to be scoured in order to achieve armoring. An active layer thickness is defined as:

$$T = \frac{D_a}{(1 - \phi)P_a} \quad (4-8)$$

where T is the thickness of the active layer (cm); D_a is the smallest armor size (cm); ϕ is the porosity of the bed material; and P_a is the fraction of all the armor sizes present in the bed material. D_a is computed using a modified version of the Shields Curve (Shields, 1936; van den Berg and van Gelder, 1993). The scour depth is then computed as:

$$E = T - D_a \quad (4-9)$$

where E is the scour depth (in cm). These equations have been applied and the results validated for laboratory (Little and Mayer, 1972) and field (Karim and Kennedy, 1982) data.

4.2.4 Time Scale of Erosion Estimates

The cohesive sediment scour calculations result in a mass estimate at the peak flow for an event assuming that the event peak shear stress is established essentially instantaneously. Experiments by Lick et al. (1995) indicate that this mass is eroded over the time scale of approximately one hour. The non-cohesive computations provide a mass estimate corresponding to scour down to the armoring depth. However, the time required to reach armoring depth cannot be directly calculated with the available models. Model predictions for non-cohesive sediments should therefore be considered “upper bound” estimates, as they are based upon the assumption that the flood event is of sufficient duration to allow erosion to proceed all the way down to the armoring depth. This upper bound estimate is suitable for determining the likelihood that the buried contamination can

be "reactivated", but it is not suitable for direct use in HUDTOX. Hence, non-cohesive sediment resuspension rates in HUDTOX were calibrated.

4.3 DOSM PARAMETERIZATION

4.3.1 Data

4.3.1.1 Distribution of Types of Bottom Sediment

The bedded sediments in Thompson Island Pool were differentiated as cohesive and non-cohesive based on side-scan sonar profiles of fine and coarse sediments (Flood, 1993). The analysis of sonar and sediment data suggested that the results of the 500 kHz digital image (i.e. mean digital number, or DN) can be successfully correlated to mean grain size. It was found that DN values less than about 40 generally correspond to finer grain sizes (mean size less than about 4 phi) while DN values greater than about 60 generally correspond to coarser sediments (coarse sand, gravel). For the purpose of characterizing the sonar images, sediment type is described as "finer" for DN less than 40, or as "coarse" or "coarser" for DN greater than 60.

The sonar maps were qualitatively divided into several categories including "coarse", "coarser", "finer", "island", and "rocky". These maps were digitized into a GIS coverage by TAMS Consultants, Inc. No sediments described as "coarse" were listed for Thompson Island Pool. The two sediment categories considered for this analysis to be significant sources of potentially erodible materials (due to magnitude of area and/or substrate type) were "coarser" – representing non-cohesive sediments – and "finer" – representing cohesive sediments. The area of non-cohesive sediments in Thompson Island Pool is approximately three times that of cohesive sediments.

4.3.1.2 Resuspension Experiments

Data used to parameterize the DOSM for cohesive Thompson Island Pool sediments were obtained from resuspension experiments described in a report by HydroQual (1995). This report contained two different sets of experimental data.

The first dataset came from an annular flume study, wherein sediments from three different locations in Thompson Island Pool were transported to a laboratory at the University of California at Santa Barbara and subjected to two types of experiments involving shear stress. Multiple shear stress tests were conducted by filling the flume with sediment, allowing it to compact for 1, 3, or 14 days with the flume at rest, and running (i.e., rotating) the flume at successively higher levels of shear stress, with steady state suspended sediment concentrations achieved (as indicated by concentration measurements at 30 minute intervals) before each shear stress increase. A continuous flow test was conducted by filling the flume with sediment and running it continuously for 47 days at a shear stress of about one dyne/cm², except that on several days the shear stress was increased to 5 dynes/cm² for two hours. Also, one multiple shear stress test similar to those described above was conducted.

The purpose of these experiments was to investigate the effects of bed compaction and to estimate the value of the critical shear stress, within the framework of the Lick equation, Equation 4-2.

Based upon these laboratory flume experiments, HydroQual (1995) concluded that: 1) the critical shear stress was approximately 1.0 dyne/cm^2 , 2) the maximum time since deposition (t_d) was 7 days (i.e., after 7 days no further significant bed compaction takes place), and 3) the exponent, n , for t_d was 0.5.

Although laboratory-derived values were used in the DOSM, there are environmental factors that were not accounted for in the laboratory experiments. Critical shear stresses from resuspension can vary seasonally due a number of factors. These include disturbance of sediments by benthic organisms, generation of gases from decomposition of organic matter, and uprooting of macrophytes. Also, the bed surface in the river may be much more varied than the planar surfaces achieved in the laboratory annular flume experiments. Nonetheless, these laboratory data were the best available information.

The second set of sediment resuspension measurements described in HydroQual (1995) consisted of field studies using a portable resuspension device, commonly called a shaker. Surficial sediment cores were collected at 20 cohesive sediment locations in Thompson Island Pool and 8 locations downstream; each location had one (Thompson Island Pool) or two (downstream) sets of three cores each. Each core was subjected to a shear stress in the shaker and the resulting resuspension potential was determined. The field study produced 107 resuspension potential-shear stress data pairs for the Hudson River, with 60 measurements specific to Thompson Island Pool. The shear stresses used in the field study ranged from 5 to 11 dynes/cm². Observed sediment erosion rates in Thompson Island Pool ranged from 0.06 to 28.84 mg/cm².

From the Thompson Island Pool-specific data, HydroQual (1995) assumed a Thompson Island Poolwide constant value of 3 for m , and back-calculated the core-specific values for a_0 necessary to produce the observed erosion. The methodology used to determine the value for m was not provided. HydroQual reported a mean value and standard deviation for a_0 of 0.071 (in units of mg-day^{1/2}/cm²) and 0.062, respectively, excluding certain results deemed to be outliers.

4.3.1.3 Non-Cohesive Particle Size Distributions

The Borah formulation described above (Equations 4-8 and 4-9) requires sediment data on particle size distribution, particle density, and wet bulk density (to calculate porosity). Unfortunately, a large percentage of the cores had missing or incomplete data for one or more properties. This obstacle was overcome in two ways: 1) missing data on particle density and bulk density were replaced by random deviates from the distributions found for the existing data, and 2) particle size distributions, which were occasionally incomplete on the large-particle end, were extrapolated by plotting the data for each core as $\ln(\text{size})$ vs. $\ln(\text{fraction})$ and extending the curves smoothly (this was done for 81 cores with data to extrapolate). The distribution used for particle density was normal with a mean of 2.438 g/cm^3 and a standard deviation of 0.262. The distribution used for wet bulk density was normal with a mean of 1.452 g/cm^3 and a standard deviation of 0.212; random deviates greater than 1.8 or less than 1.04 were rejected on the grounds of physical improbability and were replaced with new deviates. Particle size distributions were extrapolated as far as size fraction 2.7 percent or size 20 mm.

The data synthesis procedures (extrapolations and data substitutions) contribute to uncertainty. However, it was judged that more uncertainty would result from ignoring the sample datasets entirely where one parameter was missing.

4.3.1.4 1984 Cohesive Sediment PCB Concentration

The DOSM was used separately from HUDTOX to develop a conservative estimate of PCB mass and associated sediment eroded from cohesive sediment areas in response to a 100-year peak flow. This was accomplished by using the 1984 NYSDEC sediment PCB data from grab samples and coarsely-segmented sediment cores. Surface sediment core sections for these data were on average about 10 inches thick. The mean cohesive sediment surface sediment PCB concentration is approximately 32.5 mg/kg (USEPA, 1998a). This value was applied to the DOSM cohesive sediment elements, which are the same as the hydrodynamic model elements in Figure 3-2. The depth of scour in each element at the 100-year flow was converted to PCB mass eroded using this concentration.

Use of the 1984 median surface concentration results in a conservatively high estimate of PCB mass likely to be eroded under a future 100-year event for the following reasons:

1. The surface concentrations at the present have decreased significantly from those observed in 1984; and
2. The coarse vertical segmentation of the 1984 core samples likely resulted in an over-estimate of mean surface concentrations because peak concentrations are buried.

It should also be noted that the 1984 NYSDEC data do not represent total PCB and therefore do not provide an estimate of total PCB mass eroded. These data more closely represent the sum of the tri- and higher-chlorinated congeners, which is discussed in detail in Section 6.3.3.

Results of the mass erosion estimates from cohesive sediment are presented below in Section 4.4.3.1

4.3.2 Parameterization for Cohesive Sediments

There are several assumptions inherent in the application of Equations 4-3 and 4-6 to the shaker data for parameterization of the DOSM. These include:

- The value for critical shear stress obtained from the annular flume study is constant and applies throughout Thompson Island Pool;
- The sediment cores used in the resuspension studies represent an unbiased random sample of Thompson Island Pool cohesive sediments;
- The experimental shear stress values are exact;
- The statistical model is valid for extrapolation to higher values of shear stress than were used experimentally; and,

- The bulk density, at a specific location, used for converting erosion to depth of scour can be represented as a single number.

All statistical analyses were conducted using SYSTAT[®] Version 6.0 for Windows[®] (SPSS, 1996), and only data from Thompson Island Pool were considered. A linear regression of natural log erosion (in mg/cm²) vs. natural log τ produced an intercept (A) value of -3.829 and a slope (m) value of 2.906 (Figure 4-1). Of 60 Thompson Island Pool data points, two outliers were deleted; 58 data points were used. The outliers were identified solely on the basis that their Studentized residuals were too large (absolute value greater than 3.0). The regression R-squared value was 0.541, and p-values for both the regression constant and the slope were <0.00001. An analysis of the residuals strongly indicated that they could be assumed to be normally distributed. It was concluded on the basis of these and other statistical indications that the use of linear regression was supported by the data.

The value of 2.906 obtained for m is similar to the value of 3 reported by HydroQual (1995). Assuming from the flume studies that the maximum time since deposition (t_d) was 7 days, and the exponent, n, for t_d was 0.5, the lumped term corresponds to a value of a_0 of 0.0575. This value is well within one standard deviation of the value reported by HydroQual (1995), (Section 4.3.1.2).

4.3.3 Parameterization for Non-cohesive Sediments

The Borah formulation described previously was used to develop a relationship between depth of scour and shear stress for the various size fractions in each core sample. The data points were plotted on a log-log plot. One linear relationship was found for shear stresses below about 5 dynes/cm², and another for shear stresses above 5 dynes/cm² (Figure 4-2).

Data for determining particle size distributions are not available throughout Thompson Island Pool, but shear stresses are available on a fine scale. A predictive relationship between armoring depth and shear stress was sought. Assuming that the core particle size distributions are typical of particle size distributions throughout Thompson Island Pool, the relationships between armoring depth and shear stress discussed above can be considered predictive, even where the particle size distribution is unknown. Therefore, a linear regression was performed to fit the 355 data points above 5 dynes/cm² (shear stresses lower than 5 would not be, of course, as significant in producing erosion) to Equation 4-10.

$$\ln(\text{Depth}, cm) = A + m \times \ln(\text{ShearStress}, \text{dynes} / \text{cm}^2) \quad (4-10)$$

A constant (A) value of -1.6335 and a slope (m) value of 1.2407 were found. The R-squared value was 0.5, and the p-values were less than 0.00001. The spread around the regression line is considerable, encompassing approximately two orders of magnitude. This is not unexpected, since a similarly large spread was observed for the cohesive sediment correlation. The graph of armoring depth vs. shear stress, with the regression line shown, is provided in Figure 4-2.

4.4 DOSM APPLICATION

4.4.1 Application Framework

An ARC/INFO-based Geographical Information System (GIS) (ESRI, 1997) was utilized to associate sediment and hydrodynamic properties with geographic locations and areas in Thompson Island Pool. Computations made use of shear stresses estimated at the nodal locations where flow field information was available from the Thompson Island Pool Hydrodynamic Model (Chapter 3). The sediments were spatially differentiated into cohesive and non-cohesive areas, as described in Section 4.3.1, with separate analyses conducted for each sediment type.

It is important to note that the DOSM, as a stand-alone model, has not been designed to simulate the subsequent transport and redeposition of eroded sediments. It evaluates only the mass of bottom sediments potentially mobilized at a specified peak flow. The HUDTOX mass balance model includes a dynamic representation of solids and PCB transport and fate in the water column and bedded sediments.

The DOSM was used to develop relationships between river flow and cohesive sediment resuspension in Thompson Island Pool that were subsequently used in the HUDTOX model to compute flow-dependent cohesive sediment resuspension. Details of the development of these equations are presented in Section 5.2.3.2. The relationship between the DOSM and HUDTOX ensures internal consistency in representation of flow-dependent resuspension for cohesive sediments between these two models. Use of the non-cohesive sediment scour equations to determine non-cohesive resuspension rates in HUDTOX was not possible due to limitations of the theoretical formulations. As discussed in Section 4.2.4, the non-cohesive armoring equation only represents the maximum potential scour and the actual armoring depth depends on the dynamic characteristics of the flood hydrograph.

4.4.2 Probabilistic Model Application to High Resolution Coring Sites

As discussed above, a Monte Carlo approach was used to assess probability of sediment scour depths based on the variability in site-specific measurements of cohesive sediment resuspension properties. This was done specifically for cohesive sediment locations where USEPA collected high-resolution sediment core PCB profiles, and the range of probable scour depths was compared to these profiles to assess the likelihood that higher PCB concentrations would be uncovered in response to scour under a 100-year flow event. Probabilistic calculations were not conducted for non-cohesive sediments because the method already provides an upper-bound calculation.

As part of the Phase 2 monitoring program, sediment cores were taken at five locations in areas containing cohesive sediments in Thompson Island Pool, and analyzed at a high vertical resolution. These sediment cores exhibited fairly high long-term sediment burial rates and showed peak PCB concentrations in excess of 2,000 ug/g (dry weight). Core collection locations were specifically established in highly depositional areas of the River. Although these five locations are not necessarily representative of PCB profiles in cohesive sediments in the entire Pool, they were used because each site contained detailed measurements of sediment physical-chemical properties that were required for a finely resolved analysis of resuspension potential. Location-specific inputs consisted of predicted shear stress at each coring location and sediment bulk density

measured for each core. Table 4-1 lists location-specific input data for each of the five cores. For depths greater than 2 cm, core average values of dry bulk density were used for calculating depths of scour.

Table 4-2 contains summary results for each of the five sediment core locations. The predicted median depths of scour for the five locations, shown in the second column of Table 4-2, range from less than 0.08 (HR-19) to almost 4 cm (HR-25). The third and fourth columns in Table 4-2 show the range of predicted scour depths encompassing the middle 90 percent of expected values (i.e. 5th to 95th percentile) for each core location. By comparing the depth of scour estimates in Table 4-2 with the input data in Table 4-1, one can see that bottom shear stress is a very strong determinant of erodibility in these cohesive sediments.

The median predicted depth of scour provides information on quantities of solids that can potentially resuspend during an event; however, this information alone does not define the quantity of PCBs that can potentially resuspend. The last column in Table 4-2 contains the observed depth of the total PCB peak at each of the five core locations. By comparing median predicted depths of scour and observed depths of PCB peaks, a more complete picture of potential PCB erodibility emerges. These results are depicted graphically in Figure 4-3, which show the total PCB (as originally measured) profiles with depth for each of the five sediment cores, along with the 5th, 50th and 95th percentile predicted depth of scour for each of the five core locations. Results indicate that Core HR-25 is likely to experience scour of sufficient magnitude to substantially erode the PCB peak at that location. However, even if erosion occurs at the 95th percentile depth, PCB peaks at the other four locations are predicted to be unscoured (i.e. the PCB peaks are likely to stay intact after a 100-year peak flow event).

4.4.3 Poolwide Model Application

4.4.3.1 Cohesive Sediments

Equations 4-3 and 4-6 can conveniently be used to estimate the total mass of solids remobilized from cohesive sediments throughout Thompson Island Pool, and the mean depth of scour in cohesive sediments, by means of a Monte Carlo Analysis. The cohesive sediment areas of Thompson Island Pool were subdivided into polygons of constant shear stress and dry bulk density by intersecting coverages for these properties in the GIS system discussed in Section 4.4.1. The Monte Carlo technique was employed to calculate the depth of scour and the mass scour by randomly varying parameters in the resuspension equation according to variability in the site-specific resuspension measurements. Poolwide results for mass scour were obtained by summing the results at all locations, while an area-weighted average was calculated as the mean depth of scour. The calculation was repeated many times to get a valid statistical distribution of results.

Monte Carlo calculations were performed with the Crystal Ball[®] computer program (Decisioneering, Inc., 1996). Depth and mass of scour were computed together, with 3,000 repetitions conducted; a sensitivity analysis of the number of repetitions demonstrated that 3,000 repetitions were adequate to produce consistent results. The results were plotted as cumulative percent vs. mean depth of scour or mass of scour, respectively. Expected values for mean depth and mass of scour were estimated by the mean of the Monte Carlo trials and are shown in Table 4-3.

Figure 4-4 shows the results for mean depth of scour. Most of the predictions fall into the range of about 0.3 to 0.4 cm. There is, therefore, a high probability that a future 100-year peak flow would result in a mean depth of scour of between 0.3 and 0.4 cm. Figure 4-5 shows the results for total solids scoured. Most of these predictions fall into the range of about 1,500,000 to 2,000,000 kg. There is, therefore, a high probability that a future 100-year peak flow would result in a mass scour of between 1,500,000 and 2,000,000 kg.

The PCB concentration in Thompson Island Pool surficial sediments was estimated to be 32.5 mg/kg (USEPA, 1998a). Using this concentration value in Equation 4-6 with the above estimate of 1,500,000 to 2,000,000 kg of solids erosion provides an approximate range of gross PCB erosion of 49 to 65 kilograms. This is a conservative estimate due to the use of the 1984 PCB data, as discussed in Section 4.3.1.4. The range of solids scoured represents uncertainty due to variability in sediment properties. This range could be applied to a more recent estimate of surface sediment concentrations to get a more refined estimate of the range of expected PCB mass scoured.

4.4.3.2 Non-Cohesive Sediments

Equation 4-9 was applied using estimated shear stresses in non-cohesive sediment areas. For the 100-year peak flow, the mean, non-area-weighted Thompson Island Pool non-cohesive sediment armoring depth is 13.1 cm. Therefore, 13.1 cm is an estimate of the expected average upper bound erosion from non-cohesive sediment areas in Thompson Island Pool resulting from a 100-year peak flow. Upper bound estimates of erosion at specific non-cohesive sediment locations throughout Thompson Island Pool ranged from 1.5 to 42 cm. This estimate of erosion in non-cohesive sediment areas is fundamentally different from, and not directly comparable to, the above estimates of erosion in cohesive sediment areas. Those cohesive estimates are predictive of the actual erosion expected to occur under the specified conditions, including an uncertainty band for the prediction. It is reasonably certain that the actual erosion would be less than the non-cohesive sediment erosion estimate, perhaps much less. Given the difference in the nature of the estimates, it is not surprising that the 13.1 cm upper bound on the average erosion from non-cohesive sediment areas of Thompson Island Pool substantially exceeds the 0.317 cm expected value of the mean depth of scour from cohesive sediment areas of Thompson Island Pool. If this upper bound scour depth were achieved in non-cohesive sediments, *some* areas *might* result in increased surface sediment PCB concentrations based on observations of the PCB distribution in the various sediment PCB datasets. For example, the 1977 NYSDEC sediment core data and 1991 GE composite core data show that higher PCB concentrations exist below the surface sediment layer in non-cohesive sediments. This can be observed from inspection of Figures 6-34 and 7-21 through 7-23, which present data used in the development of sediment initial conditions and model calibration datasets.

4.5 DOSM FINDINGS

The Depth of Scour Model (DOSM) was developed for Thompson Island Pool specifically to address the likelihood of a 100-year flood event uncovering buried high concentrations of PCBs due to erosion of surface sediments. Two separate applications of the DOSM model were conducted to address this question. These applications found that:

4. A probabilistic calculation of 100-year peak flow scour depths at the five USEPA

high resolution sediment coring locations in Thompson Island Pool; and,

5. A conservatively high estimate of total PCB mass eroded during a 100-year peak flow from cohesive sediments in the Pool.

These results lead to the following major findings:

- Predicted scour depths under 100-year peak flow conditions are small and will not result in significant remobilization of buried sediments in Thompson Island Pool cohesive sediments;
- Non-cohesive scour depths could only be computed as an upper bound because the time to armoring is very uncertain and could not be determined in the DOSM framework. If this upper bound were achieved, scour in non-cohesive sediment areas may result in increased surface sediment PCB concentrations in some areas;
- Even at the 95th percentile of scour depth, the 100-year peak flow does not cause scour to elevated PCB concentrations at the high-resolution sediment core locations; and,
- Based on a conservative estimate of the mass of PCBs resuspended under a 100-year peak flow, the 100-year flow will result in only a slightly larger amount of PCBs resuspended than may be expected during typical annual high flow events.

5. FATE AND TRANSPORT MASS BALANCE MODEL DEVELOPMENT

5.1 INTRODUCTION

Chapter 5 describes the development of the Hudson River Toxic Chemical Model (HUDTOX), the principal transport and fate modeling tool in this Reassessment. This chapter presents the conceptual framework and the governing equations for model state variables and process mechanisms as well as details on the computer hardware and software operating environment. The following major sections are included in Chapter 5:

- 5.2 General Model Approach
- 5.3 Water Transport
- 5.4 Solids Dynamics
- 5.5 PCB Dynamics
- 5.6 Model Spatial Segmentation
- 5.7 Model Implementation

5.2 MODEL APPROACH

5.2.1 Introduction

HUDTOX is the principal transport and fate modeling tool in this Reassessment. HUDTOX is a time-variable, three-dimensional mass balance model. It is a fully-integrated representation of solids and PCB concentrations in the water column and bedded sediments. HUDTOX was applied to the entire Upper Hudson River from Fort Edward to Federal Dam at Troy. Because a disproportionate amount of PCB-contaminated sediments is contained in Thompson Island Pool (TIP), and because there is substantially more data available for the Pool HUDTOX included greater spatial resolution for the Thompson Island Pool than for the river downstream of Thompson Island Dam (TID). In the Pool, HUDTOX is two-dimensional in the water column and three-dimensional in the sediments. Between Thompson Island Dam and Federal Dam, it is one-dimensional in the water column and three-dimensional in the sediments.

The principal model application was a long-term historical calibration for a 21-year period from 1977 to 1997 for Tri+ PCBs. Short-term hindcast applications were also conducted from 1991 to 1997 in order to test the long-term historical calibration for several PCB forms (5 congeners, and total PCBs) exhibiting a range of physical-chemical properties (e.g., sorption to solids, Henry's Law constants, molecular weights, etc.). The calibrated model was also used to conduct a validation simulation with an independent dataset acquired in 1998 for the Upper Hudson River. Calibration parameters were not changed in this validation exercise. The calibrated model was then used to conduct forecast simulations for 70-year periods beginning in 1998. These forecast simulations were intended to estimate long-term system responses to continued No Action and impacts due to a 100-year peak flow.

5.2.2 Conceptual Framework

Three different mass balances are represented in HUDTOX: (1) a water balance; (2) a solids balance; and (3) PCB mass balances. A water balance is necessary because PCB dynamics are influenced by river flow rates and mixing rates. A solids balance is necessary because PCB dynamics are influenced by the tendency of PCBs to sorb, or attach, to both suspended and bedded solids in the river. Finally, a PCB mass balance itself is necessary to account for all sources, losses and internal transformations of PCBs in the river.

HUDTOX represents PCBs in both the water column and bedded sediments. PCBs in each medium are comprised of three phases:

- Truly dissolved;
- Bound to dissolved organic carbon (DOC); and,
- Sorbed to total solids.

Organic carbon is the principal sorbent compartment for hydrophobic organic chemicals in aquatic systems. A time-dependent mass balance was developed for the suspended and bedded solids, and organic carbon fractions were assigned to these solids based on data. Dissolved organic carbon (DOC) was not simulated in the mass balance. Instead, concentrations were held constant in the sediment bed and the water column. These concentrations were developed from site-specific data and specified as model inputs.

HUDTOX computes time-dependent mass balances for two state variables: solids and PCBs (total PCBs, Tri+, and congeners BZ#4, BZ#28, BZ#52, BZ#[101+90], or BZ#138, depending on the particular application). It assumes that within each model spatial segment a local equilibrium exists among the three different PCB phases. It computes the PCB distribution among these phases by applying an organic carbon-based partition coefficient to the organic carbon concentration of each sorbent (dissolved and particulate organic carbon). This local equilibrium assumption allows the mass balance model to compute only a single PCB state variable while still representing the specific process kinetics operating on each PCB phase. For example, only the solids-sorbed PCBs will settle; therefore, the settling velocity determined through the solids mass balance is applied to only the solids-bound phase of PCBs within each spatial segment. On the other hand, only truly dissolved PCBs can exchange across the air-water interface; hence, that process is applied to only dissolved phase PCBs in water column segments at the air-water interface.

Figure 5-1 contains a conceptual diagram for HUDTOX that illustrates PCBs in the water column and surface sediment spatial segments. This diagram displays the three phases into which PCBs can be partitioned, as well as the model processes which are applied to either the whole PCB form or to an individual PCB phase. Thus, each arrow into or out of a given control volume (or spatial segment) represents a distinct source or sink flux process that operates on the PCB state variable and forms its full mass balance equation for that segment. The simultaneous solution of those mass balance equations permits quantification of the relationship between external inputs and within-system concentrations of PCBs over space and time.

5.2.3 Governing Equations

This section presents a summary of the state variables and processes in the HUDTOX mass balance model. The HUDTOX model is a modified version of the USEPA WASP toxic chemical model WASP5/TOXI5. The equations and framework are essentially the same except for two major enhancements; one relates to handling of sediment bed segments under erosion and scour, and the second relates to sediment scour formulations.

The HUDTOX model code was originally developed using an earlier version of the WASP model (WASP4/TOXI4) which was later updated by EPA to reflect coding changes and various enhancements. The primary source for documentation of the updated WASP5/TOXI5 model is Ambrose et al. (1993). This document can be obtained via the Internet by downloading it from the USEPA Center for Exposure Assessment Modeling (CEAM) web site located at "http://www.epa.gov/epa_ceam/wwwhtml/ceamhome.htm." The HUDTOX model description presented in this section is a summarized version of the WASP5/TOXI5 documentation contained in Ambrose et al. (1993). Details are presented for those processes in HUDTOX that were modified from the WASP5/TOXI5 model. Unless specifically noted, the HUDTOX model processes are identical to those in the WASP5/TOXI5 model.

The mass balance for the HUDTOX model accounts for all user-specified material entering and leaving the system by external loading, advective and dispersive transport, settling and resuspension, and physical, chemical, and biological transformations. The generalized HUDTOX mass balance (partial differential) equation for an infinitesimally small fluid volume in three-dimensions is:

$$\begin{aligned} \frac{\partial C}{\partial t} = & - \frac{\partial}{\partial x}(U_x C) - \frac{\partial}{\partial y}(U_y C) - \frac{\partial}{\partial z}(U_z C) \\ & + \frac{\partial}{\partial x}\left(E_x \frac{\partial C}{\partial x}\right) + \frac{\partial}{\partial y}\left(E_y \frac{\partial C}{\partial y}\right) + \frac{\partial}{\partial z}\left(E_z \frac{\partial C}{\partial z}\right) \\ & + S_L + S_B + S_K \end{aligned} \tag{5-1}$$

where:

- C = concentration of the water quality constituent state variable, mg/L (g/m³) [M/L³]
- t = time, days [T]
- U_x, U_y, U_z = longitudinal, lateral, and vertical advective velocities, m/day [L/T]
- E_x, E_y, E_z = longitudinal, lateral, and vertical diffusion (dispersion) coefficients, m²/day [L²/T]
- S_L = direct and diffuse loading rate, g/m³-day [M/L³/T]
- S_B = boundary loading rate (including upstream, downstream, sediment, and atmospheric), g/m³/day [M/L³/T]
- S_K = total kinetic transformation rate; positive indicates a source,

negative indicates a sink, g/m³/day [M/L³/T].

By expanding the infinitesimally small control volumes into larger adjoining “segments” and specifying transport, loading, and transformation parameters, HUDTOX implements a finite-difference form of Equation 5-1 to solve for the concentration of each water quality state variable over time. A one-dimensional simplification of Equation 5-1 may be expressed by assuming vertical (z-domain) and lateral (y-domain) homogeneity:

$$\frac{\partial}{\partial t}(AC) = \frac{\partial}{\partial x} \left(\overset{\text{Term 1}}{-U_x AC + E_x A \frac{\partial C}{\partial x}} \right) + \overset{\text{Term 2}}{A (S_L + S_B)} + \overset{\text{Term 3}}{A S_K} \quad (5-2)$$

where:

A = cross-sectional area, m² [L²]

This equation represents the three major classes of water quality processes:

- Transport (term 1);
- External loading (term 2); and,
- Transformation (term 3).

These processes, which describe the fate of each HUDTOX solids and PCB model state variable, are discussed in the following paragraphs. The finite-difference derivation of the general WASP mass balance equations and the specific solution technique implemented to solve these equations are described in Ambrose et al. (1993).

5.3 WATER TRANSPORT

The physical transport of water column solids and PCBs in HUDTOX is governed principally by advective flow and dispersive mixing in the water column. Each are described below. Advective water column flows are important because they control the downstream transport of dissolved and particulate pollutants in many water bodies. In addition, changes in velocity and depth resulting from variable flows can affect such kinetic processes as reaeration, volatilization, and photolysis. HUDTOX tracks each separate inflow specified by the user from its point of origin and through each segment until it exits the model network. For each inflow, the user must supply a continuity or unit flow response function (i.e., flow routing) and a time function. For the HUDTOX model, the flow routing information is based upon the RMA-2V results for the Thompson Island Pool two-dimensional water column segmentation grid. The advective flows are simply routed directly through the one-dimensional HUDTOX segmentation existing downstream of the Thompson Island Pool. Representation of short-term transient effects due to storage and drainage were deemed unimportant considering the goal of the HUDTOX model, which was to describe long-term PCB concentration trends.

The flow continuity function describes how various flow inputs are routed throughout the model network. The time function describes the temporal variability of the inflow. The actual flow

between segments that results from a given inflow is the product of the time function and the continuity function. If several inflow functions are specified between any segment pair, then the total flow between segments is computed as the sum of the individual flow functions. In this manner, the effect of several tributaries joining, density currents, and wind-induced flow patterns can be described in a simple manner.

Hydraulic relating describing depth and velocity to stream flow are based on formulations developed by Leopold and Maddox (1953) which describe empirical observations of the velocity and depth to stream flow relationship. These relationships, which are used for determining chemical air-water mass transfer rates (gas phase absorption and volatilization), are described in Ambrose et al. (1993). For the Thompson Island Pool portion of the Upper Hudson River, the HUDTOX model coefficients describing this relationship were developed from the RMA-2V hydrodynamic model described in Chapter 3. The relationship for downstream reaches was developed using correlations between surface water elevations and flow (USEPA, 1997). Note that these relationships are only used to affect chemical gain or loss within a water column model segment (through volatilization); they do not affect water volume or advective or dispersive transport of chemicals between model segments.

Dispersive water column exchanges significantly influence the transport of dissolved and particulate pollutants by mixing between water of different concentrations. In rivers, longitudinal dispersion can be an important process in diluting peak concentrations that may result from dynamic (unsteady) loads or spills. Natural or artificial tracers such as dyes, salinity, conductivity or heat (temperature) are often used to calibrate dispersion coefficients for a model network.

The dispersive exchange between HUDTOX segments i and j at time t is given by:

$$\frac{\partial M_i}{\partial t} = \frac{E_{ij}(t) \cdot A_{ij}}{L_{cij}} (C_j - C_i) \quad (5-3)$$

where:

M_i = mass of constituent (state variable) in segment i , g [M]

C = total constituent (state variable) concentration, mg/L (g/m^3) [M/L^3]

$E_{ij}(t)$ = dispersion coefficient time function for exchange "ij", m^2/day [L^2/T]

A_{ij} = interfacial area shared by segments i and j , m^2 [L^2]

L_{cij} = characteristic mixing length between segments i and j , m [L] .

The exchange coefficient may also be expressed as a mass transfer velocity by dividing the dispersion coefficient by the characteristic mixing length:

$$v_{ij}(t) = \frac{E_{ij}(t)}{L_{cij}} \quad (5-4)$$

where:

$$v_{ij}(t) = \text{mass transfer rate for exchange "ij", m/day [L/T]} .$$

5.4 SOLIDS DYNAMICS

HUDTOX calculates sediment and PCB concentrations for every segment in a model grid that includes surface water, surficial sediment bed, and underlying sediment bed layers. During simulation, solids are treated as a conservative constituent that is advected and dispersed through water column segments, settles to and resuspends from surficial sediment segments, and moves through the subsurface bed through burial/scour of the surficial bed or through particle mixing. Due to large uncertainties in externally contributed solids loads (see Chapter 6), internal production and decay of water column biotic solids through primary production was not included in the HUDTOX model calibration application to the Upper Hudson River. The contributions of primary production and decay of solids is dwarfed by the high upstream and tributary solids loads.

5.4.1 Solids Gross Settling

HUDTOX differs from WASP5/TOXI5 with respect to gross settling of suspended solids from the water column to the sediment bed in order to capture effective differences in settling characteristics between cohesive and non-cohesive sediment areas. Constant settling velocities (not dependent on flow or other factors) are specified in HUDTOX with different rates specified for cohesive and non-cohesive sediment areas. Settling velocities are constant for each sediment type throughout the river under all flow conditions. This approach was developed to be consistent with the model calibration strategy presented in Chapter 7. The differences between cohesive and non-cohesive settling velocities arise as a result of lower resuspension and higher deposition for cohesive sediment areas relative to non-cohesive sediment areas. Lower resuspension occurs in cohesive sediment areas due to lower flow velocities and shear stress in these areas. Due to the lower flow velocities in cohesive sediment areas, higher deposition occurs relative to non-cohesive areas.

The rationale and approach for specification of the cohesive and non-cohesive settling rates specified for HUDTOX in this RBMR calibration is presented in Chapter 7 of this report.

5.4.2 Cohesive Sediment Flow-Driven Resuspension

The algorithm for flow-driven resuspension of cohesive sediments used in the DOSM (Equation 4-5) was incorporated into the HUDTOX model. Total sediment erosion (ϵ , mg/cm²) is incrementally applied to the rising side of the flood hydrograph. Non-linear correlations were developed relating the DOSM-predicted sediment erosion in each segment as a function of flow measured at Fort Edward. Equations of the following form were fit to DOSM results correlating the mass of cohesive sediment erosion to flow:

$$e = \alpha_1 + \alpha_2 \cdot Q_x^{\alpha_3} \quad (5-5)$$

where:

$$\begin{aligned} \epsilon &= \text{cohesive sediment erosion, mg/cm}^2 \\ Q_x &= \text{advective flow in 1000's of cfs} \end{aligned}$$

- $\alpha_1 =$ empirical constant fit to DOSM results, mg/cm^2
- $\alpha_2 =$ empirical constant fit to DOSM results, $\text{mg}/\text{cm}^2/1000 \text{ cfs}$
- $\alpha_3 =$ empirical constant fit to DOSM results, dimensionless.

The cohesive sediment erosion is converted to an effective resuspension rate (v_{RH} , m/day) in the HUDTOX model over each model time step during the rising side of a flood hydrograph. Computational time steps in the model vary between approximately 5 and 25 minutes. This approach is consistent with observations by Lick et al. (1995) that most resuspendable material is mobilized in approximately one hour.

In the HUDTOX model, resuspension occurring over previous model time steps within an increasing hydrograph is tracked such that total cumulative erosion equals the amount computed using the maximum shear stress during that event. This mass flux tracking occurs in an incremental fashion. The amount eroded during any given model time step being dependent on the change in flow and the cohesive sediment solids concentration (dry bulk density). The total amount of sediment erosion is limited by the maximum predicted erosion (ϵ_{max}) associated with the peak flow. Flow-driven resuspension effectively stops depleting the existing sediment bed once the peak flow is reached and that cohesive sediment armoring is assumed to have occurred.

HUDTOX also includes a recovery period (t_{rec} , days) in which the maximum erosion constraint prevents subsequent near-term smaller floods from eroding bedded cohesive sediments that have reached an armored condition. Any solids depositing on the sediment bed during the recovery period are allowed to erode based on Equation 5-5, but only to the extent that freshly deposited material is available. Once the recovery period is ended, no differentiation is made between freshly deposited solids and older “bedded” solids in the surficial sediment layer. At this point, all the surficial sediments are again subject to scour based on Equation 5-5 (i.e., armoring of the cohesive sediment bed ceases). Model applications employing the Lick resuspension formulation for cohesive sediments have generally used a recovery or “sediment aging” timeframe of 7 days for the surficial sediment layer (Gailani et al., 1991; Ziegler et al., 1994). Lick et al. (1995) cites a range of 1 to 28 days for the consolidation process (i.e., the consolidation or “aging” of fresh sediments to a condition consistent with sediments lying below this recently deposited material) to take place based on experiments using sediments from various freshwater river systems.

5.4.3 Non-Cohesive Sediment Resuspension

In contrast to cohesive sediments, the DOSM model only provides a single, upper-bound estimate of scour for non-cohesive sediments. The single estimate is characterized as an upper-bound because it occurs when armoring is achieved and is a function of deposition and time over which peak shear stresses are experienced (Chapter 4). Consequently, the non-cohesive scour formulation from DOSM was not incorporated into the HUDTOX model.

The representation of the flow-driven resuspension of non-cohesive sediments in HUDTOX was developed for the calibration strategy presented in Chapter 7. This strategy attempts to describe mean high and low-flow solids dynamics. It is represented in HUDTOX model by specification of a constant high-flow resuspension velocity operative during scouring conditions. Non-cohesive sediment scour is considered insignificant below specified flow thresholds, which are spatially

variable in the model. Thus, non-cohesive resuspension rates switch between zero and the specified high flow resuspension rate.

No attempt has been made in HUDTOX to simulate armoring conditions in the non-cohesive sediments. The calibration approach relies on accurately capturing the long-term behavior of the system based on solids burial rates, surface sediment PCB concentration trends, and in-river mass transport of solids and PCBs, rather than description of event dynamics which vary over small time scales. This is consistent with the overall objective of this modeling study presented in Chapter 1. Chapter 7 presents the calibration approach and a discussion of the model parameters specified to simulate non-cohesive resuspension during high flow scouring conditions. These parameters include: the transition flow between scouring and non-scouring conditions for each reach of the river, and the calibrated non-cohesive resuspension rate for scouring flow conditions.

5.4.4 Sediment Bed Particle Mixing

Bioturbation and other physical processes can result in vertical mixing of solids (and sorbed chemicals) within the bedded sediment. Particle mixing rates tend to be site-specific and can vary seasonally due to temperature influences on biological activity (e.g. McCall and Tevesz, 1982). Sediment bed particle mixing is an important model consideration.

Sediment mixing processes are represented in HUDTOX by effective particle diffusion coefficients. The resulting particle diffusion transfer between sediment layers induces a flux of sorbed contaminants between sediment layers in the model. The direction of flux is determined by the concentration gradient between layers. The form of the particle mixing equation is similar to that represented by Equation 5-3, but with the concentration gradient expressed in terms of the solids concentrations (and sorbed chemical concentrations) in the sediment layers across which the flux takes place. Particle mixing rates are not subjected to temperature influences in the model.

The parameterization of particle mixing in HUDTOX requires specification of the depth over which particle mixing occurs and the effective particle diffusion rates between sediment layers. Specification particle mixing depths and particle diffusion rates is presented in Chapter 6 and further developed in Chapter 7.

5.4.5 Scour and Burial

The HUDTOX model uses an improved sediment bed handling approach from that in WASP5/TOXI5. The HUDTOX approach maintains and allows the formation of a distinct vertical chemical profile through the bedded sediments. This modified sediment bed handling routine is a better representation of transport of PCB mass through the sediment bed because it maintains the integrity of the deeply buried sediment layers as burial or scour occurs. The standard WASP5/TOXI5 model can exhibit significant numerical dispersion over long simulation periods, leading to a “smearing” of vertical contaminant profiles.

To insure the maintenance and formation of a distinct vertical profile, the following modifications were made to WASP5/TOXI5: 1) use of a quasi-Lagrangian sediment bed handling routine; and, 2) use of an archival stack of deep sediment layers as a dynamic boundary condition to track PCB mass beneath the computational grid. The following paragraphs describe the implementation of

this alternative bed handling through a set of modifications to the WASP5/TOXI5 scour and burial processes.

The revised sediment bed handling routine maintains the integrity of the deeply buried sediment profile as sedimentation and erosion occur. With the revised framework, the surficial sediment layer volume varies over time due to deposition and resuspension. Thus variation continues until either erosion or burial is triggered based on the volume (or equivalently, the thickness) reaching a specified minimum or maximum level. For burial, the trigger is based on a doubling of the surficial sediment thickness. Erosion is triggered by depletion (or near depletion) of the original surficial sediment volume. Essentially, the HUDTOX model bed handling implements a quasi-Lagrangian (or floating frame of reference) approach to burial and scour versus the WASP/TOXI5-based quasi-Eulerian (fixed frame of reference) approach.

Figures 5-2 and 5-3 illustrate the manner in which HUDTOX implements respectively scour and burial of surface sediment segments. In the HUDTOX bed handling framework, burial results in no numerical mixing of chemicals to deeper sediments, because the surface sediment segment is simply split into two and renumbering of the segments is triggered whenever its volume doubles. Erosion of the surface sediments still provides a degree of mixing between the surface sediments and the immediate segment below. The degree of this mixing is dependent on the amount of sediment remaining in a surface segment once it has been effectively depleted. However, no additional mixing occurs through the deeper sediment segments as a result of the HUDTOX bed handling procedure. These deeper segments are subject to renumbering when erosion occurs, but they still maintain their original pre-erosion characteristics. As described in the previous discussion of particle mixing, HUDTOX allows user-specified vertical mixing (via particle mixing and/or diffusion) through the active sediment bed to represent the effects of bioturbation and other processes (e.g., ice scour, propagation of bed load waves, prop wash, etc.) which serve to maintain partially mixed conditions through some depth of the sediment bed. Thus, the degree of vertical “smearing” of sediment concentration profiles is user-controlled, rather than being dependent upon the sedimentation time utilized in the standard WASP5/TOXI5 model framework.

In order to provide long-term tracking of sediment layer PCB concentration, and allow possible future exposure of deeply buried PCBs, a second modification of the WASP5/TOXI5 framework maintains an “archival” stack of deep sediment layers beneath the existing simulated bed segments. A user-defined reserve stack of deep sediment layers can be specified to underlie the existing simulated bed segments with distinct stacks for each surface sediment segment. In essence, the archive stacks provide a dynamic boundary condition for the bottom sediments. The stacks are not part of the computational grid, except to the extent that layers are moved between the stack and the model grid to compensate for burial or erosion of the surface sediment segments. The process of constituent decay is not represented in the archive stack.

When erosion results in a surface sediment segment being depleted, then “renumbering” of the segments is triggered as previously described. Additionally, the top layer of the archival stack is then incorporated within the computational grid as a new bottom sediment segment. During periods of deposition, the surface layer is allowed to grow in thickness (the bed solids density is kept constant) until renumbering is triggered, based on a doubling of the surface sediment volume. The surface segment is then split into two layers and the sediment segments are renumbered accordingly. Additionally, the bottom sediment layer is removed from the computational grid and

placed on the top of the archive sediment stack. The archive stack is allowed to grow or shrink as needed in response to burial or erosion of the surface sediment segments. A significant advantage of using the sediment archive stack relates to its minimal effect on the computational requirements and execution speed of the model. This allows for improved vertical resolution of the sediment bed without excessively increasing memory and runtime requirements.

The HUDTOX approach for sediment scour and burial requires that the upper portion of the sediment bed be composed of vertical layers of equal thickness at the beginning of the model computations. This insures that long periods of scour and deposition will not cause changes to the basic physical characteristics (e.g. original volume and thickness) of the surface layer sediments when deposition or scour triggers the bed handling mechanism.

5.5 PCB DYNAMICS

In the environment, organic chemicals may transfer across the different environmental media (air, water, and sediment) and may be degraded and/or transformed by a number of physical-chemical and biological processes. Cross-media PCB transfer processes within the HUDTOX model framework include equilibrium sorption and volatilization (air-water exchange). PCBs may also be transformed within HUDTOX through degradation as expressed by a first-order rate equation to represent the effect of dechlorination and/or destruction as a net mass loss over time. PCB dechlorination or degradation processes are not represented in the HUDTOX model for this application to the Upper Hudson River. Other chemical transformation processes (hydrolysis, photolysis, and chemical oxidation) are included within the overall WASP5/TOXI5 framework. Detailed descriptions of these processes are contained in Ambrose et al. (1993).

5.5.1 Equilibrium Sorption

Sediment particle dynamics are important in controlling the transport, transformation and fate of PCBs in aquatic systems due to the tendency of PCBs to sorb, or bind, to both suspended and bedded solids (Eadie and Robbins, 1987). Karickhoff et al. (1979) and Karickhoff (1984) have shown that organic carbon is the principal sorbent compartment for hydrophobic organic chemicals, such as PCBs, in aquatic systems. In addition to organic carbon in particulate form, dissolved organic carbon (DOC) can also be an important sorption compartment in determining PCB fate (Eadie et al., 1990; Bierman et al., 1992). Partition coefficients are used to characterize the distribution of chemical among three apparent phases: dissolved, particulate-bound, and DOC-bound.

The assumption of equilibrium partitioning in a natural system is reasonable when PCB sorption kinetics are rapid relative to other processes affecting water and sediment concentrations. There is some evidence of non-equilibrium conditions in the mainstem of the Upper Hudson River; however, a detailed investigation by USEPA (1997) found that the assumption of equilibrium partitioning was a valid approach for the spatial-temporal scales in the HUDTOX model applications. Section 6.9 provides further information on the available site-specific data for estimating the partition coefficients used for the PCB forms in the HUDTOX model.

The partition coefficients depend upon characteristics of the chemical and the sediments or DOC on which sorption occurs. PCBs are non-polar, hydrophobic, organic compounds. The sorption

of these compounds correlates well with the organic carbon fraction (f_{OC}) of the sediment. Rao and Davidson (1980) and Karickhoff et al. (1979) developed empirical expressions relating equilibrium coefficients to laboratory measurements, leading to reliable means of estimating appropriate values. Dissolved organic materials are typically assumed to be composed entirely of organic carbon ($f_{OC} = 1$). The partitioning expressions implemented in the HUDTOX model are:

$$K_p = f_{oc} \times K_{POC} \quad (5-10)$$

$$K_B = 1.0 \times K_{DOC} \quad (5-11)$$

where:

K_p = Solids partition coefficient, L_w/kg_{solid} [L^3/M].

K_{POC} = particulate organic carbon partition coefficient, L_w/kg_{OC} [L^3/M]

f_{oc} = organic carbon fraction of sediment, kg_{OC}/kg_{solid} [M/M].

K_B = DOC-bound partition coefficient, $L_w/kg_{DOC-sorbent\ material\ (or\ DOM)}$ [L^3/M]

K_{DOC} = dissolved organic carbon partition coefficient, L_w/kg_{DOC} [L^3/M].

The dissolved organic carbon (DOC) partition coefficient, K_{DOC} , is commonly estimated as K_{POC} times a binding efficiency factor based on analysis of field data measurements of each chemical phase.

HUDTOX differs from WASP5/TOXI5 in that it includes temperature-dependent partitioning, as well as segment-specific parameters which allow for both spatial and compartmental (i.e., water column vis-à-vis sediment bed) variations in partitioning. The dependence of partitioning on temperature was developed and presented in the DEIR (USEPA, 1997). The general form of the resulting empirical relationship, applicable to both the particulate and DOC partition coefficients, is represented by:

$$\log K_{p,T} = \log K_{p,25} + tsf \times \left(\frac{1}{T - T_0} - \frac{1}{25 - T_0} \right) \quad (5-12)$$

where:

$K_{p,25}$ = partition coefficient at 25°C, L/kg

T = water temperature, °C

T_0 = Absolute zero temperature (0 °K) = -273.15 °C

tsf = temperature slope factor, °K.

The HUDTOX model can include particle interaction effects on solids partition coefficients using the approach proposed by DiToro (1985). This approach is described in Ambrose et al. (1993). Analysis of site-specific data for the Upper Hudson River indicated that particle interaction effects on PCB partitioning were minimal (USEPA, 1997). Consequently, none of the present HUDTOX applications included particle interaction effects on PCB partitioning.

The total chemical concentration is the sum of the three phase concentrations:

$$C = C'_w n + C'_s M_s + C'_B B \quad (5-13)$$

where:

$$\begin{aligned} C'_w &= \text{concentration of dissolved chemical in water, mg/L}_{\text{water}} \\ n &= \text{porosity (Volume}_{\text{water}} / \text{Volume}_{\text{water + solids}}), L_{\text{water}}/L \\ C'_s &= \text{concentration of solids-sorbed chemical on a mass basis, mg/kg}_{\text{solid}} \\ M_s &= \text{concentration of solids, kg}_{\text{solids}}/L \\ C'_B &= \text{concentration of DOC-bound chemical on a mass basis, mg/kg}_{\text{DOC}} \\ B &= \text{concentration of DOC, kg}_{\text{DOC}}/L. \end{aligned}$$

The dissolved fraction f_d is given by:

$$f_d = \frac{C'_w n}{C} = \frac{1}{1 + K_B B' + K_p M'_s} \quad (5-14)$$

The particulate (solids-sorbed) and DOC-bound fractions, respectively f_p and f_b , are given by:

$$f_p = \frac{C'_s M_s}{C} = \frac{K_p M'_s}{1 + K_B B' + K_p M'_s} \quad (5-15)$$

$$f_b = \frac{C'_B B}{C} = \frac{K_B B'}{1 + K_B B' + K_p M'_s} \quad (5-16)$$

where:

$$\begin{aligned} M'_s &= M_s/n = \text{solids concentration on a water volume basis, kg}_{\text{solid}}/L_w \\ B' &= B/n = \text{DOC concentration on a water column basis, kg}_{\text{DOC}}/L_w \end{aligned}$$

These fractions are determined in time and space throughout a simulation from the partition coefficients, internally calculated porosities, simulated solids concentrations, and externally-specified DOC concentrations. Bulk volumetric concentrations for each phase (C_w for dissolved, C_p for particulate chemical, and C_B for DOC-bound chemical) are simply determined from the product of each relative fraction and the total chemical concentration.

5.5.2 Air-Water Exchange

Air-water exchange, or volatilization, is the mass transfer of a chemical across the air-water interface as dissolved chemical attempts to equilibrate with the gas phase concentration of that chemical in the atmosphere. In HUDTOX the air-water mass transfer exchange rate, S_v , is a function of dissolved chemical gradient between the liquid and vapor phase by the following equation:

$$\frac{\partial C}{\partial t} |_{volat.} = S_v = \frac{K_v}{D} \left(f_d C - \frac{C_a}{\frac{H_T}{RT_K}} \right) \quad (5-17)$$

where:

- S_v = air-water chemical mass transfer rate, g/m³/day
- K_v = air-water chemical transfer rate, m/day
- R = universal gas constant, 8.206x10⁻⁵ atm m³/mole °K
- T_K = water temperature, °K
- H_T = Henry's Law constant at temperature T (°C), atm m³/mole.
- D = depth (m) C_a = atmospheric chemical concentration (g/m³)

Equilibrium occurs when the ratio of the atmospheric partial pressure of a chemical to its dissolved concentration in the water column equals its temperature-corrected Henry's Law constant. Atmospheric partial pressure is expressed as a boundary condition in HUDTOX and the determination of its value is described in Chapter 6.

HUDTOX employs the same two-layer resistance model (Whitman, 1923) utilized by WASP5/TOXI5 to calculate the air-water exchange rate. This model assumes that two "stagnant films" exist at the air-water interface, bounded by well-mixed compartments on either side. The air-water mass transfer rate is controlled by the combined effect of liquid and gas phase resistance described by the following equation:

$$K_v = (R_L + R_G)^{-1} = \left[K_L + \left(K_G \frac{H_T}{RT_K} \right)^{-1} \right]^{-1} \quad (5-18)$$

where:

- K_v = Air-water chemical transfer rate, m/day
- R_L = liquid phase resistance, day/m
- R_G = gas phase resistance, day/m
- K_L = liquid phase transfer coefficient, m/day
- K_G = gas phase transfer coefficient, m/day

Diffusion of chemical through the liquid (water) layer is driven by concentration differences, whereas the gas (air) layer diffusion is controlled by partial pressure differences. The Henry's Law constant generally increases with increasing vapor pressure and decreases with increasing solubility of a compound. Therefore, highly volatile compounds that have low solubility are likely to exhibit mass transfer limitations in water (i.e., high liquid phase resistance). Similarly, mass transfer in air is limited (i.e., high gas phase resistance) when chemical compounds are relatively nonvolatile and have high solubility.

Air-water exchange is usually smaller in lakes and reservoirs than in relatively turbulent rivers and streams. Gas exchanges in rivers and river-reservoir systems can also be significantly enhanced by the highly turbulent conditions created as water flows through and/or over dams. The present HUDTOX model does not account for the possible gas exchange losses of PCBs to the atmosphere as water flows through the various run-of-the-river dams along the Upper Hudson River between Fort Edward and Federal Dam at Troy. The significance of gas exchange at dams on PCB dynamics in the Upper Hudson River is evaluated in the data analysis discussions presented in Chapter 6 of this report.

Air-water exchange in HUDTOX is the same as in WASP5/TOXI5 (Ambrose, et al., 1993) with two exceptions that are described in the following paragraphs.

The chemical-specific Henry's Law constant (H) is assumed to describe the equilibrium between the gas phase and dissolved liquid phase at the boundary between the two layers. In HUDTOX, the Henry's Law constants are temperature corrected according to the empirical relationship presented by Achman et al. (1993) in the following equation:

$$\log H_T = \log H_{25} \frac{\left(7.91 - \frac{3414}{(T - T_0)}\right)}{\left(7.91 - \frac{3414}{(25 - T_0)}\right)} \quad (5-19)$$

where:

$$\begin{aligned} H_T &= \text{Henry's Law constant at temperature } T, \text{ atm m}^3/\text{mole} \\ H_{25} &= \text{Henry's Law constant at } 25 \text{ }^\circ\text{C}, \text{ atm m}^3/\text{mole} \\ T_0 &= \text{Absolute zero temperature} = -273.15 \text{ }^\circ\text{C} \\ T &= \text{Temperature, } ^\circ\text{C}. \end{aligned}$$

As in WASP5/TOXI5, HUDTOX uses a constant gas film transfer coefficient of 100 m/day, typically applied to flowing waterbodies such as the Upper Hudson River. HUDTOX differs from WASP5/TOXI5 in that it directly adapts the O'Connor-Dobbins oxygen reaeration formula, as opposed to the Covar method which selects rates from a range of formulation (including O'Connor-Dobbins) depending on predicted water depth and current velocity within a river cross-section to predict a chemical-specific liquid film air-water transfer rate:

$$K_L = \left(\frac{D_w u}{D}\right)^{1/2} \times 8.64 \times 10^4 \quad (5-20)$$

where:

$$\begin{aligned} K_L &= \text{liquid film air-water transfer rate, m/day} \\ D &= \text{water depth, m} \\ u &= \text{water velocity, m/sec} \\ D_w &= \text{diffusivity of chemical in water, m}^2/\text{sec} \end{aligned}$$

The O'Connor-Dobbins formula internally adjusts the air-water transfer rate to determine a chemical-specific liquid film rate based on the chemical-specific diffusivity:

$$D_w = 22.0E-09 / (MW)^{2/3}, \text{ as per Ambrose et al. (1993).} \quad (5-21)$$

where:

MW = molecular weight of the chemical, g/mole

A detailed description of the two-layer resistance model used in HUDTOX and WASP5/TOXI5 is contained in Ambrose et al. (1993).

5.5.3 Dechlorination

Although the HUDTOX model framework allows for dechlorination and other degradation processes, these loss processes were assumed to be zero in the HUDTOX model calibration presented herein. Rationale for this approach is presented in Chapter 6. Dechlorination may be accommodated in the HUDTOX model in a variety of ways (e.g., first-order decay) through the use of standard WASP5/TOXI5 degradation mechanisms. However, accurate representation of dechlorination pathways from degradable higher chlorinated PCB congeners to specific lesser chlorinated PCB congeners would be an extremely difficult task to undertake in a modeling effort of this scale. Dechlorination is also not expected to be a significant loss mechanism for PCB mass in the Upper Hudson River for future conditions.

5.5.4 Sediment-Water Mass Transfer of PCBs

In river systems, non-flow dependent sediment-water exchange of contaminants, including PCBs, can result from many different physical and biological processes, which are discussed in Chapter 6. These processes include molecular diffusion in porewater as well as biologically- and hydrodynamically-enhanced transfer of both porewater and particulate phase PCBs to the water column. The net effect is observed as changes in PCB loading to the water column. The individual processes have not been directly measured or quantified for the Upper Hudson River, and not all of them are well understood. The combined effect of these processes is evident, however, in observed concentration changes of PCBs in the water column.

Non-flow dependent sediment-water mass transfer processes are represented in HUDTOX by effective particulate and/or porewater diffusion mass transfer rates. These rates move porewater and particulate chemical across the sediment-water interface based on concentration gradients of these phases between these compartments. HUDTOX represents diffusive exchanges of dissolved and DOC-bound PCBs between sediment porewater and the overlying water column with a diffusion equation similar to Equation 5-3, but with the concentration gradient expressed in terms of the dissolved and DOC-bound PCB concentrations in the porewater:

$$\frac{\partial M_i}{\partial t} = \frac{E_{ij}(t) \cdot A_{ij} \cdot n_{ij}}{L_{ij}/n_{ij}} \left(\frac{f_{dj} C_j}{n_j} - \frac{f_{di} C_i}{n_i} \right) \quad (5-22)$$

where:

M_i = mass of chemical constituent (state variable) in segment i, g [M]
 C_i, C_j = total chemical concentration in segments i and j,
 mg/L (or g/m³) [M/L³]
 $E_{ij}(t)$ = diffusion coefficient time function for exchange "ij", m²/day [L²/T]
 A_{ij} = interfacial area shared by segments i and j, m² [L²]
 $L_{c_{ij}}$ = characteristic mixing length between segments i and j, m [L] .
 f_{d_i}, f_{d_j} = dissolved or DOC-bound fraction of chemical in i and j [dimensionless]
 n_{ij} = average porosity at interface "ij", L_w/L
 (volume of water/volume total solution) [dimensionless]

Depending on the PCB concentration gradients, porewater diffusion may be a source or sink for the water column.

HUDTOX can represent mass transfer of PCBs from the particulate phase in the sediment to the overlying water column, without net mass transfer of associated solids, via application of a mass transfer coefficient applied directly to the particulate phase PCBs in the upper sediment layer.

Specific alternative approaches (i.e., porewater only versus combined porewater and particulate phase transfer) for specifying PCB sediment-water mass transfer exchanges within the HUDTOX model were investigated using data-based mass balances (see Chapter 6), and through the use of model simulations presented in Chapter 7 for a range of PCB forms.

5.6 MODEL SPATIAL SEGMENTATION

5.6.1 Water Column Segments

The HUDTOX water column spatial segmentation was developed to capture the effects of the principal factors that influence spatial patterns of water column and sediment PCB concentrations within the Upper Hudson River. A total of 47 water column segments were represented from Rogers Island (RM 194.6) to Federal Dam (RM 153.9) at Troy (Figure 5-4, Parts A through D).

The criteria for developing the water column segmentation grid were driven by locations of:

- Major tributaries to the Upper Hudson River;
- Lock and dam structures along the river;
- Phase 2 and historical water quality sampling stations;
- USGS gaging stations; and,
- Sediment PCB "hotspots" along the river.

Hydrographic survey data collected by GE during 1991 (O'Brien & Gere, 1993b) were used to estimate HUDTOX model segment cross-sections. The TAMS/Gradient Team also conducted hydrographic measurements within a portion of the Upper Hudson River; however, the GE data provides more complete coverage. No significant differences were found between the two

datasets in reaches of the river covered by both surveys, including Thompson Island Pool. Consequently the GE data were used exclusively in determining river cross-section geometry for HUDTOX.

A two-dimensional segmentation for the water column was developed within Thompson Island Pool to better resolve potential differences in impacts from cohesive and non-cohesive sediment areas. The 28 water column segments within the Pool are configured as three lateral segments across the river, except at Rogers Island, with longitudinal resolution on the order of $\frac{1}{2}$ to $\frac{3}{4}$ of a mile (Figure 5-5). At Rogers Island the east and west river channels are each represented by one lateral segment. Figure 5-6 presents a schematic representation of the HUDTOX model grid that includes references to geographical locations. Output from the RMA-2V hydrodynamic model for a flow of 8,000 cfs at Fort Edward was used to provide flow-routing information for this two-dimensional segmentation grid within the Pool. An evaluation of the variation in flow through the HUDTOX segments at a given TIP cross-section for different upstream flows showed only minor variations, so the flow routing pattern was held constant over the entire range of flows simulated (also see Section 5.2.3.1).

The 19 one-dimensional water column segments between Thompson Island Pool and Federal Dam were developed to capture the impacts of hydrologic features of the river, including dams and locations of tributary inputs. The water column segmentation was also specified based on locations of sediment PCB “hotspots”. Consequently, the longitudinal resolution of these segments is variable, ranging from less than one mile to greater than four miles. The geometry of the HUDTOX water column segmentation is presented in Tables 5-1a and 5-1b. Figure 5-7 illustrates how the HUDTOX water column segment depths vary from upstream to downstream, indicating the important impacts of the lock and dam systems on river geometry.

5.6.2 Sediment Segments

Tables 5-2a and 5-2b present the spatial configuration and geometry of the HUDTOX surface sediment segmentation (layer 1), including the assignment of cohesive and non-cohesive sediment areas. Historically delineated sediment PCB “hotspots” are not explicitly represented by individual model segments. The finer model grid in Thompson Island Pool does, however, better represent these areas than it does in segments downstream of the Thompson Island Dam. As such, care must be taken in the use of the model for simulating future responses to remedial scenarios that focus on bedded sediment areas which may be much smaller than the model segmentation spatial scale. The longitudinal variation in cohesive sediment abundance in the HUDTOX model is depicted in Figure 5-8 and was developed according to the procedure described in the following paragraphs.

Surface sediment segment areas for the HUDTOX model were computed using two GIS coverages. First, a GIS coverage developed from side scan sonar studies conducted as part of the USEPA Phase 2 investigation (USEPA, 1997) was used to define sediment segments within TIP and downstream to the Northumberland Dam (RM 183.4). The side scan sonar measurements were used to distinguish river bottom areas of finer (representing cohesive solids) and coarser (representing non-cohesive solids) sediments. Rocky and mounded bed areas identified by the river bottom coverage were excluded from the sediment segmentation grid, as were all islands.

Two additional criteria were used in developing the sediment segmentation from the side scan sonar data:

- Water column segments underlain by 15 percent or more cohesive sediment area were assigned both cohesive and non-cohesive sediment segments, unless they contained more than 85 percent cohesive sediment area, in which case only a cohesive sediment segment was assigned; and,
- Water column segments underlain by less than 15 percent cohesive sediment area were assigned only non-cohesive sediment segments.

The second GIS coverage was based on GE's 1997 sediment bed type sampling between Northumberland Dam and Federal Dam (QEA, 1998). This coverage was used to define the HUDTOX sediment segmentation in reaches of the Upper Hudson River that were not covered by the side scan sonar surveys.

These two GIS coverages of sediment type were intersected with the HUDTOX water column segments to develop a two-dimensional picture of the surface sediments, and to define 27 cohesive and 43 non-cohesive sediment segments for the Upper Hudson River between Fort Edward and Federal Dam. Figure 5-4 (Parts A through D) depicts the two sediment types underlying each water column segment for the entire upper river. Figure 5-5 provides a large-scale view of the same information within just TIP, which was represented with 15 cohesive and 27 non-cohesive surface sediment segments.

A vertical discretization of two centimeters was used for the HUDTOX sediment segmentation to provide adequate resolution of vertical PCB profiles for simulating sediment-water interactions and long-term system responses. This resolution also provides flexibility in the use of HUDTOX model output for PCB sediment exposures in terms of an "active" surface sediment layer for the bioaccumulation models. A summary of the HUDTOX surficial sediment segmentation geometry is provided in Tables 5-2a and 5-2b. The model grid includes sediments down to 26 cm (13 layers), resulting in a total of 1035 water column and sediment segments in the entire model grid.

5.7 MODEL IMPLEMENTATION

The HUDTOX model was developed from the USEPA WASP toxic chemical model framework. The model was originally constructed from the WASP4/TOXI4 version of the code and subsequently modified to include relevant code corrections and changes that were implemented by USEPA in the WASP5/TOXI5 version. The WASP5 model is documented in Ambrose et al. (1993) and is distributed by the Center for Exposure Assessment Modeling (CEAM) at the USEPA Environmental Research Laboratory, Athens, Georgia.

The HUDTOX model FORTRAN source code was compiled and run using Lahey FORTRAN 90 (Version 4.50b, Lahey Computer Systems, Inc.) for personal computers running Microsoft DOS or Windows (95, 98 or NT) operating systems. Development, testing and application of the HUDTOX model was conducted on IBM-PC compatible computers. The computer hardware system requirements vary, depending on the type of HUDTOX model simulations being conducted. A Pentium II microprocessor (266 Mhz or higher), 64 Megabytes of RAM, and available disk

storage space of 1.0 Gigabyte are minimum requirements for the simulations presented in this report. As a general indication of model execution speed, a 21-year simulation from 1977 to 1997 required on the order of 10 hours of real time on a 450 Mhz Pentium II computer. This simulation included a model grid consisting of 1035 spatial segments and computational time steps ranging from 0.0027 to 0.019 days over the 21-year simulation period. Most model calibration and forecast simulations were conducted on 600 Mhz Pentium III computers.

THIS PAGE INTENTIONALLY LEFT BLANK

**Table 3-1
Comparison of Manning's 'n' from Previous Studies.**

Source	Main Channel 'n'	Floodplain 'n'
Zimmie, 1985	0.027	0.065
FEMA, 1982	0.028 - 0.035	0.075

**Table 3-2
Modeled Hudson River Flows at the Upstream Boundary of Thompson Island Pool.**

Flow Description	River Discharge, (cfs)
Peak flow during spring and fall surveys, 1991	8,000
Peak flow for GE high flow survey, April 23-24, 1992	19,000
Peak flow for TAMS Phase 2 survey, April 12, 1993	20,300
Peak flow for spring 1994 (Bopp, 1994)	28,000
Peak flow in 1983	35,000
5-year high flow	30,126
25-year high flow	39,883
100-year high flow	47,330

**Table 3-3
Comparison of Model Results with Rating Curve Data**

Flow (cfs)	Downstream Boundary Condition feet (NGVD)	Model Predicted Upstream Elevations feet (NGVD)	Rating Curve Gauge 119 (Upstream) Elevations feet (NGVD)
10,000	120.6	121.5	121.2
20,000	122.2	123.8	123.6
30,000	123.8	126.1	126.1

**Table 3-4
Effect of Manning's 'n' on Model Results
for 100-Year Flow Event**

	Main Channel Manning's 'n'	Floodplain Manning's 'n'	River Elevation at Roger's Island feet (NGVD)
Baseline	0.020	0.060	129.1
High 'n'	0.035	0.075	131.1
Low 'n' Main Channel	0.015	0.060	128.6
Low 'n' Floodplain	0.020	0.040	128.9
High 'n' Floodplain	0.020	0.080	129.3

**Table 3-5
Effect of Turbulent Exchange Coefficients on Model Results**

	Turbulent Exchange Coefficients (lb-sec/ft²)	River Elevation Roger's Island feet (NGVD)
Baseline	100	129.1
Low Turbulent Exchange Coefficients	50	128.8
High Turbulent Exchange Coefficients	200	129.7

Table 4-1
Summary of Inputs for Depth of Scour Model at Each High Resolution Core.

Core Name	100 Year Flood Shear Stress (dynes/cm²)	Surficial Dry Bulk Density (g/cm²)
HR-19	12.7	0.369
HR-20	29.8	0.207
HR-23	19.1	0.619
HR-25	53.1	0.590
HR-26	31.7	0.276

Source: TAMS/Gradient Database/Release 4.1b
 Thompson Island Pool Hydrodynamic Model results

Table 4-2
Predicted Depth of Scour Range for 100 Year Flood at Each High Resolution Core Location.

Core Name	Depth of Scour (cm)			Depth of PCB Peak (cm)
	Median	5th Percentile	95th Percentile	
HR-19	0.074	0.016	0.356	20-24
HR-20	1.820	0.311	7.695	24-28
HR-23	0.158	0.030	0.819	28-32
HR-25	3.714	0.500	21.789	2.5
HR-26	1.643	0.275	8.262	12-24

Source: TAMS/Gradient Database/Release 4.1b

Table 4-3
Thompson Island Pool Cohesive Sediment Expected Values of Solids Erosion and Mean Depth of Scour for 100-Year Flood, from Monte Carlo Analysis.

Erosion Type	Expected Value
Depth (cm)	0.317
Solids (kg)	1,740,000

Table 5-1a.
HUDTOX Water Column Segment Geometry in Thompson Island Pool (2-dimensional segmentation).

	HUDTOX Segment Number	Location Description	Downstream River Mile	Length (m)	Depth (m)	Surface Area (m ²)	Volume (m ³)	Cross-sectional Area (m ²)	Adjacent Segments		
									Below		Downstream
2-dimensional segmentation	1	West R. Island	194.11	721	1.66	111,167	184,239	256	48		3
	2	East R. Island	194.11	721	1.33	124,233	164,924	229	49		4
	3	West R. Island	193.59	845	1.66	179,319	301,100	357	50		5,6
	4	East R. Island	193.59	845	2.19	100,373	219,502	260	51		7
	5	west	193.00	942	1.55	93,705	145,320	154	53	52	8
	6	center	193.00	942	4.77	69,641	331,926	353	54	-	9
	7	east	193.00	942	1.60	51,501	82,167	87	55	-	10
	8	west	192.25	1,219	1.25	135,968	170,143	140	57	56	11
	9	center	192.25	1,219	3.68	118,933	437,877	359	58	-	12
	10	east	192.25	1,219	1.47	72,249	106,095	87	60	59	13
	11	west	191.69	896	1.63	116,614	190,137	212	62	61	14
	12	center	191.69	896	3.60	104,141	374,750	418	63	-	15
	13	east	191.69	896	0.72	88,892	65,047	73	65	64	16
	14	west	190.99	1,125	1.67	108,820	181,319	161	67	66	17
	15	center	190.99	1,125	4.82	98,464	481,381	428	69	68	18
	16	east	190.99	1,125	1.62	89,519	145,283	129	71	70	19
	17	west	190.33	1,054	1.71	77,285	132,461	126	73	72	20
	18	center	190.33	1,054	4.34	101,114	439,168	417	74	-	21
	19	east	190.33	1,054	2.00	66,975	133,699	127	76	75	22
	20	west	189.81	848	1.71	66,786	113,979	134	77	-	23
	21	center	189.81	848	4.29	78,114	335,126	395	79	78	24
	22	east	189.81	848	2.04	88,884	181,045	214	-	80	25
	23	west	189.22	941	2.07	76,079	157,460	167	82	81	26
	24	center	189.22	941	5.62	63,745	358,258	381	83	-	27
	25	east	189.22	941	2.01	60,339	121,202	129	85	84	28
	26	west TI Dam	188.50	1,160	1.92	106,532	200,215	173	86	-	29
	27	center TI Dam	188.50	1,160	3.58	146,361	517,870	446	87	-	29
	28	east TI Dam	188.50	1,160	1.48	157,473	232,375	200	89	88	29

Table 5-1b.

HUDTOX Water Column Segment Geometry Below Thompson Island Pool (1-dimensional segmentation).

	HUDTOX Segment Number	Location Description	Downstream River Mile	Length (m)	Depth (m)	Surface Area (m ²)	Volume (m ³)	Cross-sectional Area (m ²)	Adjacent Segments		
									Below	Downstream	
1-dimensional segmentation	29	Lock 6	186.20	3,757	1.95	837,947	1,634,430	435	91	90	30
	30		184.85	2,178	3.49	557,155	1,946,807	894	93	92	31
	31	Lock 5	183.41	2,317	3.86	474,625	1,832,981	791	95	94	32
	32		182.30	1,767	3.92	468,521	1,835,130	1,039	96		33
	33		181.40	1,446	3.12	229,378	715,684	495	97		34
	34		179.73	2,699	2.84	572,753	1,628,112	603	99	98	35
	35		178.08	2,647	3.76	501,225	1,882,175	711	101	100	36
	36		175.08	4,833	4.20	948,752	3,985,892	825	103	102	37
	37		170.98	6,597	4.24	1,377,869	5,844,528	886	105	104	38
	38		169.79	1,918	3.69	558,975	2,064,033	1,076	107	106	39
	39	Stillwater Dam	168.19	2,566	2.99	408,394	1,222,268	476	109	108	40
	40		166.67	2,454	1.93	952,848	1,835,070	748	111	110	41
	41	Lock 3 Dam	165.99	1,087	4.18	417,298	1,743,711	1,605	113	112	42
	42		164.31	2,715	3.18	623,849	1,982,413	730	115	114	43
	43	Lock 2 Dam	163.49	1,309	2.47	563,621	1,390,352	1,062	117	116	44
	44		160.87	4,214	2.89	1,090,832	3,148,431	747	119	118	45
	45	Lock 1 Dam	159.39	2,384	4.15	682,251	2,831,358	1,188	121	120	46
46		156.41	4,795	4.56	1,280,753	5,841,577	1,218	122		47	
47	Federal Dam	153.89	4,056	5.77	1,282,972	7,405,588	1,826	123		0	

Table 5-2a.
HUDTOX Sediment Segment Geometry in Thompson Island Pool for Surficial Sediment
Segments (2-dimensional segmentation).

Layer thickness = 2 cm

	HUDTOX Segment Number	Sediment Type	Surface Area (m ²)	Volume (m ³)	HUDTOX Sediment Layer	Adjacent Segments	
						Above	Below
2-dimensional segmentation	48	N	86,468	1,729	1	1	124
	49	N	64,616	1,292	1	2	125
	50	N	104,029	2,081	1	3	126
	51	N	66,458	1,329	1	4	127
	52	C	9,251	185	1	5	128
	53	N	25,142	503	1	5	129
	54	N	69,532	1,391	1	6	130
	55	N	34,250	685	1	7	131
	56	C	67,706	1,354	1	8	132
	57	N	22,071	441	1	8	133
	58	N	102,034	2,041	1	9	134
	59	C	5,886	118	1	10	135
	60	N	32,421	648	1	10	136
	61	C	16,475	329	1	11	137
	62	N	33,064	661	1	11	138
	63	N	103,509	2,070	1	12	139
	64	C	28,928	579	1	13	140
	65	N	19,719	394	1	13	141
	66	C	34,407	688	1	14	142
	67	N	23,202	464	1	14	143
	68	C	17,791	356	1	15	144
	69	N	71,668	1,433	1	15	145
	70	C	36,064	721	1	16	146
	71	N	24,256	485	1	16	147
	72	C	22,973	459	1	17	148
	73	N	22,891	458	1	17	149
	74	N	84,520	1,690	1	18	150
	75	C	8,939	179	1	19	151
	76	N	13,685	274	1	19	152
	77	N	31,066	621	1	20	153
	78	C	12,148	243	1	21	154
	79	N	53,177	1,064	1	21	155
	80	C	58,927	1,179	1	22	156
	81	C	22,523	450	1	23	157
	82	N	23,873	477	1	23	158
	83	N	50,643	1,013	1	24	159
	84	C	19,342	387	1	25	160
	85	N	4,315	86	1	25	161
	86	N	64,343	1,287	1	26	162
	87	N	138,185	2,764	1	27	163
	88	C	63,742	1,275	1	28	164
	89	N	31,981	640	1	28	165

Table 5-2b.

HUDTOX Sediment Segment Geometry Downstream of Thompson Island Pool for Surficial Sediment Segments (1-dimensional segmentation).

Layer thickness = 2 cm

	HUDTOX Segment Number	Sediment Type	Surface Area (m ²)	Volume (m ³)	HUDTOX Sediment Layer	Adjacent Segments	
						Above	Below
1-dimensional segmentation	90	C	79,269	1,585	1	29	166
	91	N	449,376	8,988	1	29	167
	92	C	189,009	3,780	1	30	168
	93	N	160,637	3,213	1	30	169
	94	C	268,967	5,379	1	31	170
	95	N	145,117	2,902	1	31	171
	96	N	468,567	9,371	1	32	172
	97	N	229,401	4,588	1	33	173
	98	C	68,901	1,378	1	34	174
	99	N	503,907	10,078	1	34	175
	100	C	97,432	1,949	1	35	176
	101	N	403,842	8,077	1	35	177
	102	C	89,073	1,781	1	36	178
	103	N	859,771	17,195	1	36	179
	104	C	346,399	6,928	1	37	180
	105	N	1,031,605	20,632	1	37	181
	106	C	295,637	5,913	1	38	182
	107	N	263,392	5,268	1	38	183
	108	C	34,953	699	1	39	184
	109	N	373,481	7,470	1	39	185
	110	C	213,454	4,269	1	40	186
	111	N	739,487	14,790	1	40	187
	112	C	171,255	3,425	1	41	188
113	N	246,085	4,922	1	41	189	
114	C	18,739	375	1	42	190	
115	N	605,171	12,103	1	42	191	
116	C	51,928	1,039	1	43	192	
117	N	511,748	10,235	1	43	193	
118	C	3,092	62	1	44	194	
119	N	1,087,846	21,757	1	44	195	
120	C	64,524	1,290	1	45	196	
121	N	617,793	12,356	1	45	197	
122	N	1,280,878	25,618	1	46	198	
123	N	1,283,097	25,662	1	47	199	

Table 5-2b.

HUDTOX Sediment Segment Geometry Downstream of Thompson Island Pool for Surficial Sediment Segments (1-dimensional segmentation).

Layer thickness = 2 cm

	HUDTOX Segment Number	Sediment Type	Surface Area (m ²)	Volume (m ³)	HUDTOX Sediment Layer	Adjacent Segments	
						Above	Below
1-dimensional segmentation	90	C	79,269	1,585	1	29	166
	91	N	449,376	8,988	1	29	167
	92	C	189,009	3,780	1	30	168
	93	N	160,637	3,213	1	30	169
	94	C	268,967	5,379	1	31	170
	95	N	145,117	2,902	1	31	171
	96	N	468,567	9,371	1	32	172
	97	N	229,401	4,588	1	33	173
	98	C	68,901	1,378	1	34	174
	99	N	503,907	10,078	1	34	175
	100	C	97,432	1,949	1	35	176
	101	N	403,842	8,077	1	35	177
	102	C	89,073	1,781	1	36	178
	103	N	859,771	17,195	1	36	179
	104	C	346,399	6,928	1	37	180
	105	N	1,031,605	20,632	1	37	181
	106	C	295,637	5,913	1	38	182
	107	N	263,392	5,268	1	38	183
	108	C	34,953	699	1	39	184
	109	N	373,481	7,470	1	39	185
	110	C	213,454	4,269	1	40	186
	111	N	739,487	14,790	1	40	187
	112	C	171,255	3,425	1	41	188
113	N	246,085	4,922	1	41	189	
114	C	18,739	375	1	42	190	
115	N	605,171	12,103	1	42	191	
116	C	51,928	1,039	1	43	192	
117	N	511,748	10,235	1	43	193	
118	C	3,092	62	1	44	194	
119	N	1,087,846	21,757	1	44	195	
120	C	64,524	1,290	1	45	196	
121	N	617,793	12,356	1	45	197	
122	N	1,280,878	25,618	1	46	198	
123	N	1,283,097	25,662	1	47	199	



Figure 1-1. Hudson River Watershed.

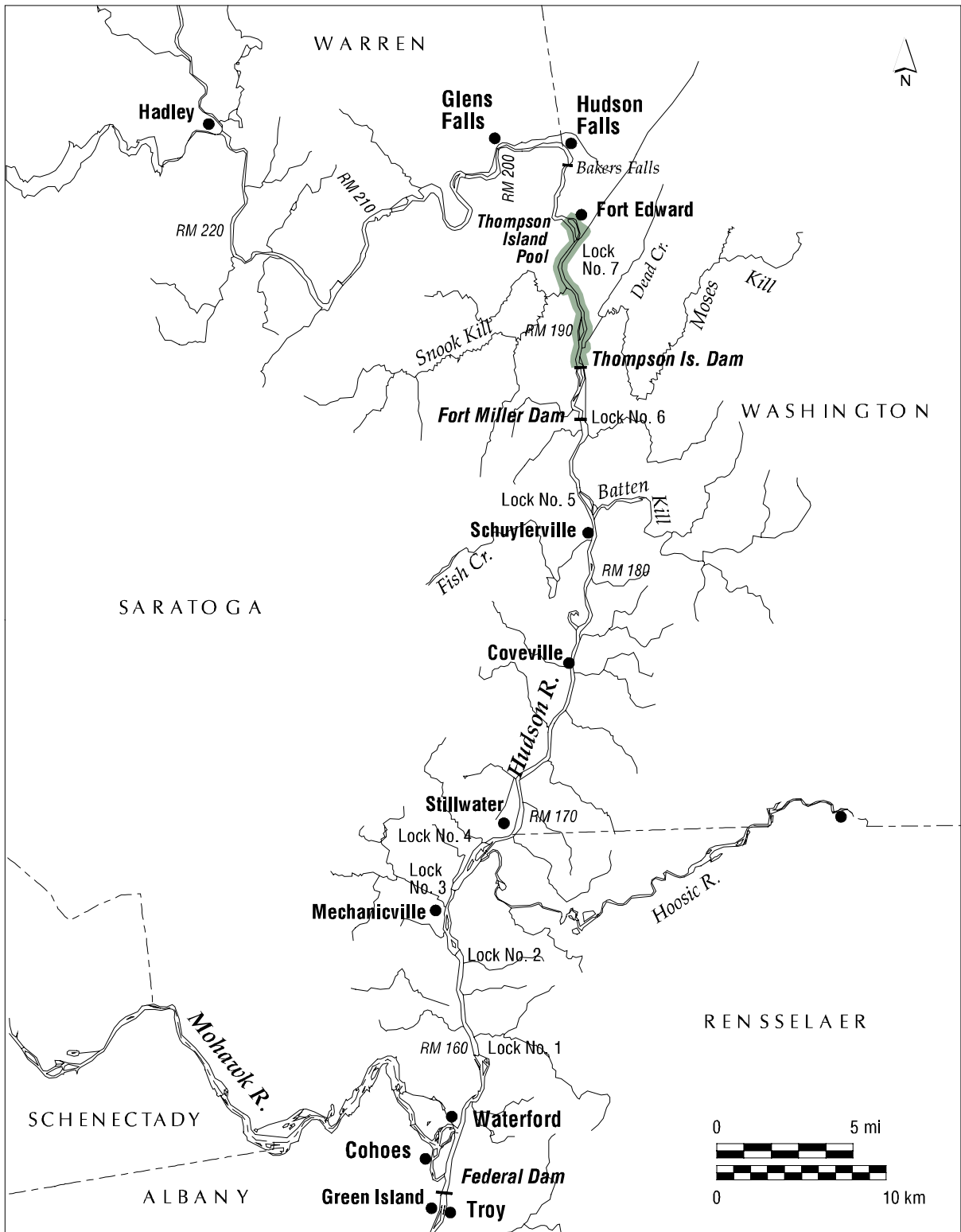


Figure 1-2. Upper Hudson River Watershed.

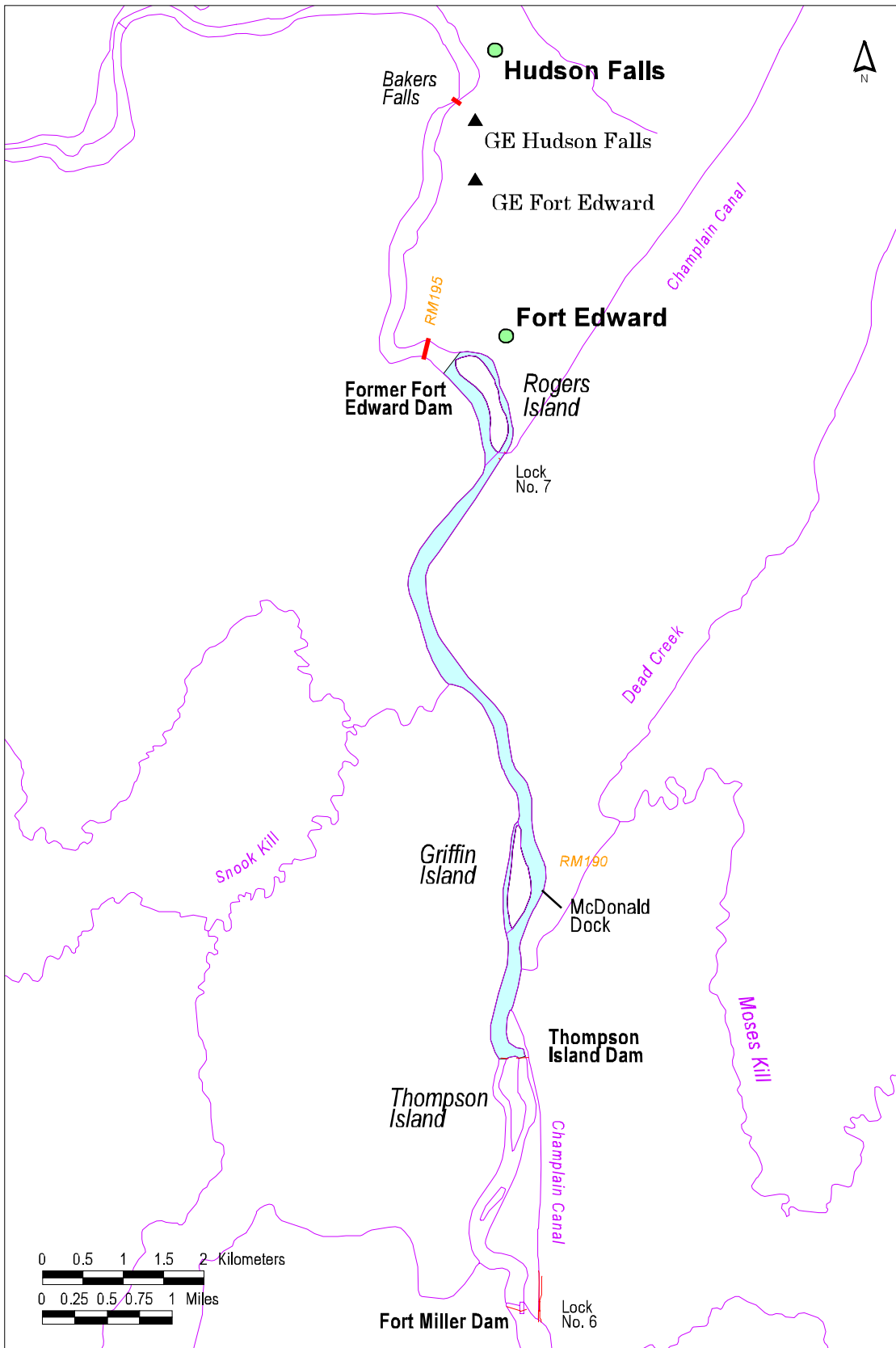
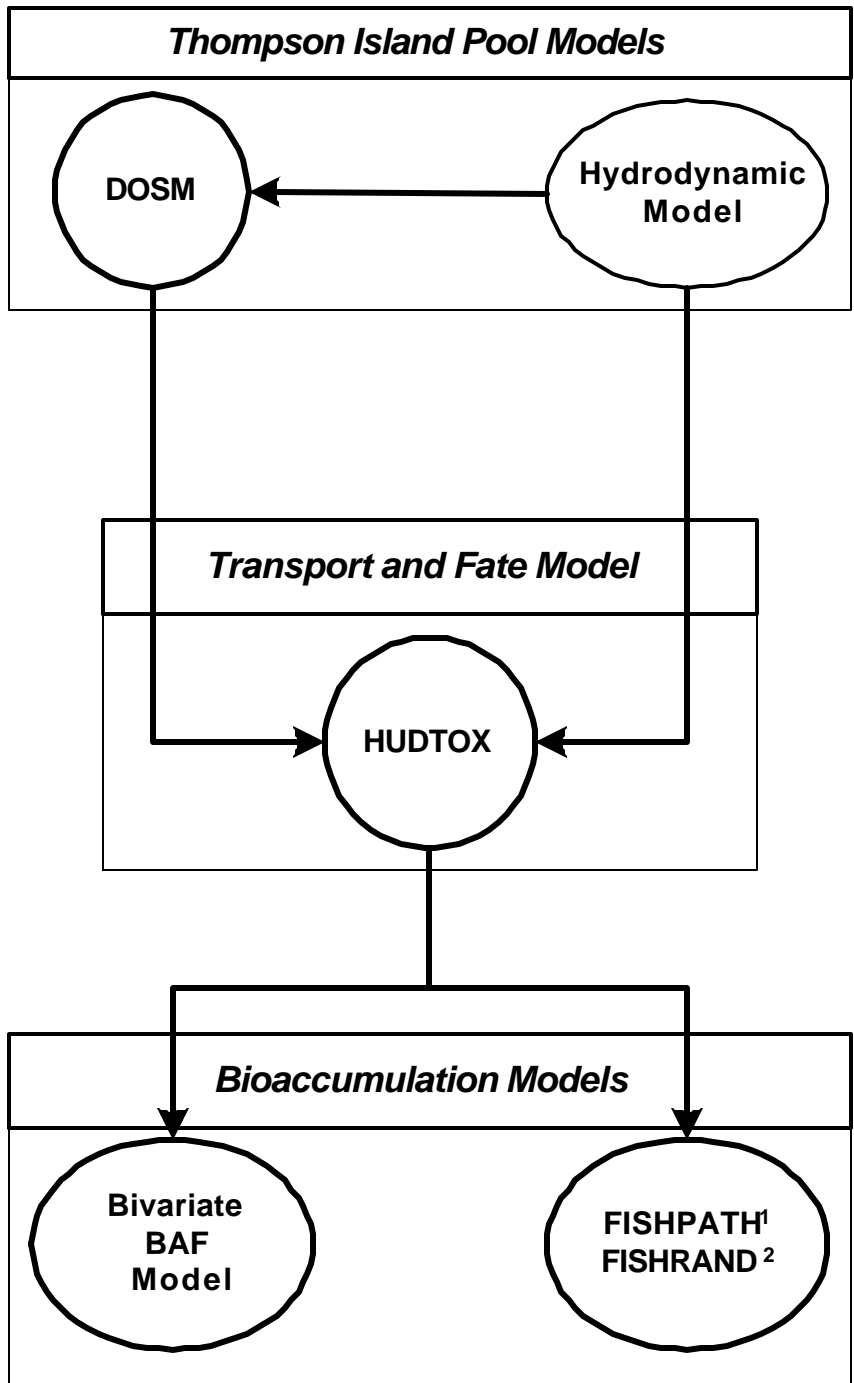
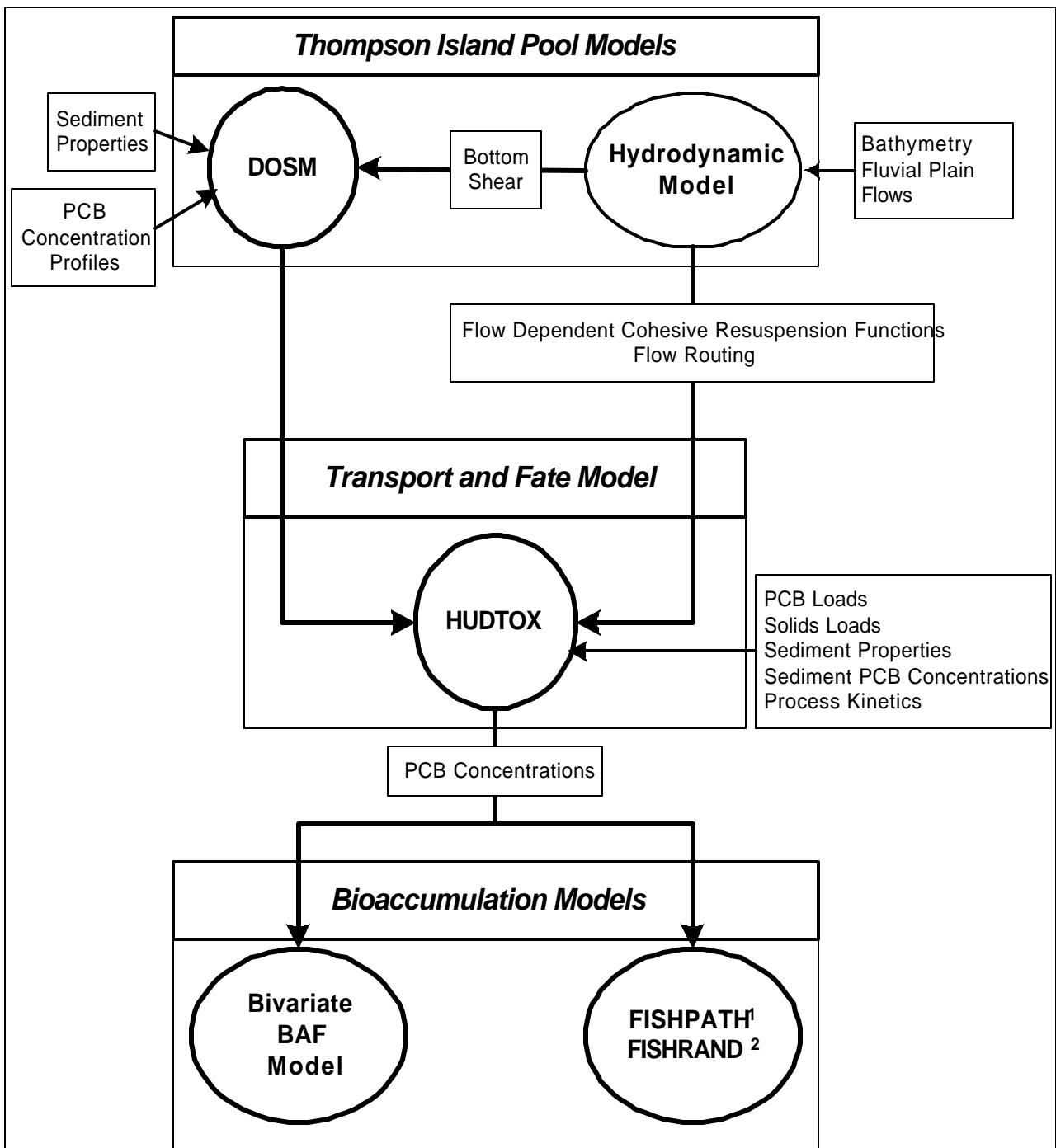


Figure 1-3. Thompson Island Pool.



¹ Deterministic Bioaccumulation Model
² Probabilistic Bioaccumulation Model

Figure 2-1. Upper Hudson River Modeling Framework .



¹ Deterministic Bioaccumulation Model
² Probabilistic Bioaccumulation Model

Figure 2-2. Upper Hudson River Modeling Framework with Model Inputs.

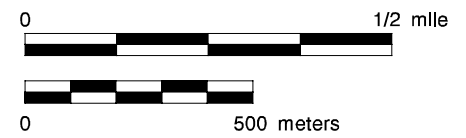
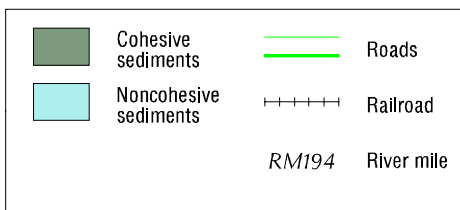
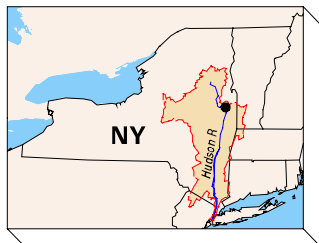
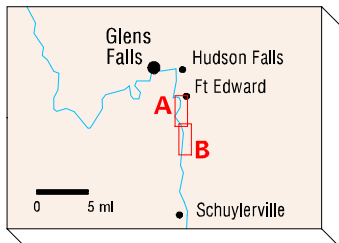
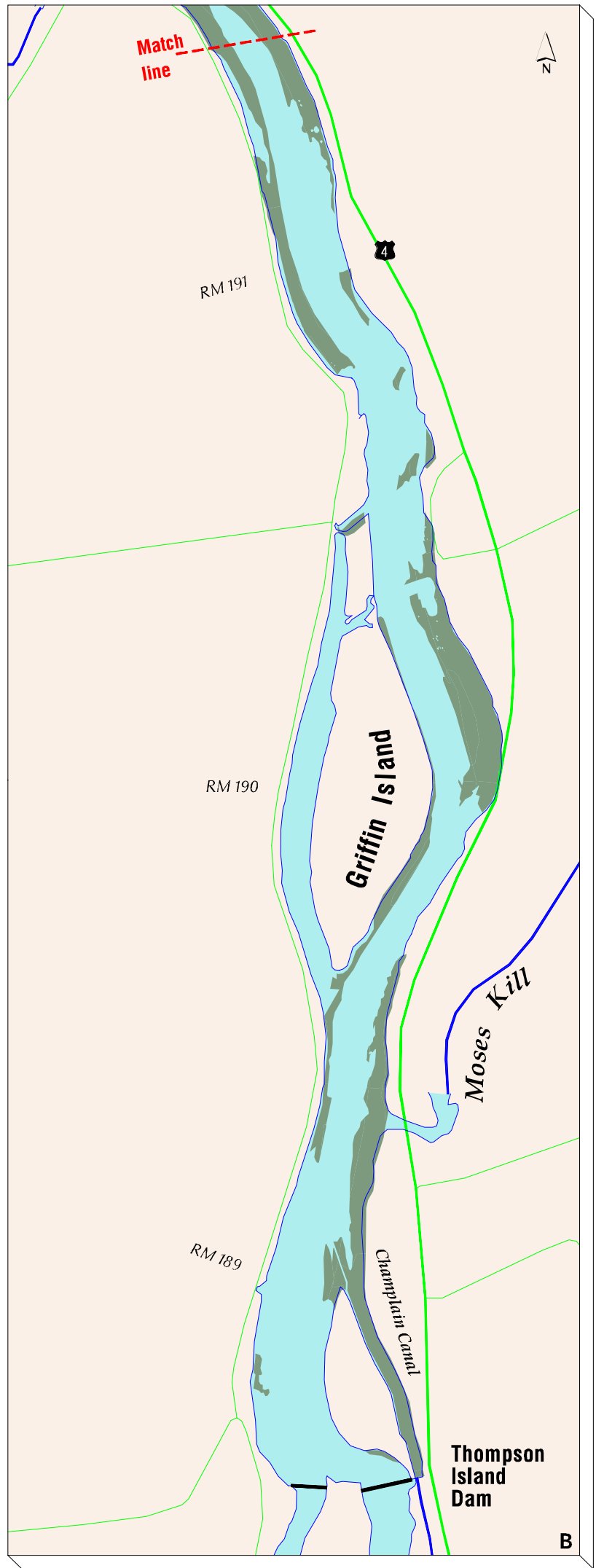
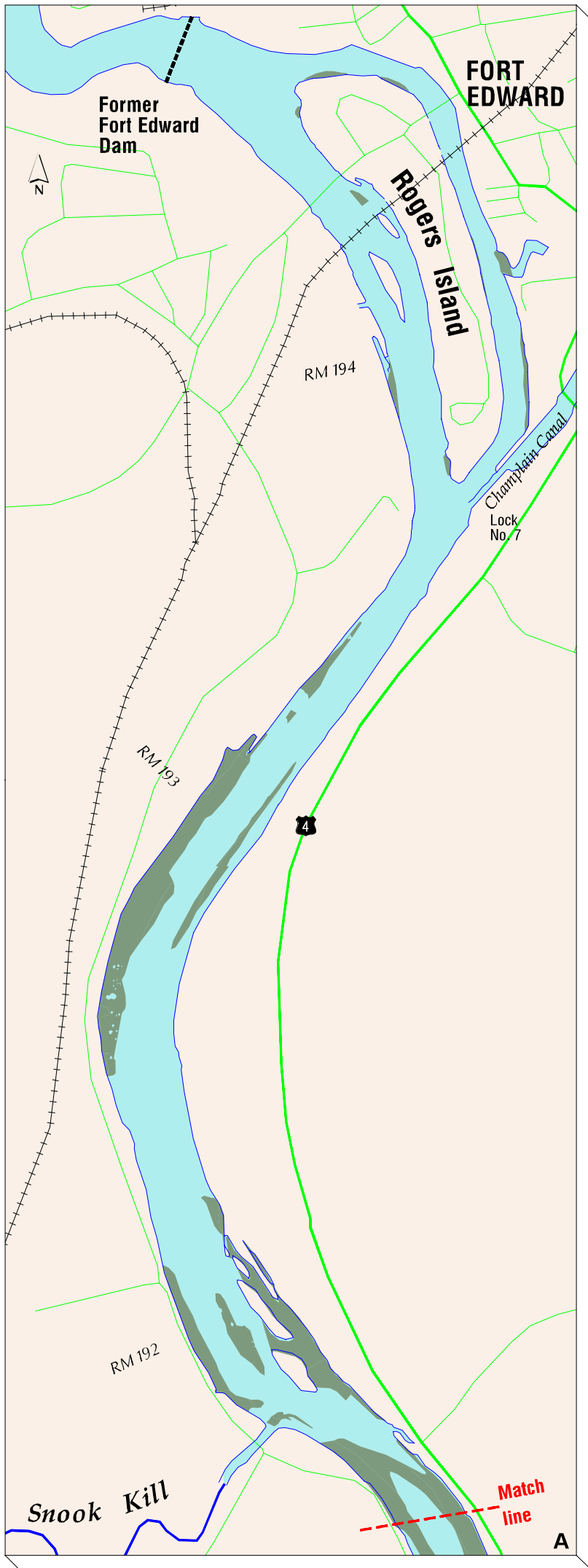


Figure 3-1. Thompson Island Pool Study Area.

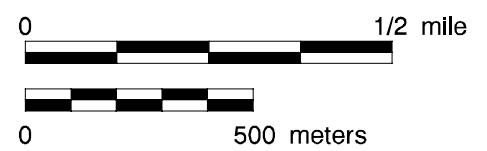
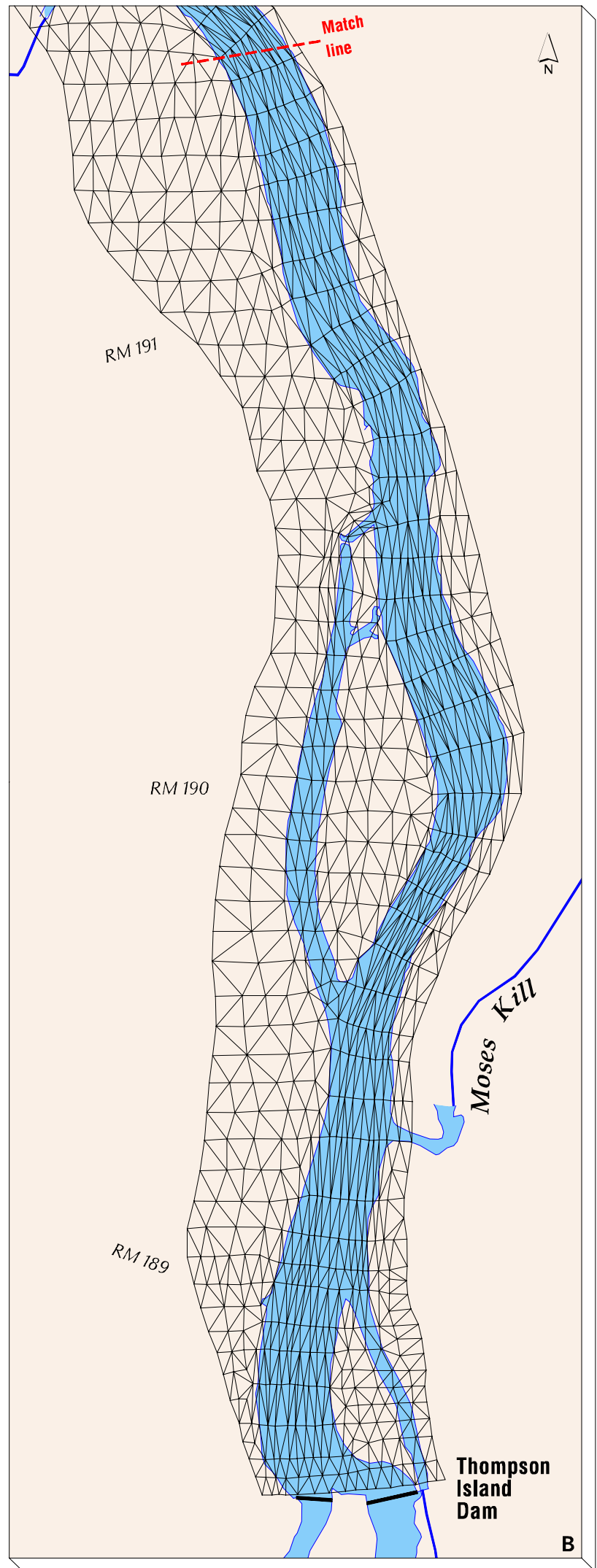
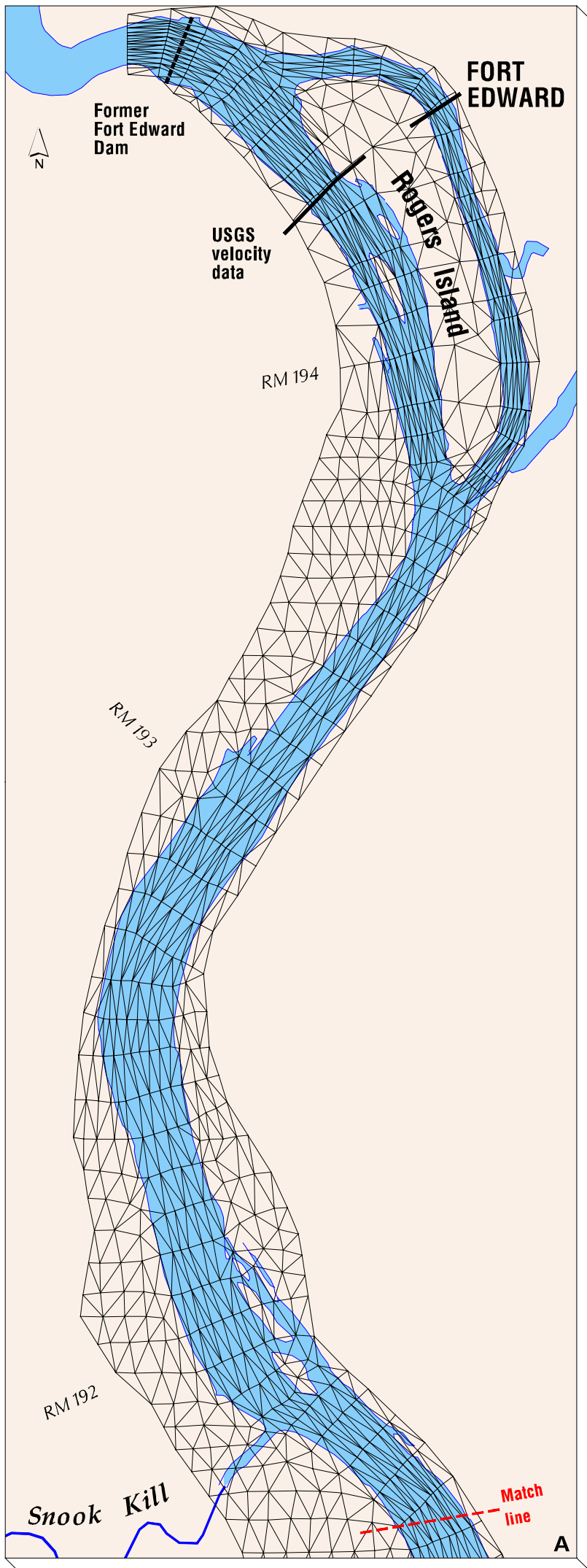


Figure 3-2. Thompson Island Pool RMA-2V Model Mesh.

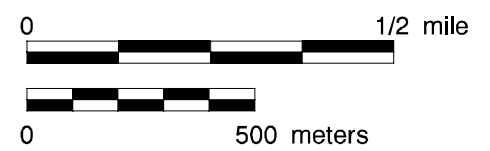
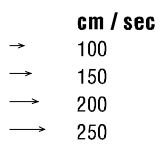
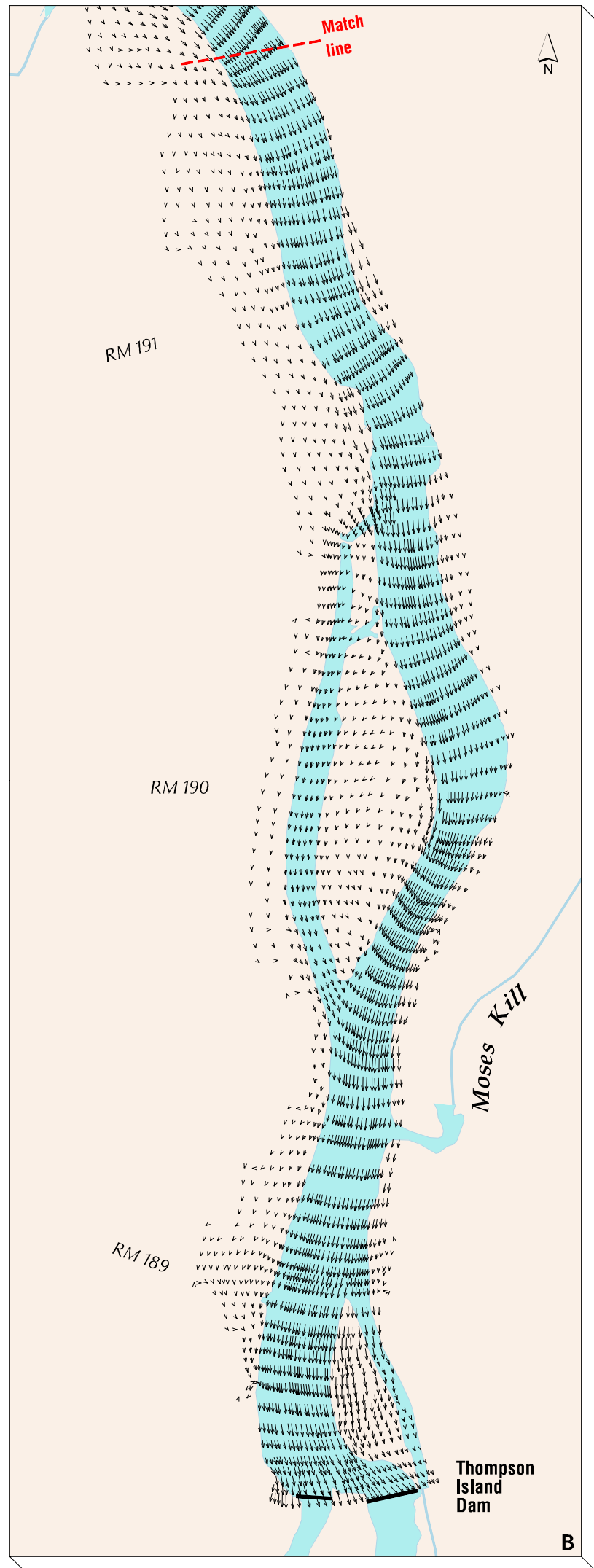
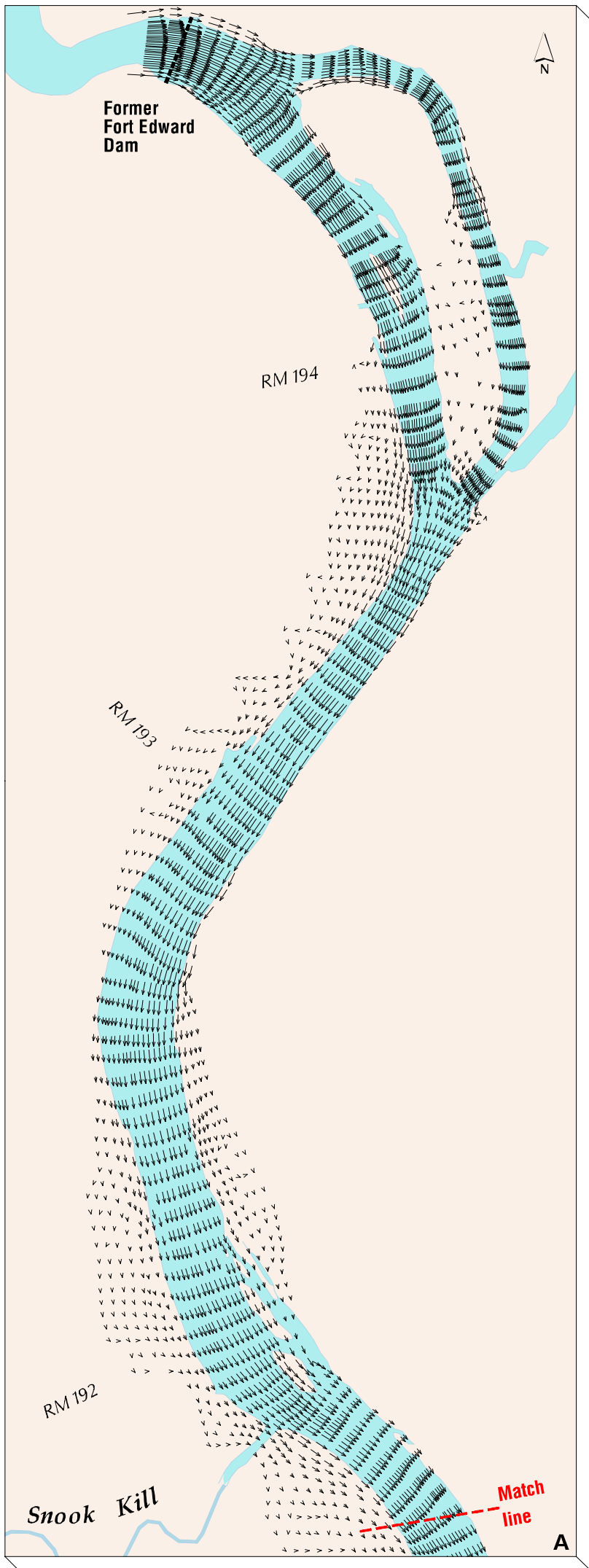


Figure 3-3. Thompson Island Pool Velocity Vectors for 100-Year Flow Event.

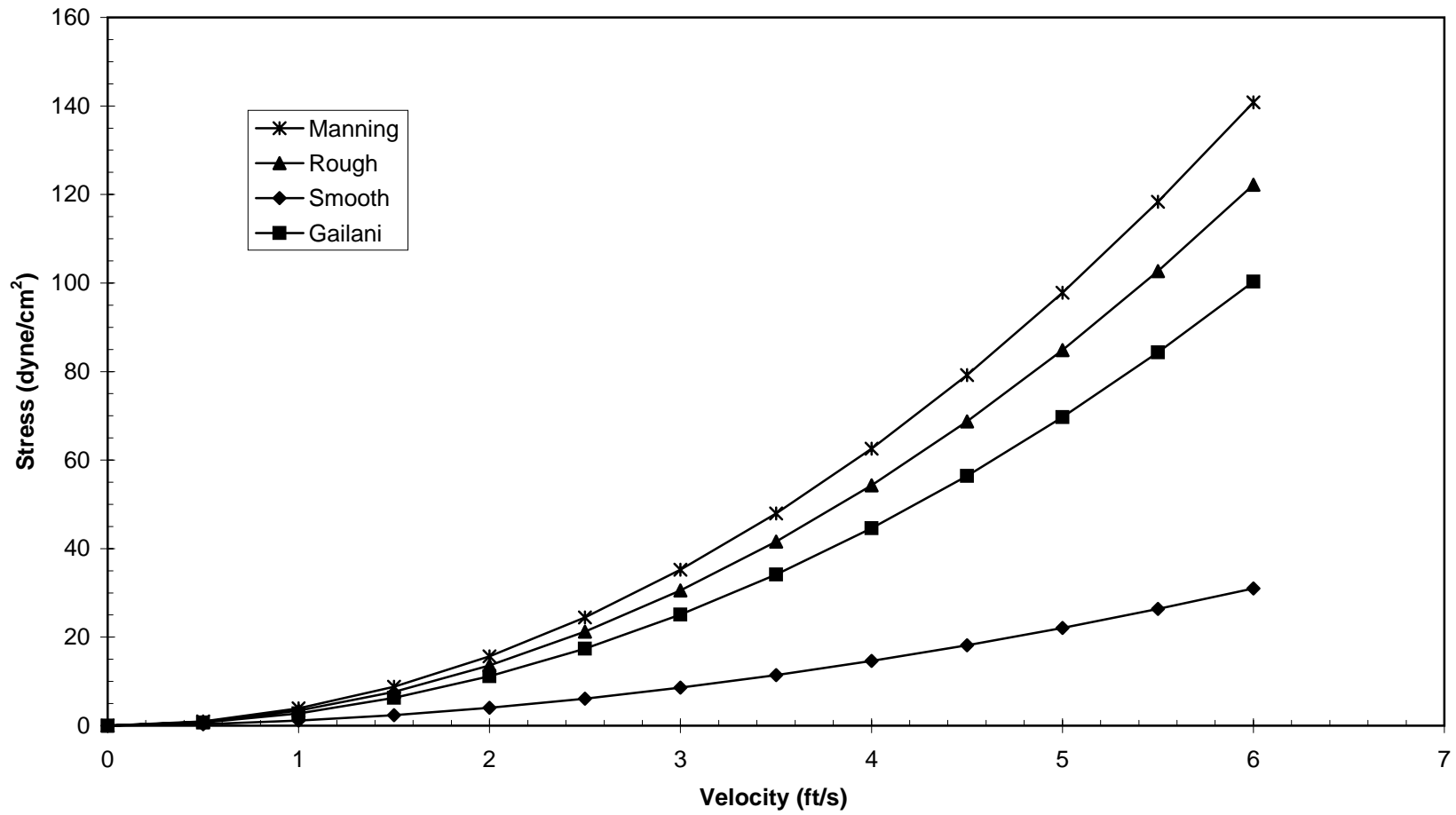


Figure 3-4. Shear Stress Computed from Vertically Averaged Velocity.

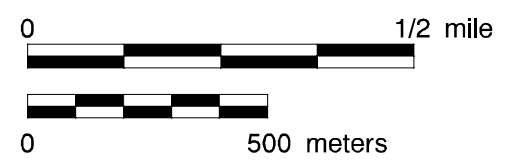
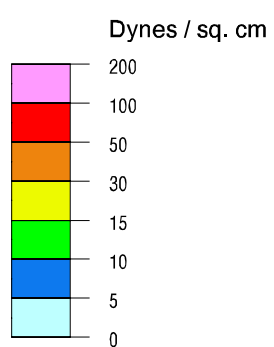
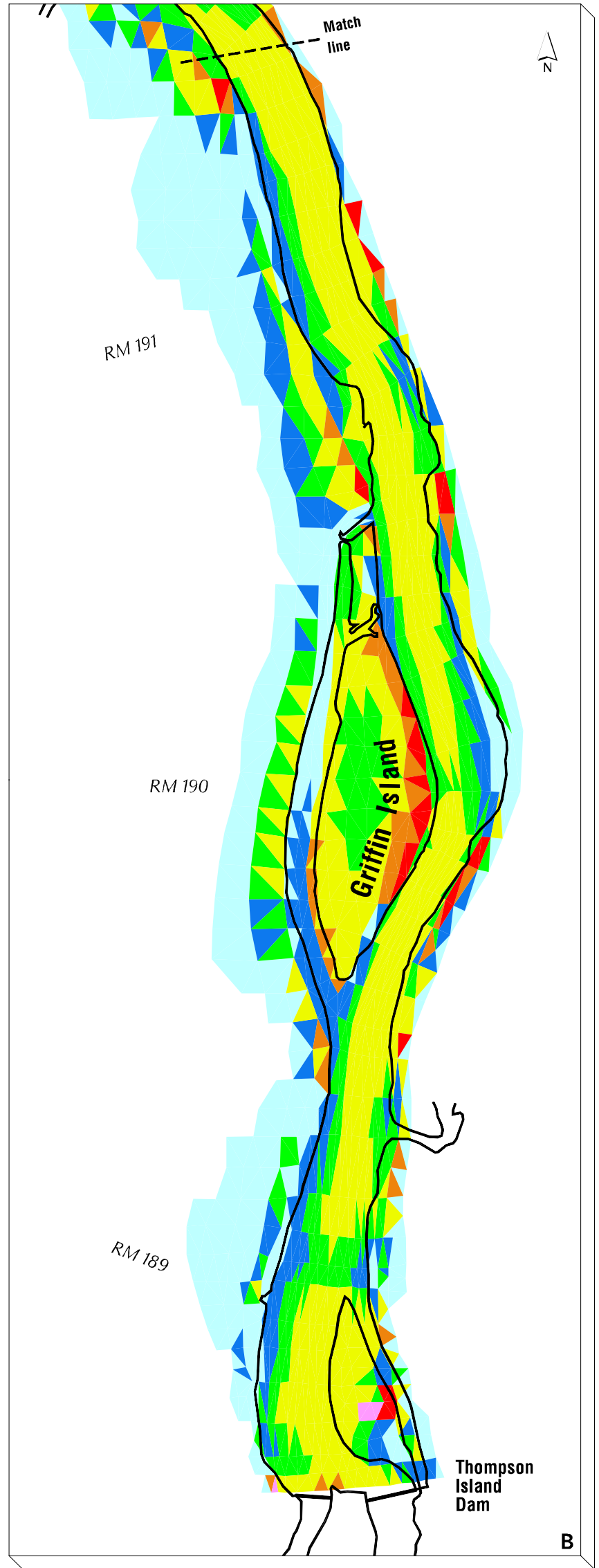
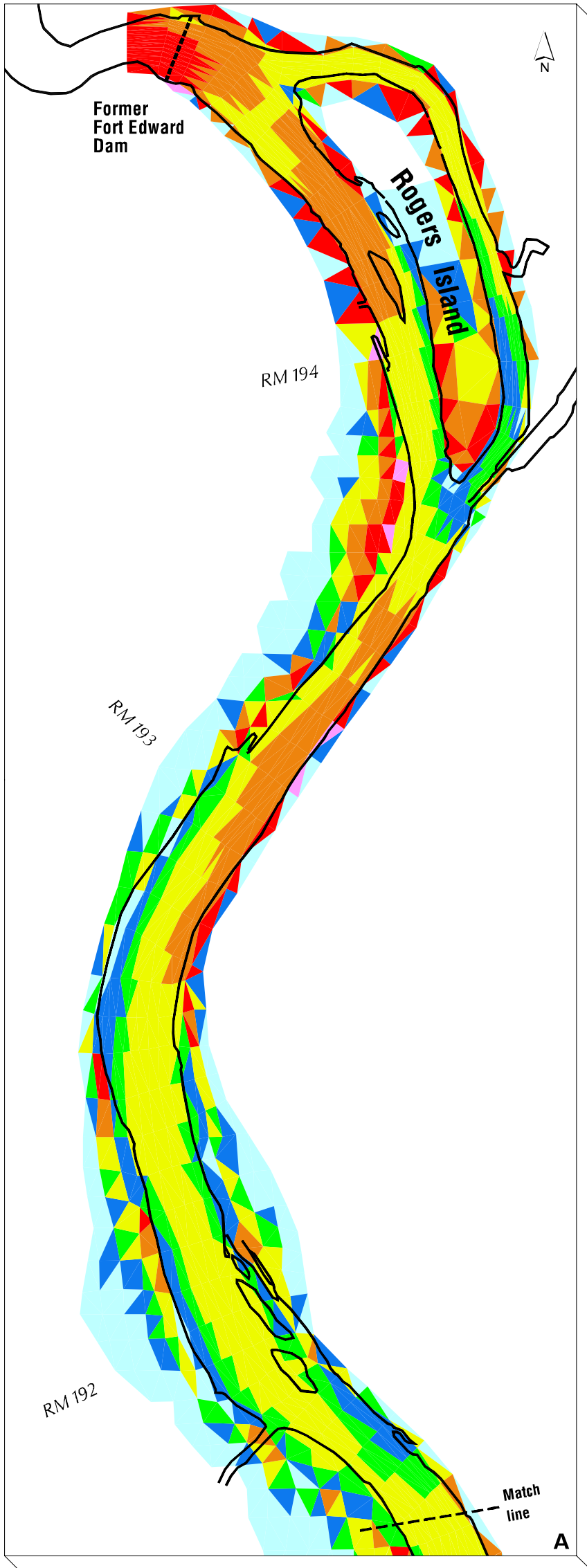
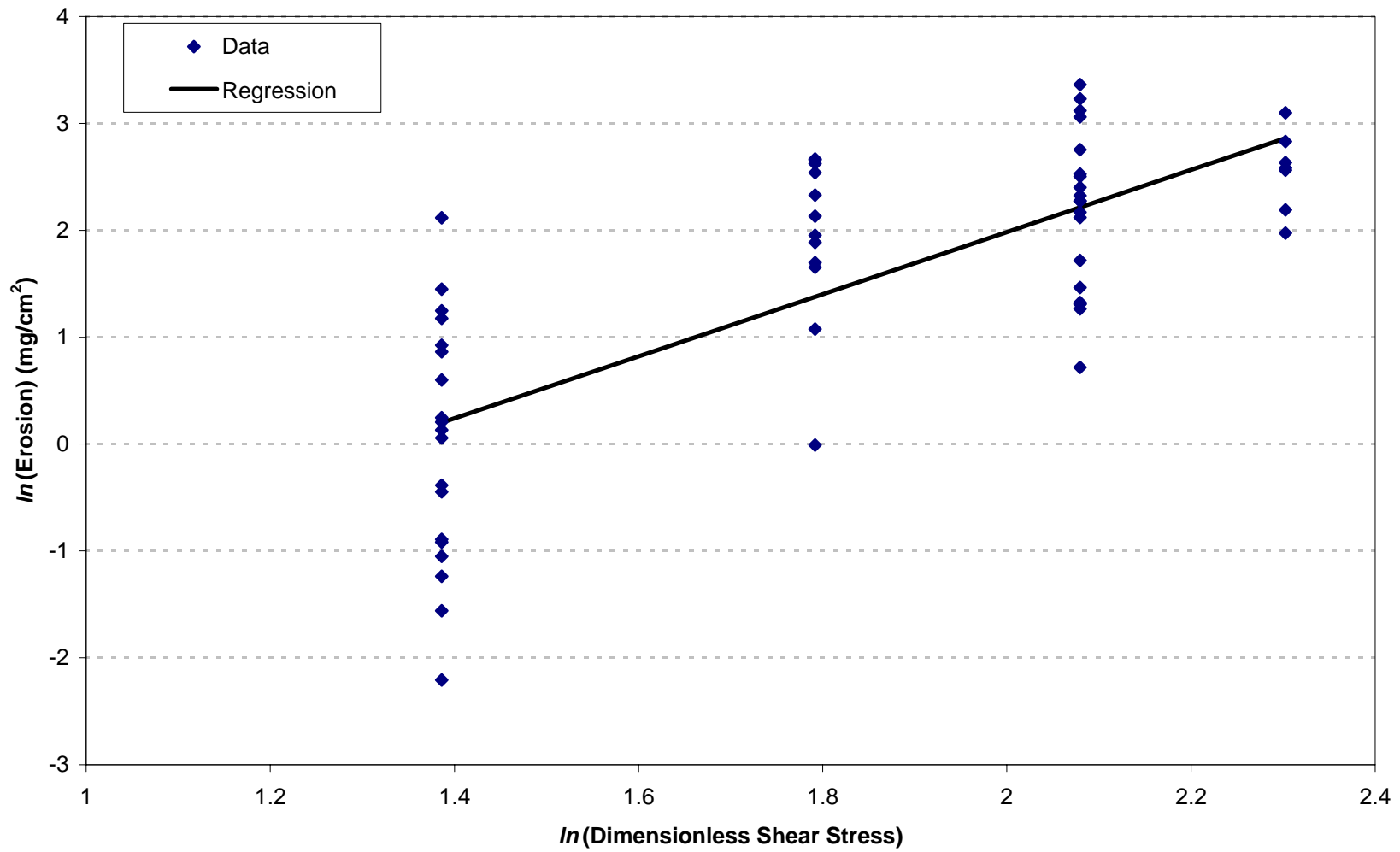


Figure 3-5. Thompson Island Pool Bottom Shear Stress for 100-Year Flow Event.



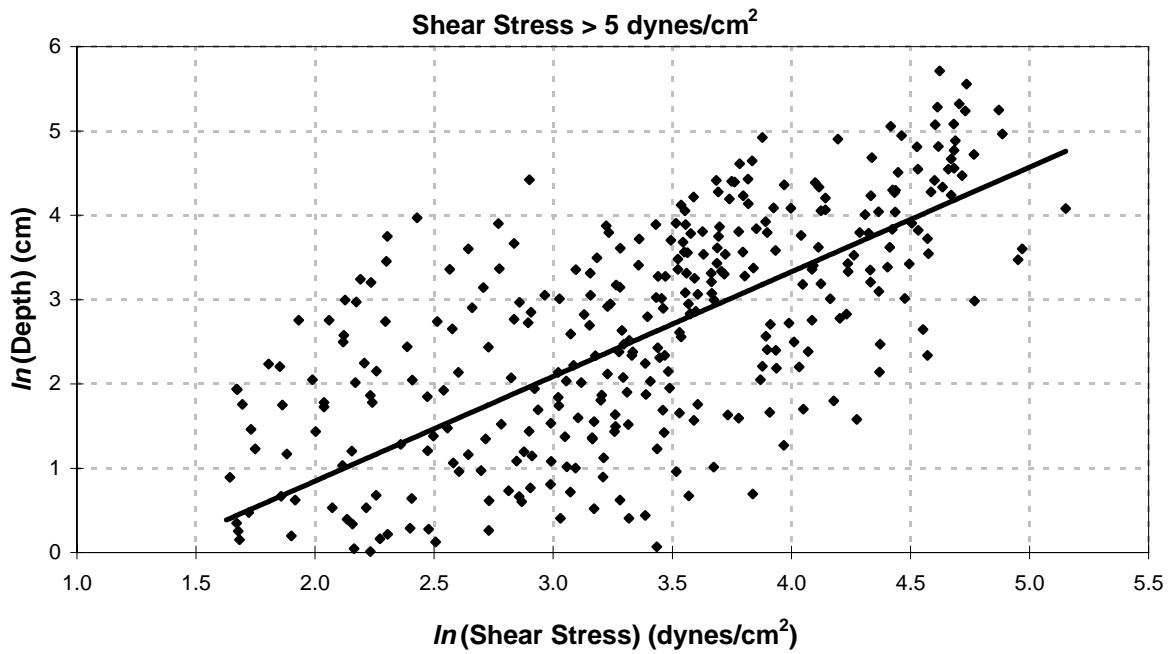
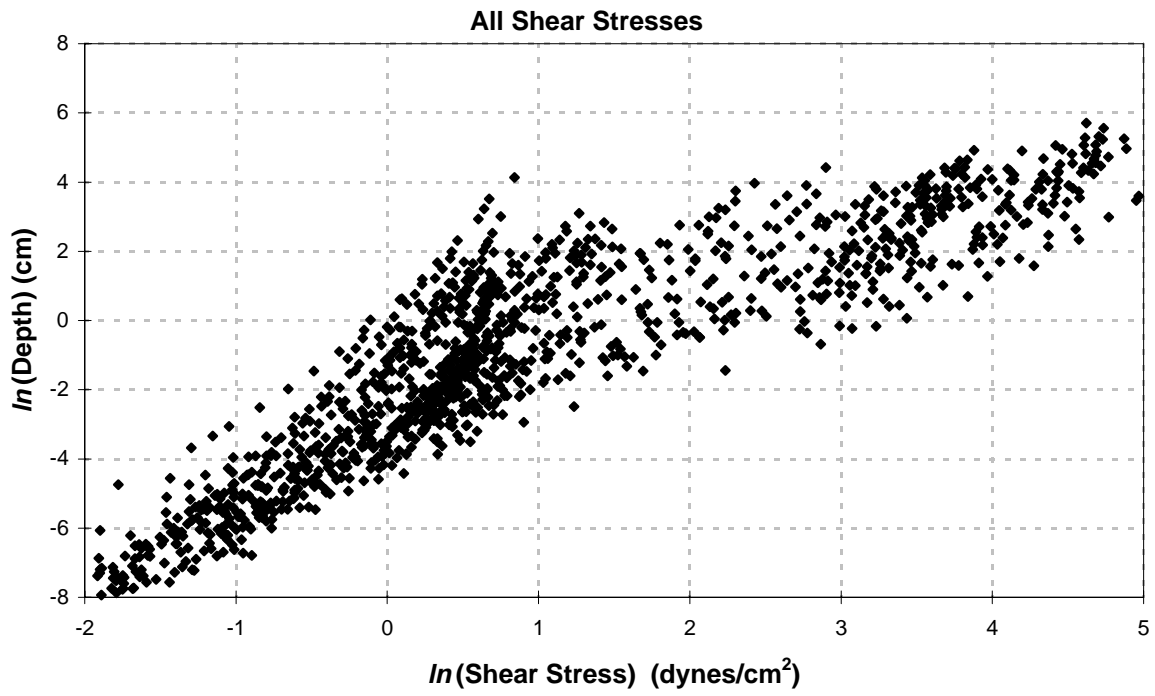


Figure 4-2. Armoring Depth versus Shear Stress.

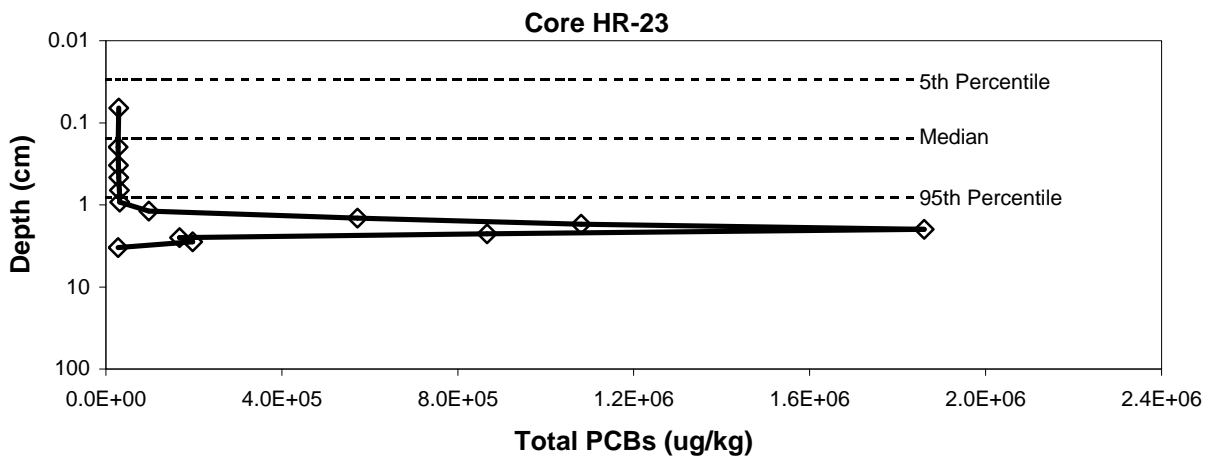
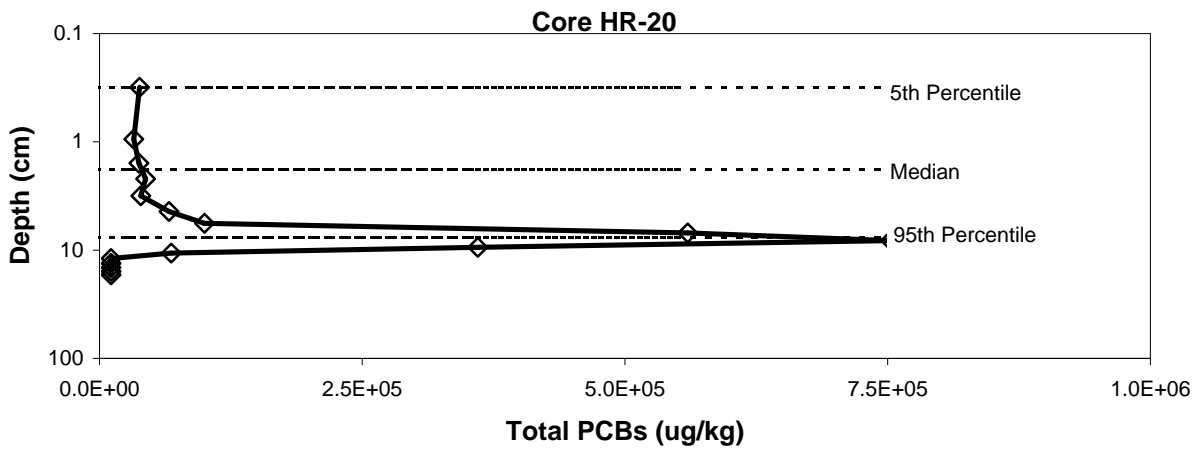
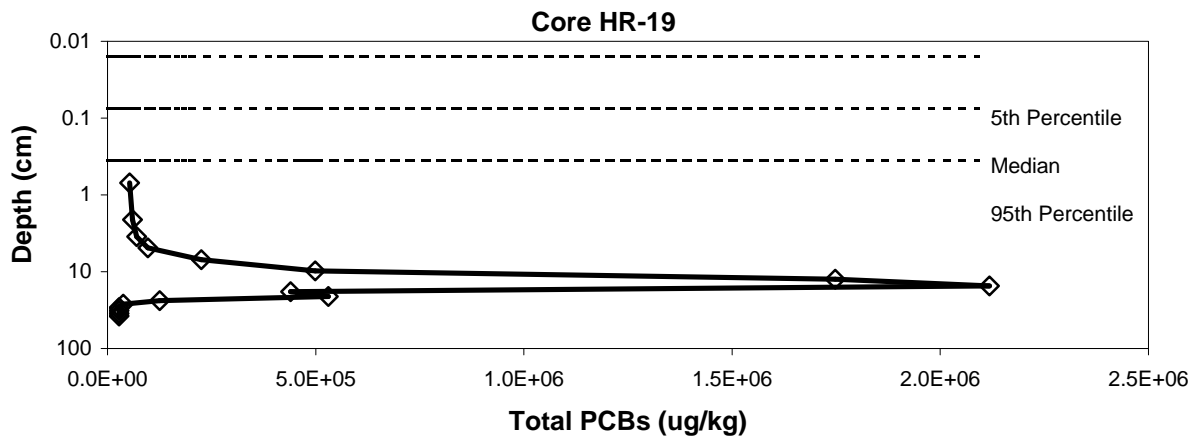


Figure 4-3a. Likelihood of PCB Scour for Selected Phase 2 High Resolution Sediment Cores.

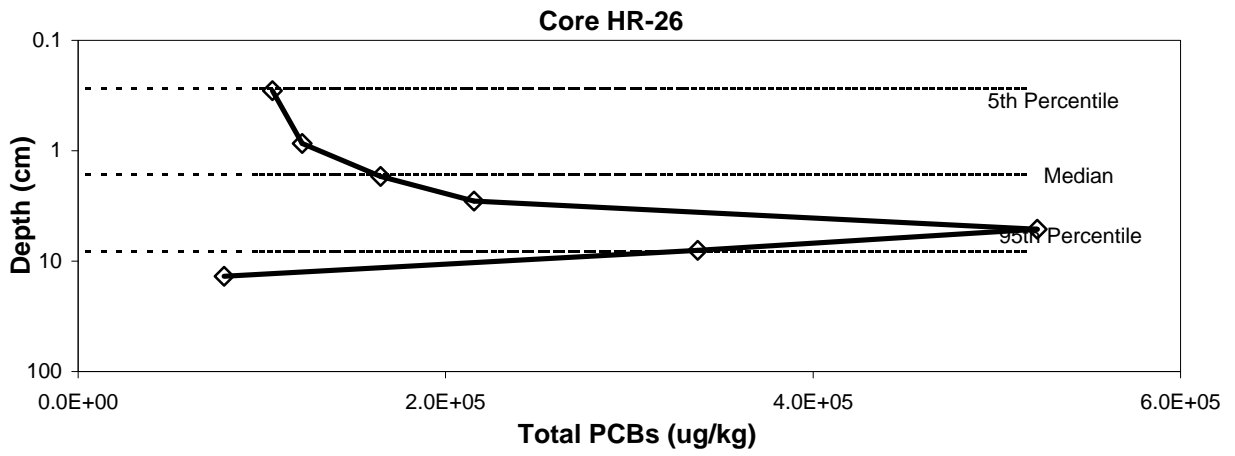
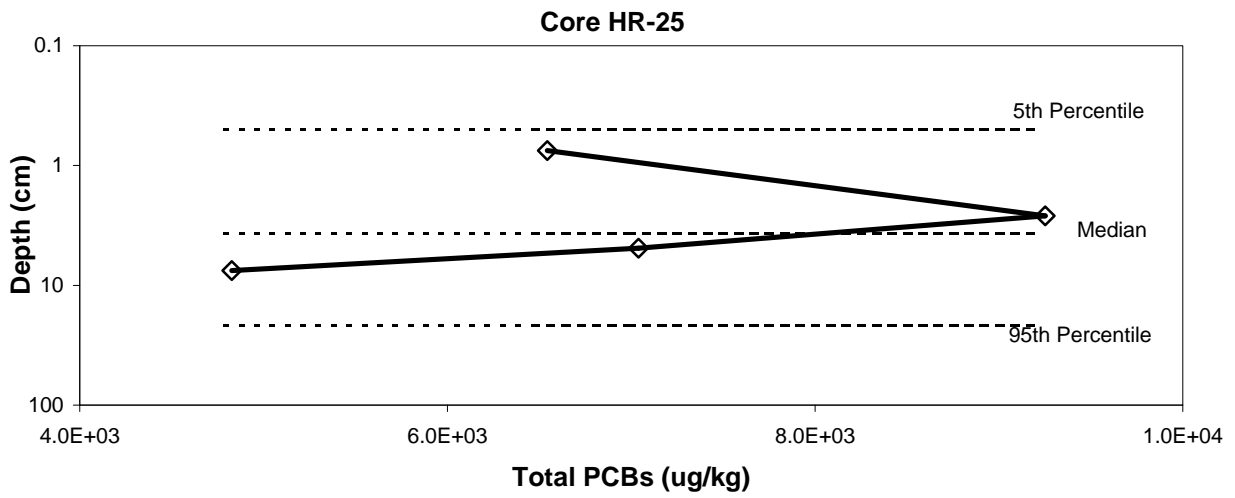


Figure 4-3b. Likelihood of PCB Scour for Selected Phase 2 High Resolution Sediment Cores.

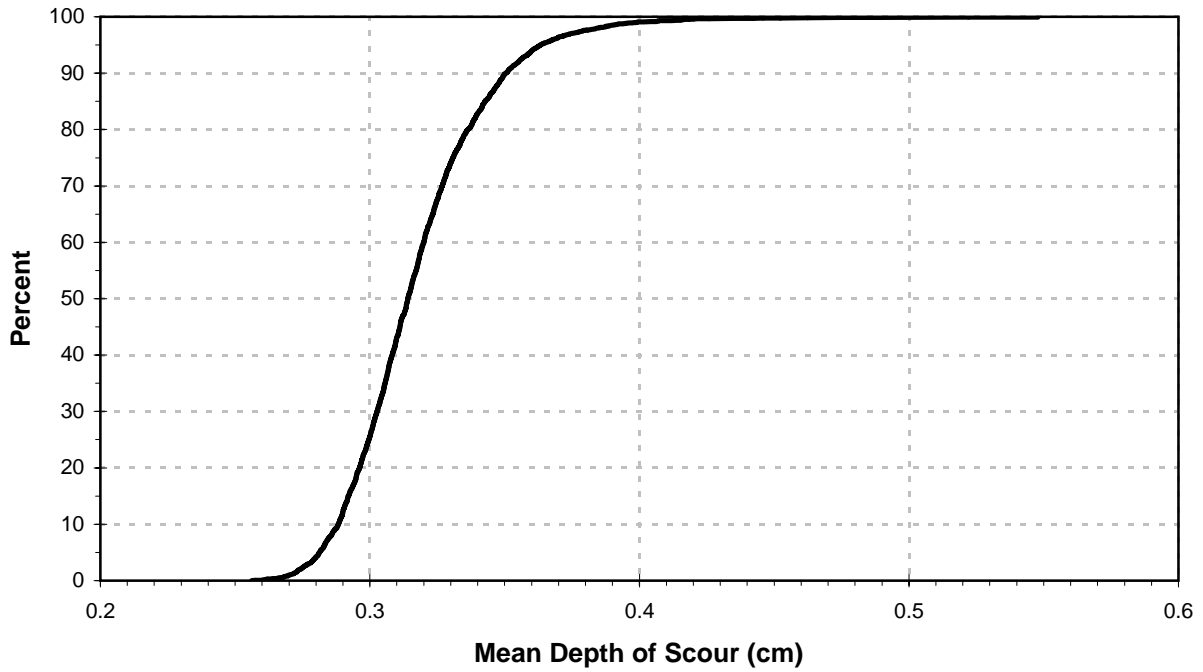


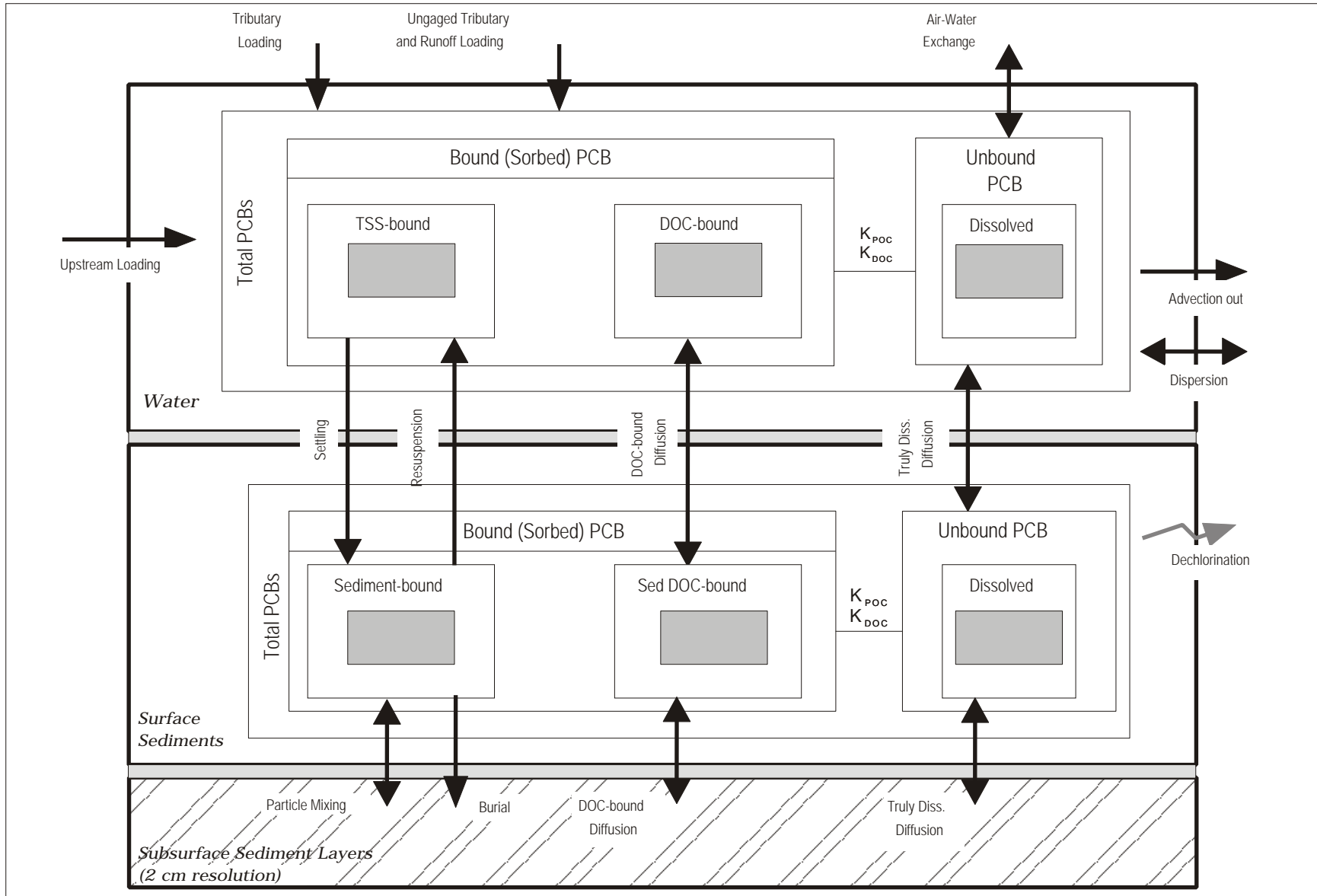
Figure 4-4. Cumulative Percent versus Mean Depth of Scour for Cohesive Sediment in Thompson Island Pool.



Figure 4-5. Cumulative Percent versus Total Solids Scoured from Cohesive Sediment in Thompson Island Pool.

Figure 5-1

Conceptual Framework for the HUDTOX PCB Model



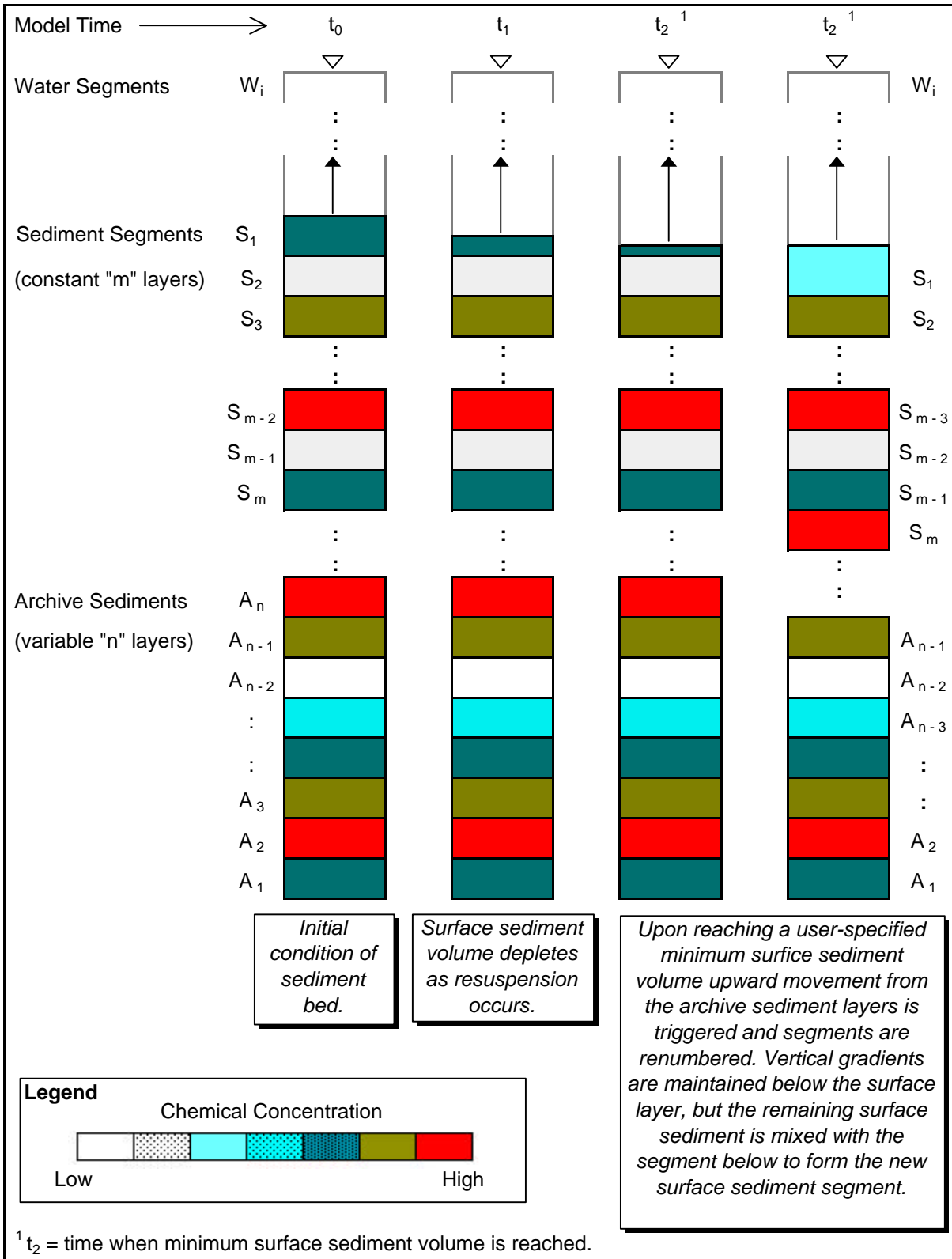


Figure 5-2. Illustration of Sediment Scour in the HUDTOX Model.

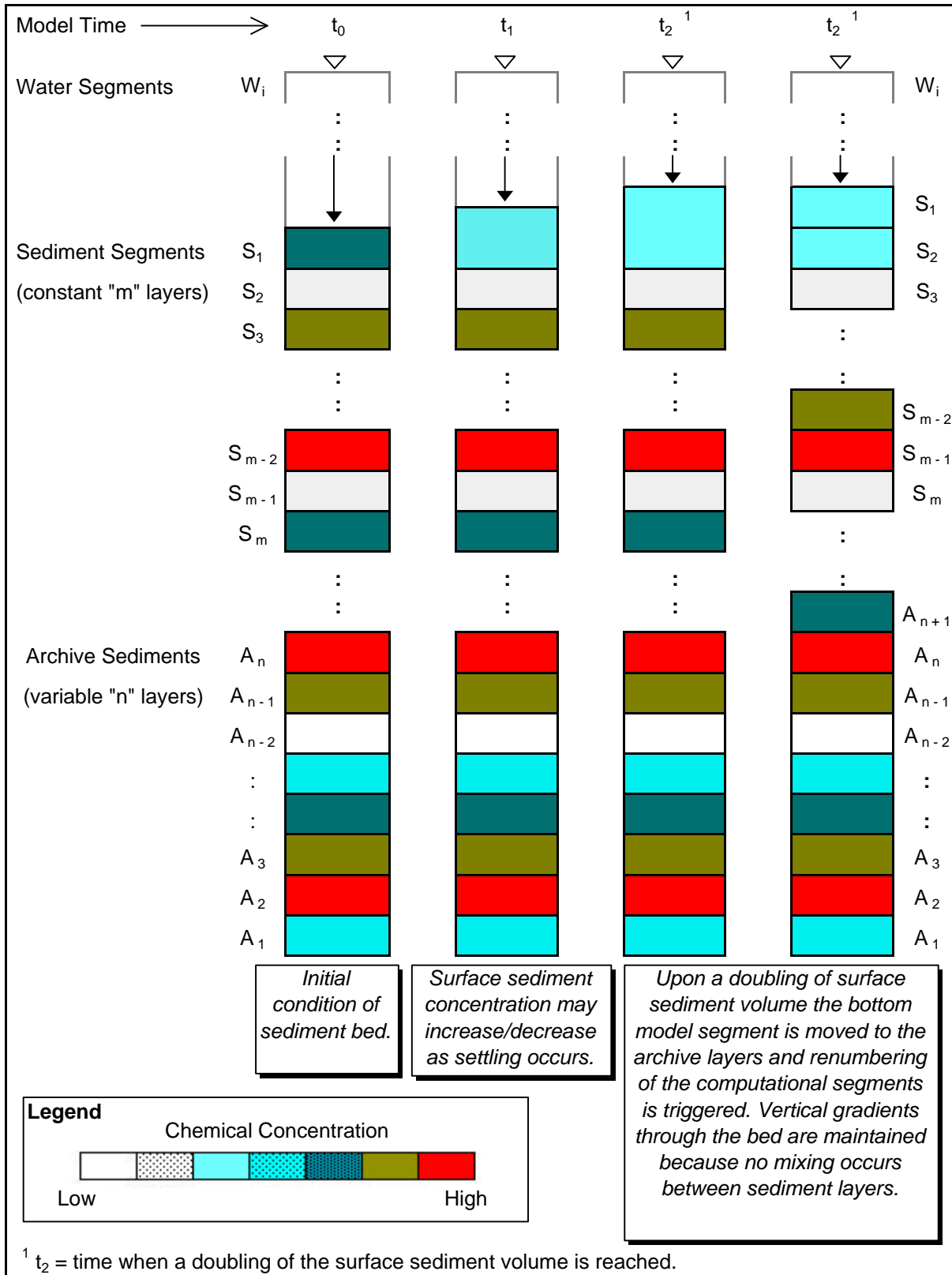


Figure 5-3. Illustration of Sediment Burial in the HUDTOX Model.

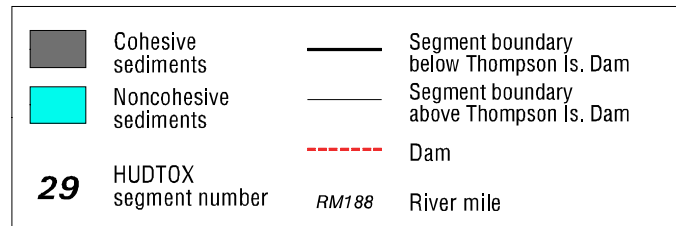
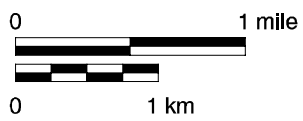
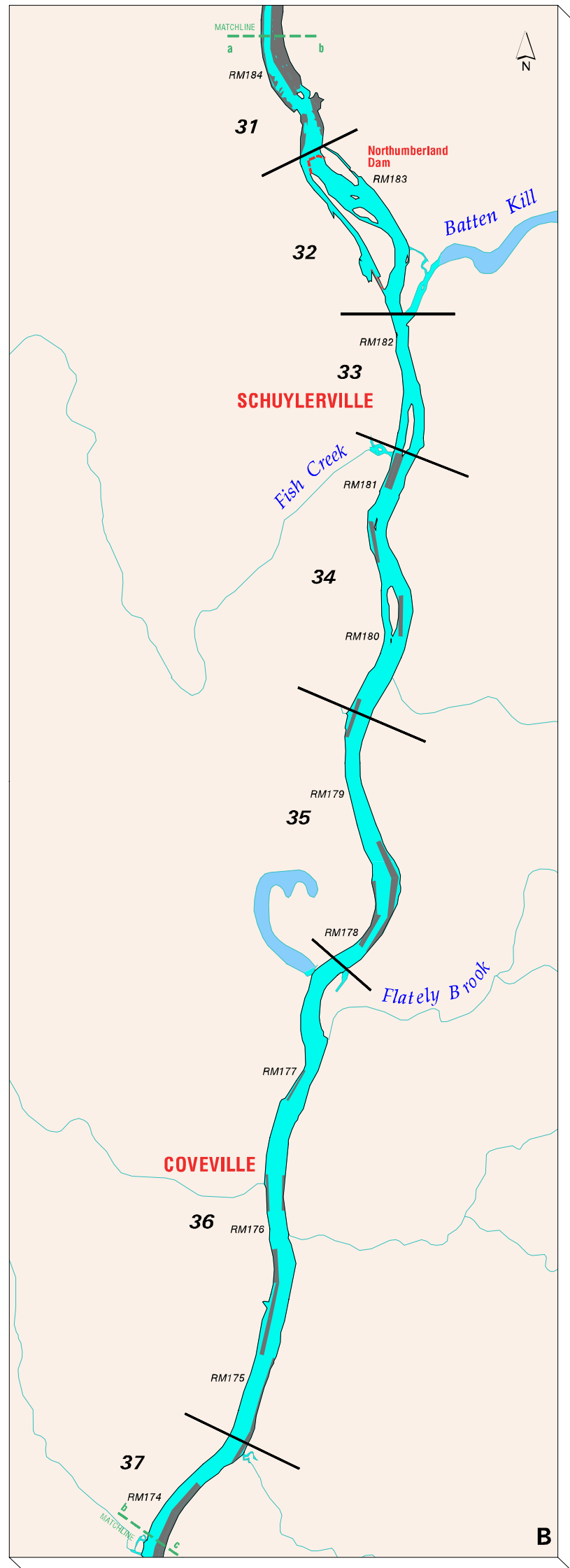
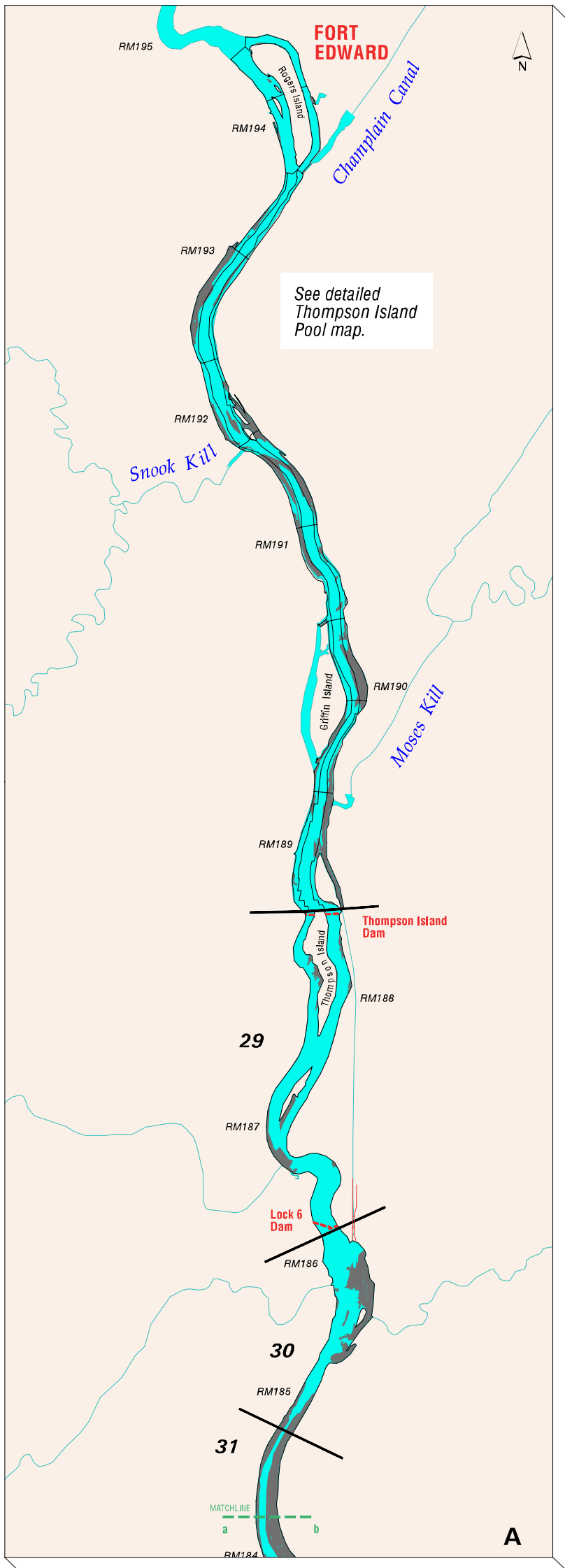


Figure 5-4 A,B. HUDTOX Model Water Column Segmentation Grid for Upper Hudson River, Parts A and B.

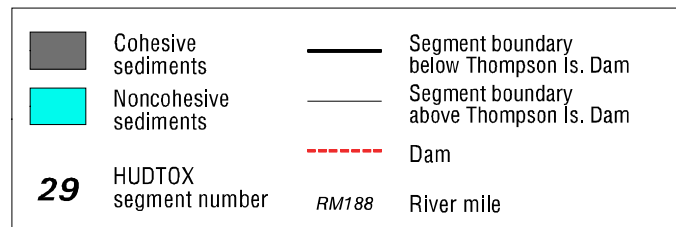
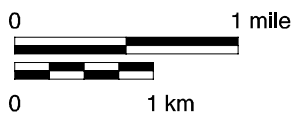
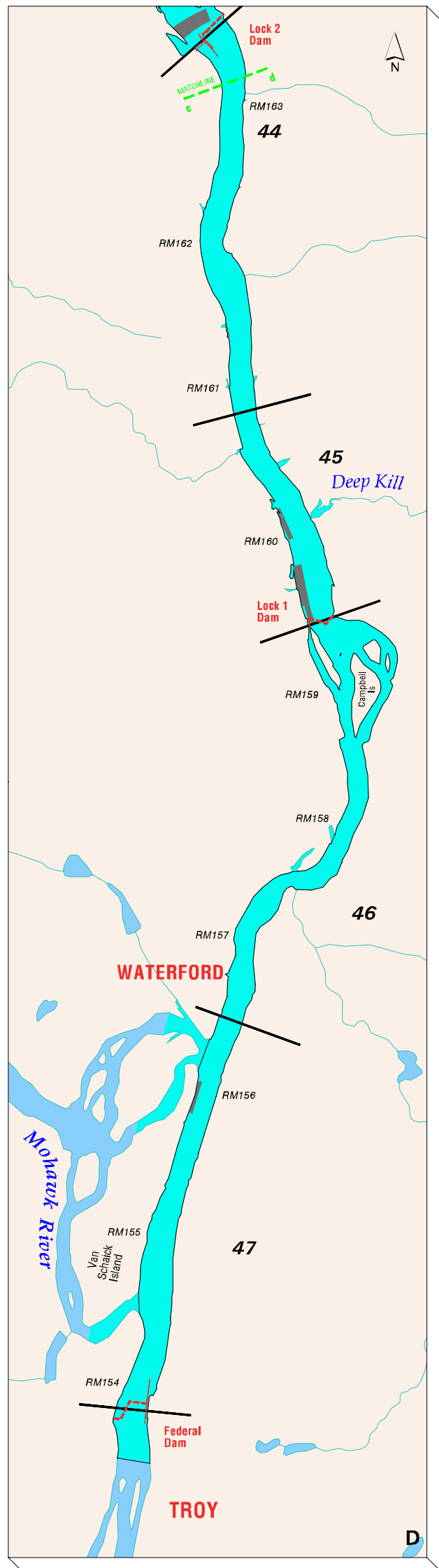
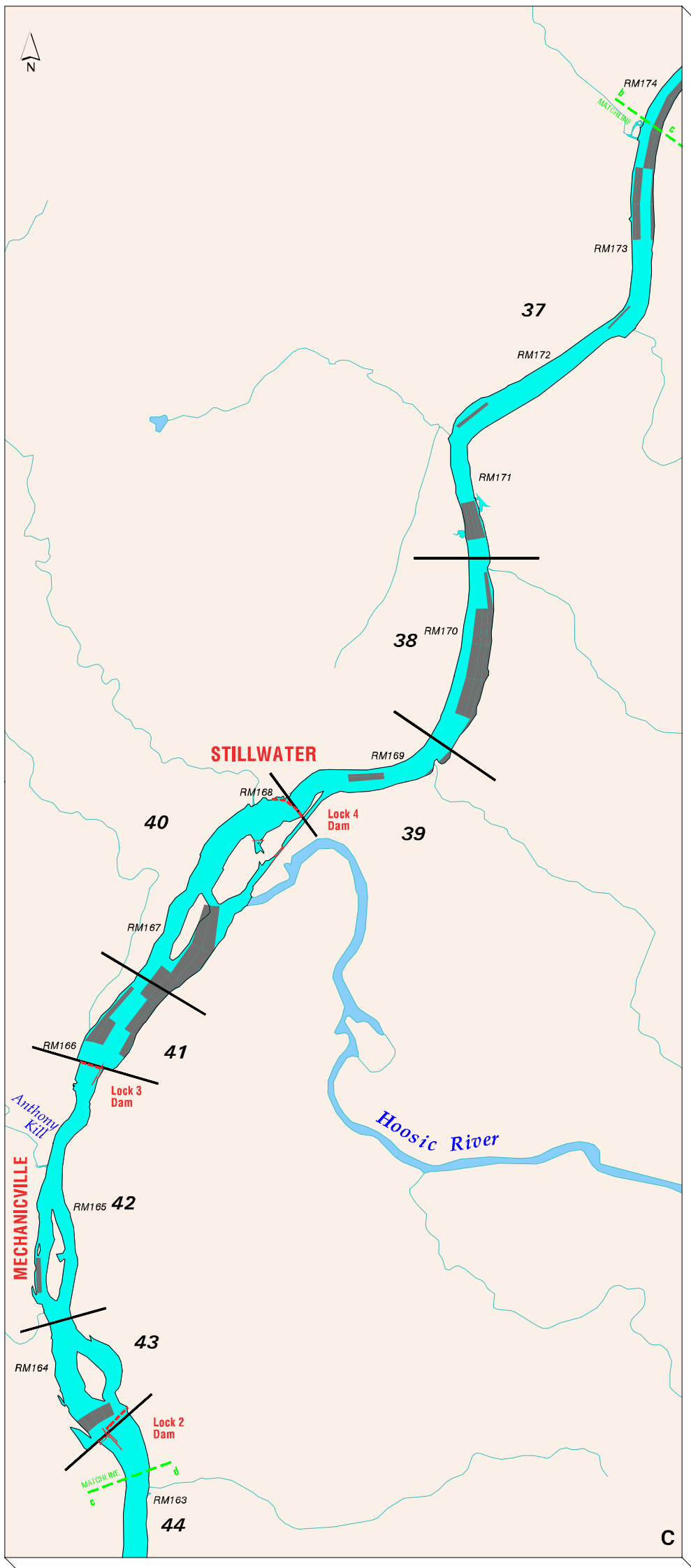


Figure 5-4 C,D. HUDTOX Model Water Column Segmentation Grid for Upper Hudson River, Parts C and D.

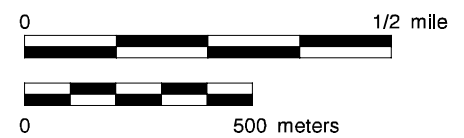
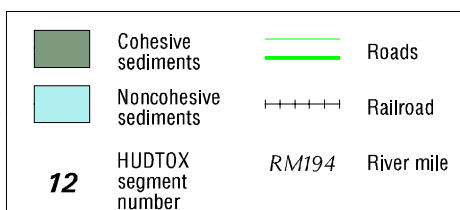
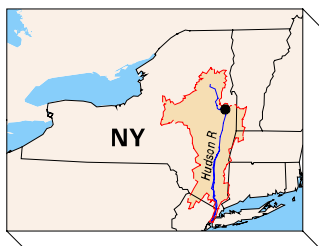
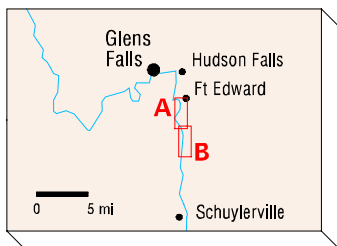
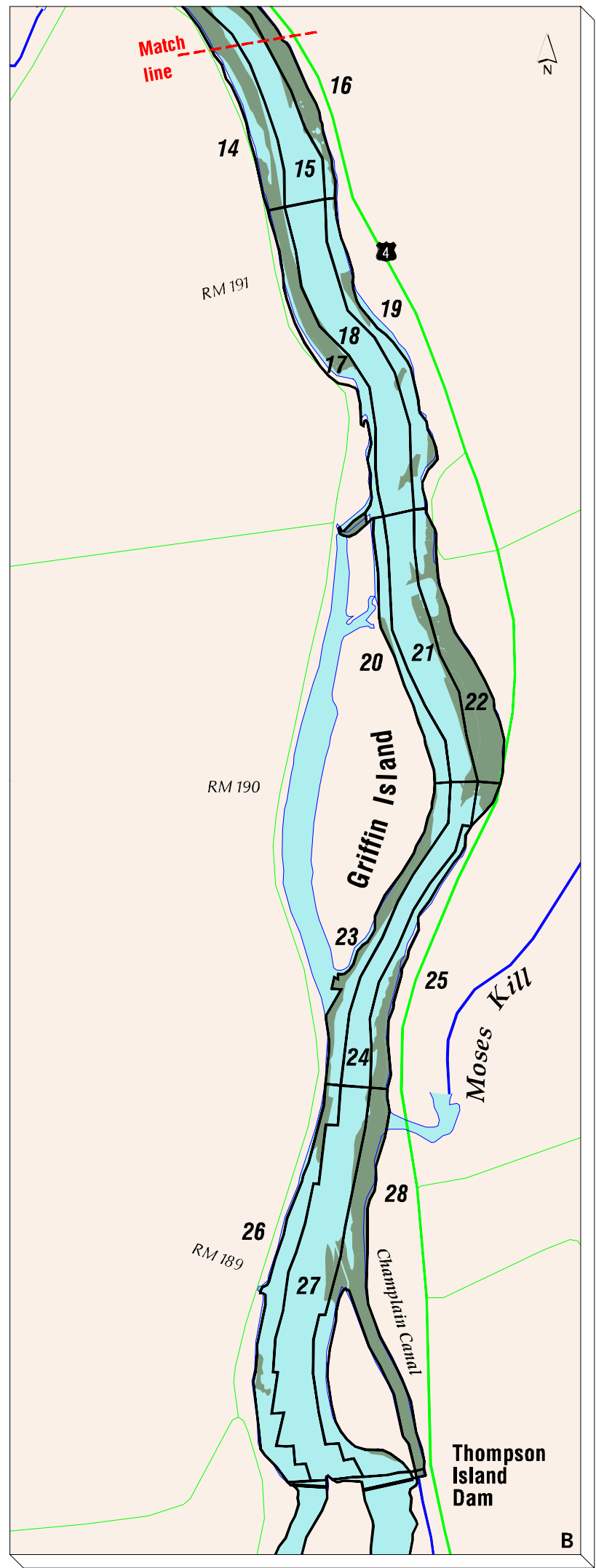
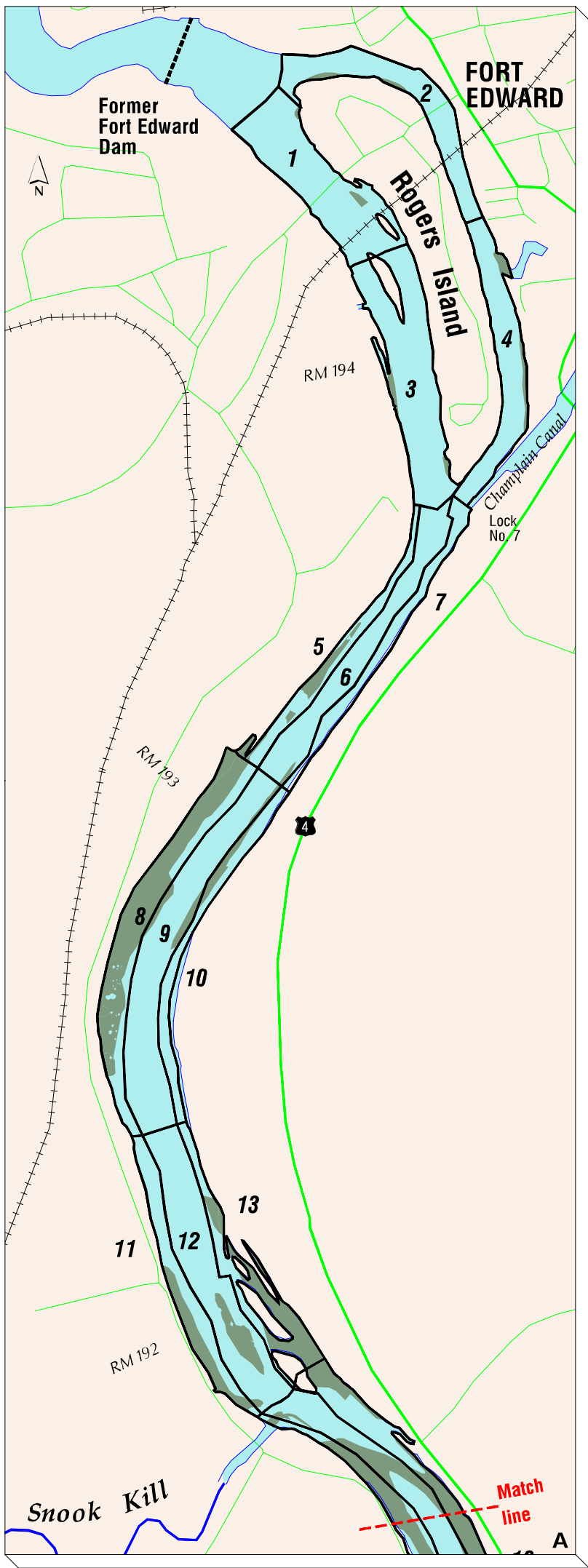


Figure 5-5. Thompson Island Pool Study Area.

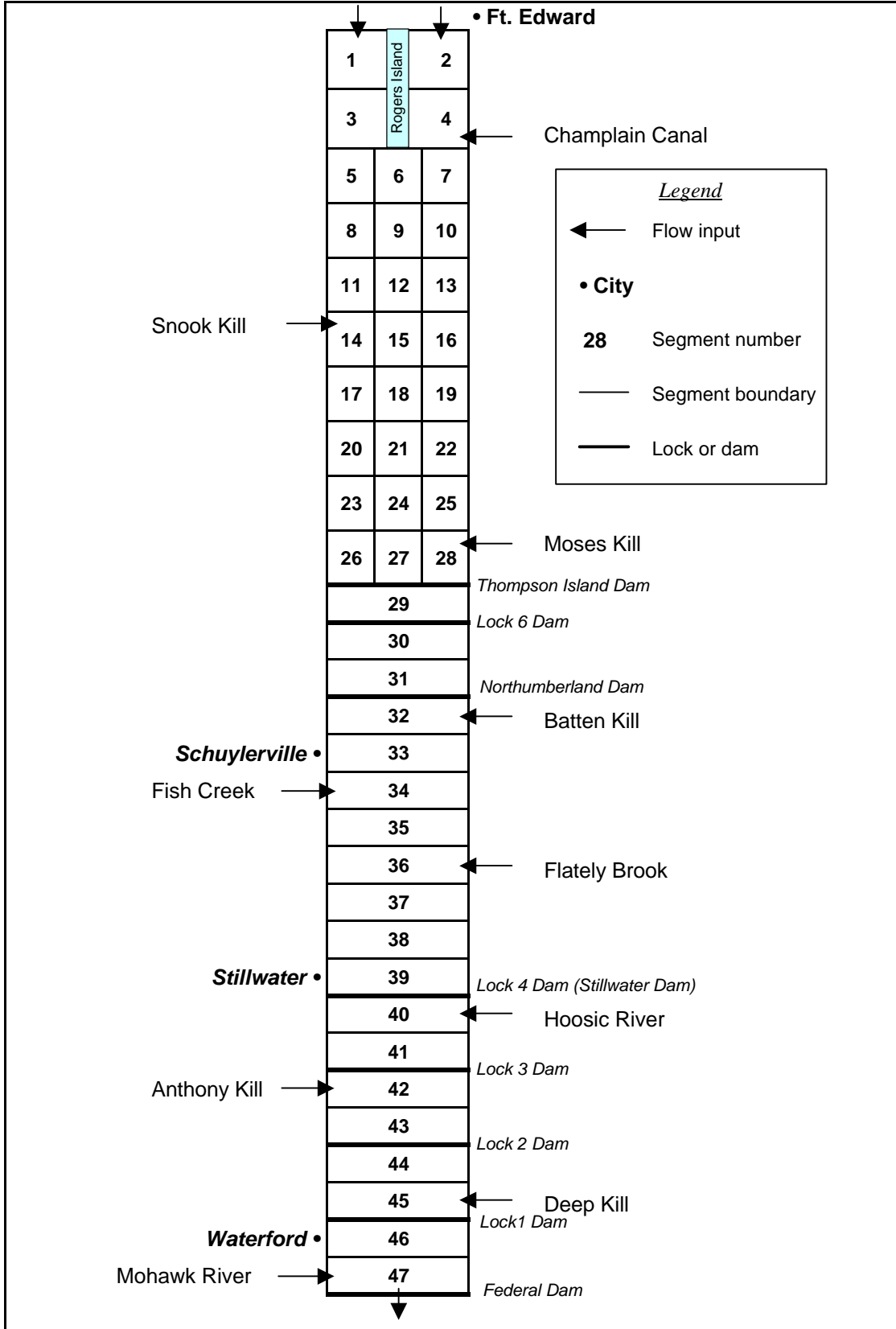


Figure 5-6. Schematic of HUDTOX Water Column Segmentation Grid.

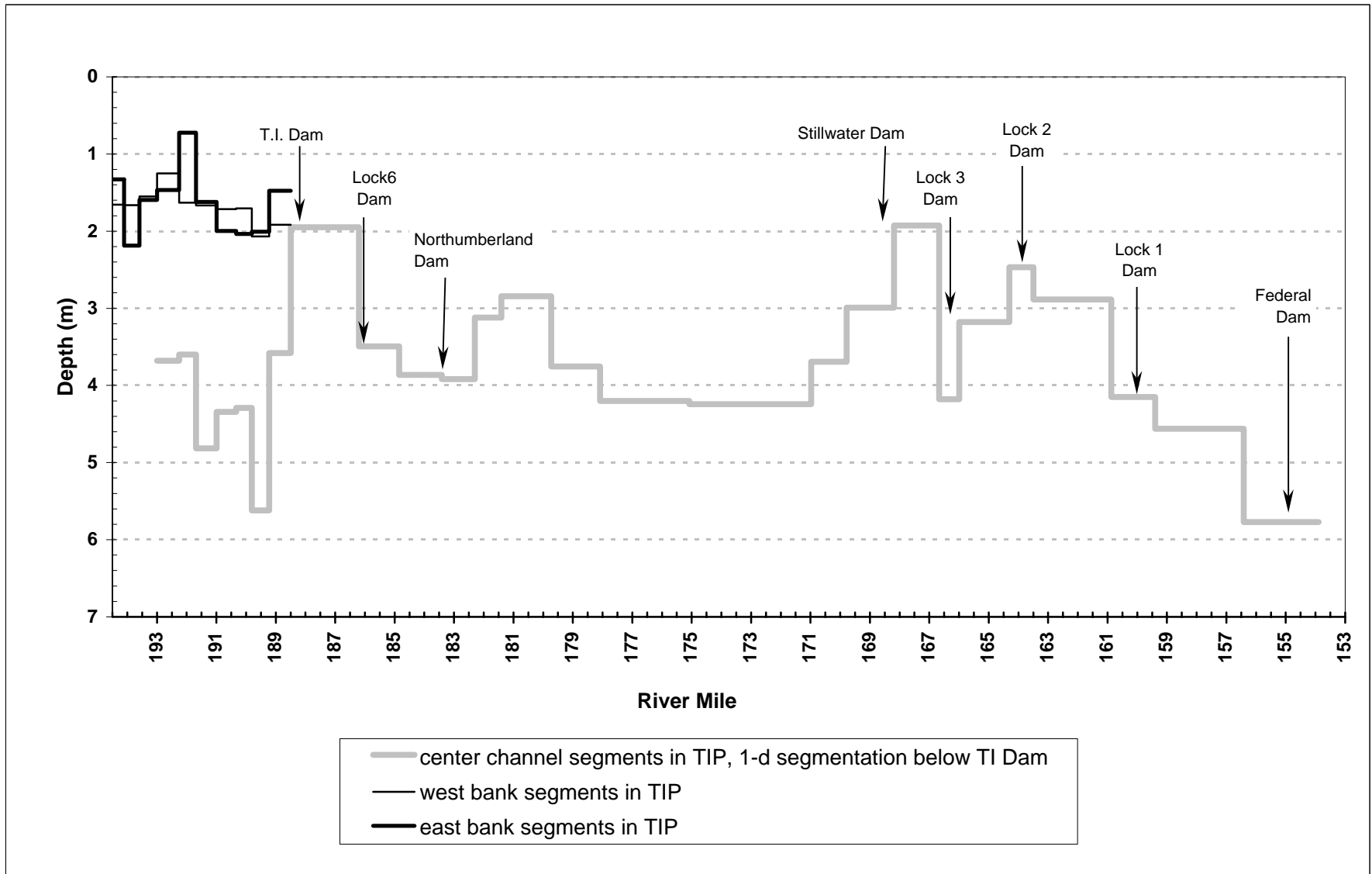
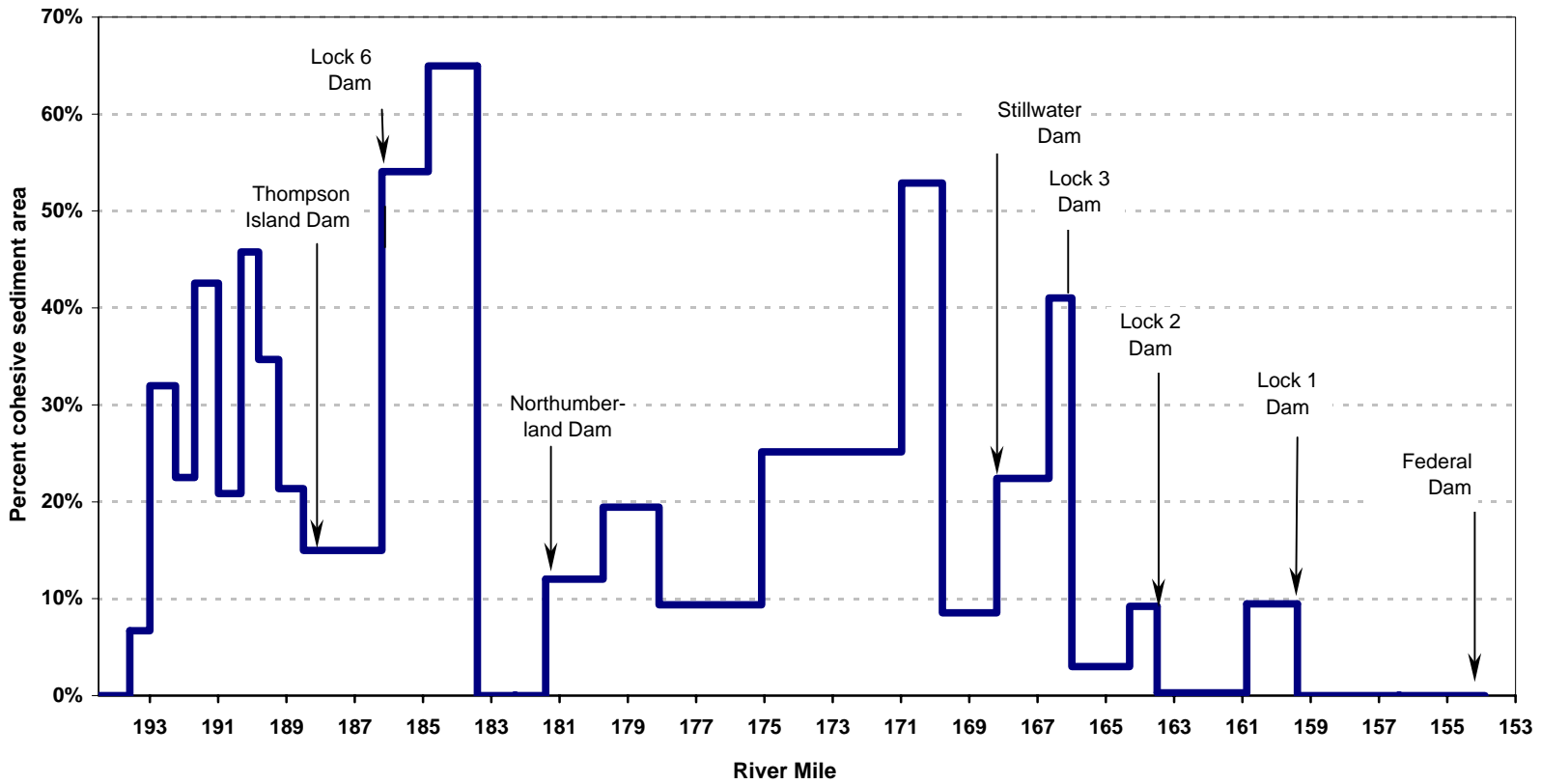


Figure 5-7. HUDTOX Water Column Segment Depths by River Mile.



Note:

1. Percent cohesive area = (cohesive sediment area) / (cohesive sediment area + noncohesive sediment area)
2. Fort Edward to Northumberland Dam cohesive and noncohesive sediment areas were determined from USEPA Phase 2 side scan sonar study (DEIR, TAMS, 1997)
3. Northumberland Dam to Federal Dam at Troy cohesive and noncohesive sediment areas were determined from the Sediment Bed Mapping Study of the Upper Hudson River from Northumberland Dam to Troy Dam (QEA, 1998).

Figure 5-8. Percent Cohesive Area Represented in HUDTOX Sediment by River Mile.